NASA Contractor Report 178228

# The Integration of a Mesh Reflector to a 15-ft Box Truss Structure, Task 3—Box Truss Analysis and Technology Development

E. E. Bachtell, W. F. Thiemet, and G. Morosow

Martin Marietta
Denver Aerospace
P.O. Box 179
Denver, CO 80201

Contract NAS1-17551
March 1987

National Aeronautics and
Space Administration

Langley Research Center
Hampton, Virginia 23665-5225

## FOREWORD

This report was prepared by Martin Marietta Denver Aerospace under Contract NAS1-17551. This report covers the results of Task 3. The contract was administered by the Langley Research Center of the National Aeronautics and Space Administration. The Task 3 study was performed from April 1985 to November 1986 and the NASA-LaRC project managers were Mr. U. M. Lovelace and Mr. J. W. Goslee.

CONTENTS

Figure



Table

GLOSSARY

| | |
|---|---|
| cm | Centimeters |
| D | Reflector Diameter |
| F | Focal Point |
| FD | Focal Length over Diameter |
| GFRP | Graphite Fiber Reinforced Plastic |
| GHz | Gigahertz |
| in. | Inch |
| m | Meters |
| mm | Millimeter |
| MT | Manufacturing Tolerance |
| N | Newtons |
| NASA | National Aeronautics and Space Administration |
| OOA | On-Orbit Assembly |
| rms | Root Mean Square |
| $TS^2$ | Area Bound by Tie Points |
| $TS_{rad}$ | Radial Tie Spacing |
| $Z_d$ | Z Coordinate of Tie Point |
| $Z_p$ | Z Coordinate of "Best-Fit" Surface |

## 1.0 INTRODUCTION--BOX TRUSS ANTENNA SYSTEM

The basic box truss structure was first designed and used on the On-Orbit Assembly (OOA) program, Contract F04701077-C-0180, for the Air Force (Fig. 1). OOA used the box truss structure to design a planar truss system to support a mesh array. Mesh support posts or standoffs were used to separate the radiating surface from the support structure. The separation provides the volume necessary to stow the mesh and mesh tie-system and to assure that neither the mesh or tie cords will impede the deployment of the box truss. Generally, the standoffs are tubes of similar cross section to the box vertical members and are inserted into the corner fittings. The mesh is attached to the top of the standoffs. In 1979, an IR&D project was performed to determine the adaptability of the box truss to nonplanar shapes, i.e., paraboloidal and spherical reflector systems. The conclusions of the study were as follows:

1) The vertical members on the box truss structure must be vertical rather than perpendicular to the surface to assure step-by-step deployment and stowability.

2) The paraboloid of revolution was the only nonflat surface that can be formed by a box truss structure using equal length standoffs and equal length surface tubes.

3) A spherical reflector can be formed by using a parabolic box truss reflector support structure and varying the mesh standoff heights.

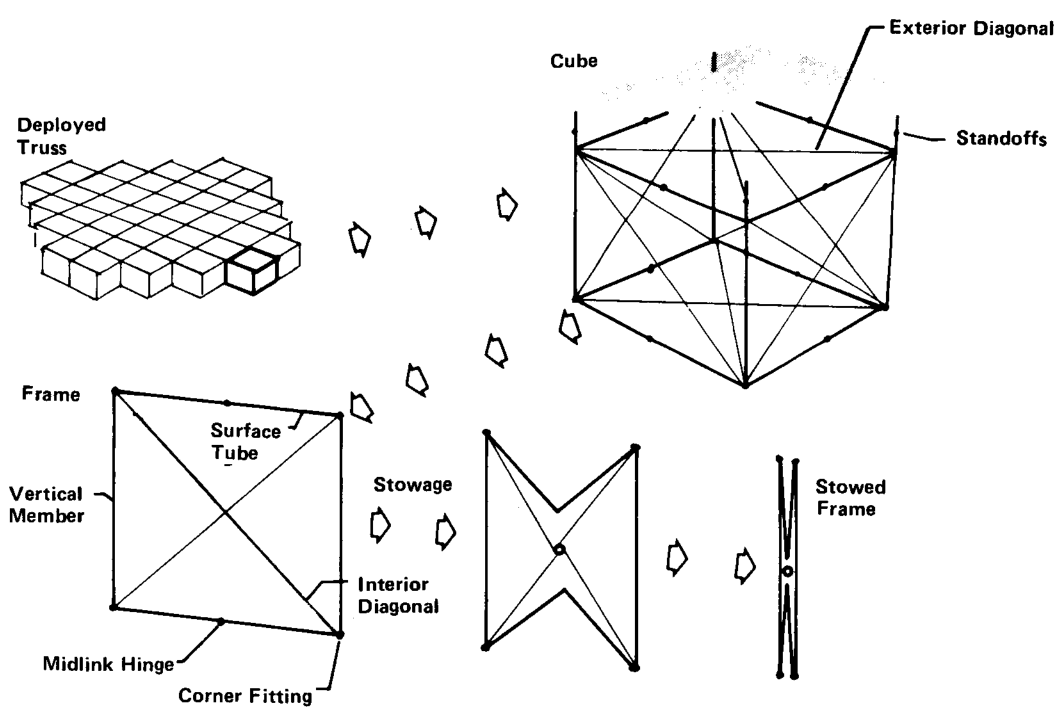


*Figure 1 Deployable Box Truss Schematic*

From 1981 through 1982, Martin Marietta's IR&D Project D-54D designed and built a single 4.572-m box truss cube using all graphite fiber reinforced plastic (GFRP) components (Fig. 2). Also, included in the D-54D effort was the geometric design of a mesh tie-system, i.e., a web of cords, which would be used to position the mesh into a paraboloid shape.

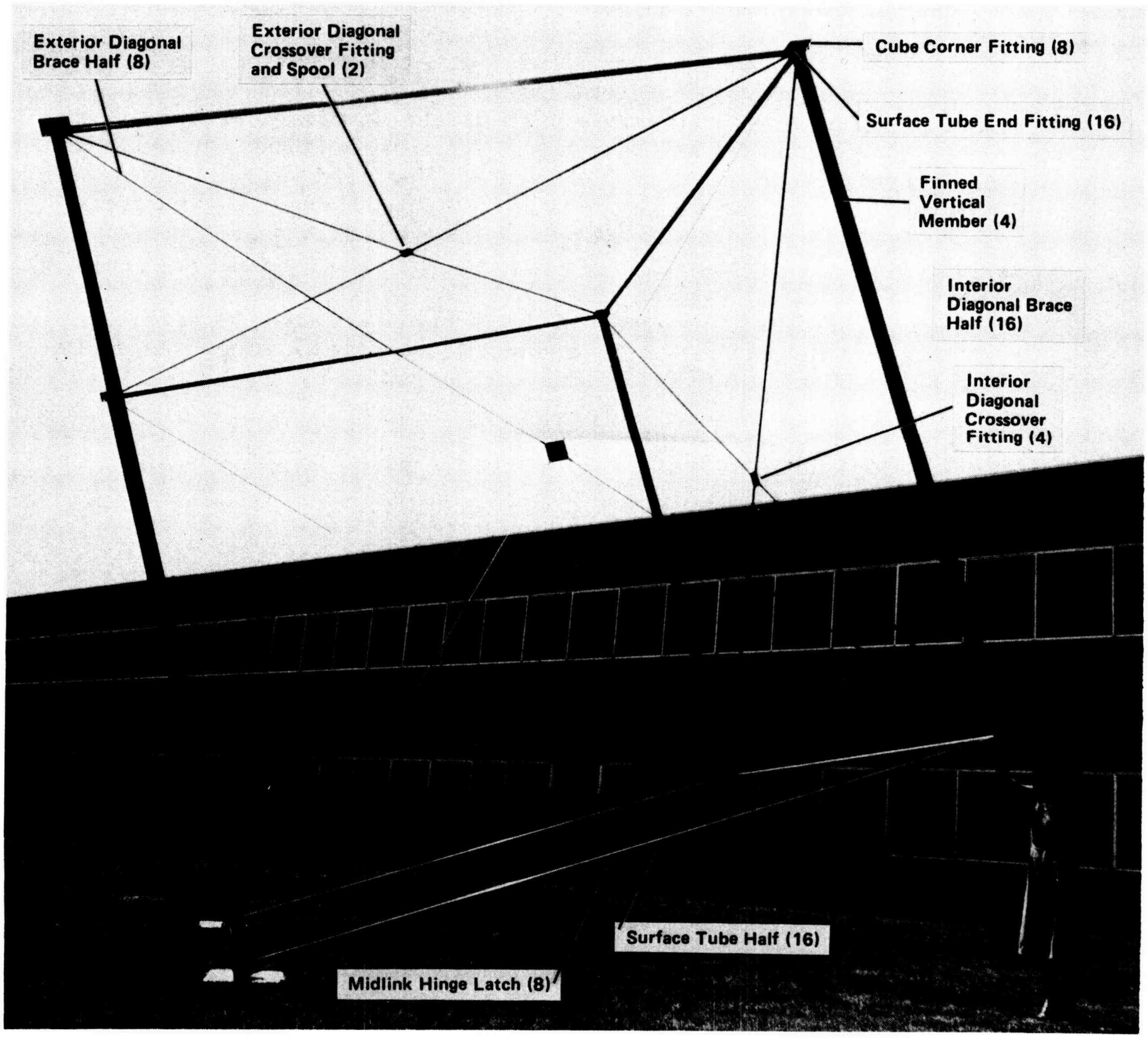


*Figure 2 Development of Box Truss (1980 and 1981)*

To demonstrate the design and integration of a reflective mesh surface to a deployable truss structure, NASA under the Box Truss Analysis and Technology Development Task Contract, Task 3 Integration of Reflector Surface to Box Truss, commissioned Martin Marietta to install a mesh reflector on the 4.572-m box truss cube. The specific features demonstrated include: (1) sewing seams in reflective mesh; (2) mesh stretching to desired preload; (3) installation of surface tie cords; (4) installation of reflective surface on truss; (5) setting of reflective surface; (6) verification of surface shape/accuracy; (7) storage and deployment; (8) repeatability of reflector surface; and (9) comparison of surface with predicted shape using analytical methods developed under Task 1--"Mesh Analysis and Control" of this contract.

## 1.1 DIRECT TIEBACK SYSTEM

From IR&D project studies on various tie system configurations, the direct tieback system has shown analytically to be one of the most stable tie system designs for applying reflective mesh to box truss antennas (Fig. 3). Also, the direct tieback system allows each box section of mesh to be manufactured separately since there are no common tie cords between box sections. This includes the edge catenaries, i.e., each box section would have four-edge catenaries. The mesh would be made continuous by simply sewing the interface together using a whip stitch. If necessary, a separate surface cord with tie backs would be installed at this sewn interface to shape the section of mesh between the two-edge catenaries. Manufacturing each box section of mesh is a desirable design feature considering a single box section may be as large as 15x15 m and having to deploy more than a single box so that the mesh and tie cords could be installed would be cumbersome, if not impractical.

Figure 3 shows that the direct tieback system consists of three types of cords: (1) the surface cross cords that bisect the mesh reflective surface; (2) the surface radial cords that extend radially from the top of the standoffs to the surface cross cords; and (3) the tieback cords that extend from the surface cords to the bottom of the standoffs. The bottom of the standoffs correspond to the location of the corner fittings on the box truss. The tieback cords are used to pull the surface into shape and are tied along each surface cord at a distance defined as the radial tie spacing. Note that the cross cords do not span the entire width of the box section. This is necessary to enable the tie system of each box section to be manufactured separately. Also, this helps to eliminate most of the interaction between the tie systems of adjacent box sections, allowing each tie system of each box to operate independently. Consequently, this produces a more stable reflector surface since local environmental effects such as shadowing of a single box section will not effect the surface of other box sections. Since each tie system can operate independently, analyzing and testing the complete reflective surface can be performed on a per box section basis.

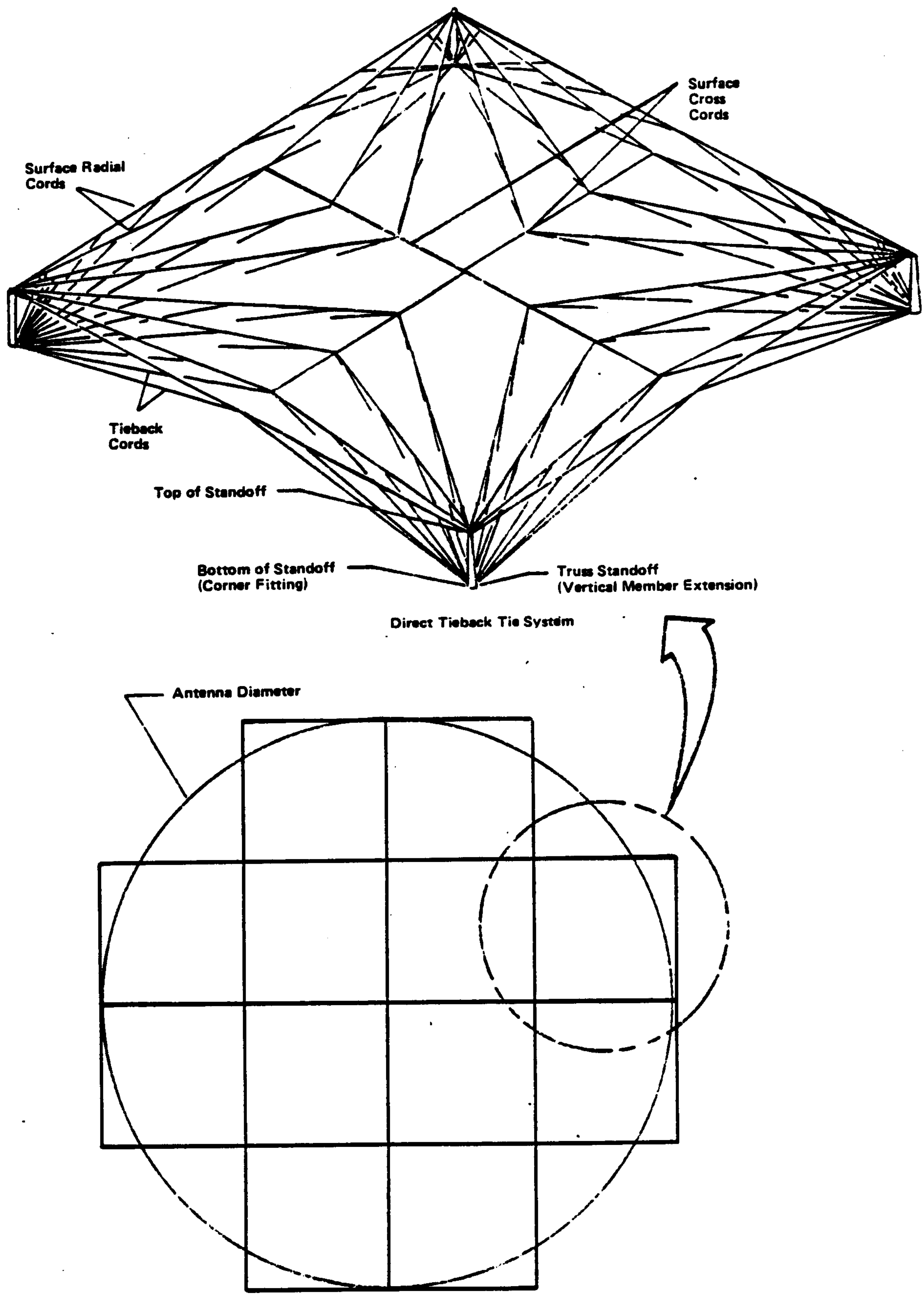


*Figure 3 Box Truss and Direct Tieback Tie System*

## 1.2 SUMMARY

The result of this task has been a 4.572-m, offset fed box truss reflector with a focal length over diameter (F/D) of 1.5. The achieved surface accuracy using the direct tieback tie system was slightly better than 1/18 of a wavelength at 10 GHz. More importantly, this task advanced box truss reflector technology by providing a physical means for answering many of the concerns associated with incorporating reflective mesh onto a box truss structure. In addition, knowledge into improving the manufacturing technics was realized.

The concerns that were directly examined included:

1) Sewing reflective mesh;

2) Stretching mesh to a desired preload;

3) Assembling and installing the reflector onto the box truss;

4) Setting and verifying the reflector surface;

5) Determining the repeatability of the surface.

Recommendations for improvement resulting from problems during the manufacturing of the reflector includes:

1) Finding a more durable material to replace the graphite cord used to build the tie system;

2) Finding ways to simplify the tieback cord adjustment so that setting the reflector surface is both faster and easier. Specific recommendations are discussed in Chapter 6.0.

This Page Left Intentionally Blank

## 2.0 DESIGN AND FABRICATION OF THE REFLECTOR SURFACE

When this task began, the mesh reflector surface was to be installed on the box truss without changing the configuration of the box truss structure. This meant designing and fabricating the reflector surface on equal length standoffs for a center-fed 4.572-m (15 ft) reflector. An F/D value of 2.0 was chosen and the tie cord system would be designed to achieve a surface accuracy compatible with 10 GHz operation and a goal of 1/25 of a wavelength. However, before the installation of the reflector onto the box truss was started, the configuration was changed to meet later test requirements and for comparison to other reflector systems. This modified reflector geometry is a 4.572-m offset-fed reflector with an F/D of 1.5 and offset from the vertex of the paraboloid by 0.61 m (Fig. 4).

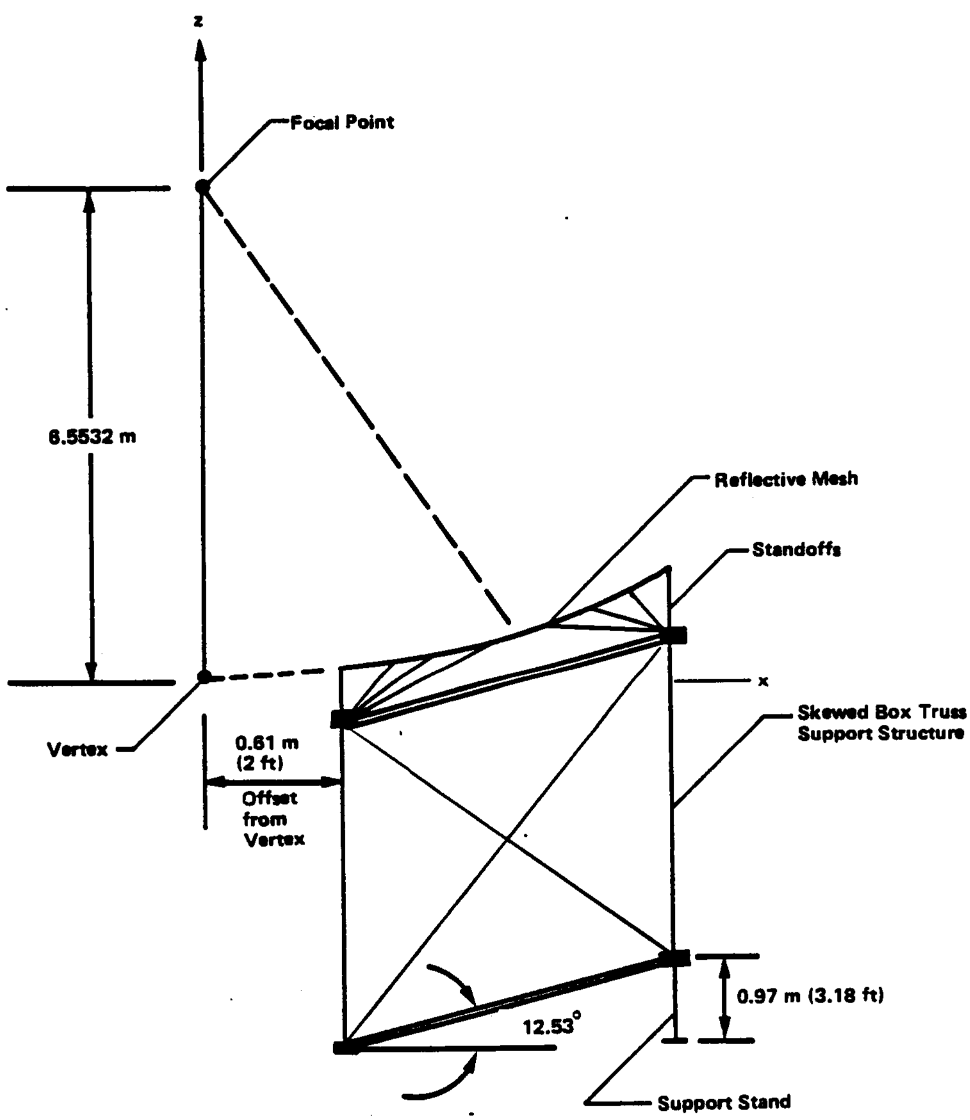


*Figure 4*
*4.572-meter Offset-Fed Reflector Geometry*



PRECEDING PAGE BLANK NOT FILMED

Even though the change from center fed to offset fed and the change from an F/D of 2.0 to 1.5 would effect the surface accuracy for a fixed tie spacing, the goal of 1/25 of a wavelength a 10 GHz was still achievable by tightening up the manufacturing tolerance.

## 2.1 DESIGN OF THE REFLECTOR SURFACE

The first step in designing the reflector was to determine the surface accuracy error budget for the system. The error budget sets the radial tie spacing for the tie system and the required manufacturing tolerance on setting the surface. The values chosen were 55% of the total error are because of pillowing and 45% are because of manufacturing. Generally, a larger value is used for manufacturing, i.e., 75%. However, this would leave only 25% for pillowing, and therefore, increases the number of tie points on the surface. Since cost on this prototype model was an issue, a tradeoff between the cost of fabricating and setting each tie point versus the cost of setting a reduced number of tie points to a closer tolerance was completed. Setting a reduced number of tie points to a closer tolerance was more cost effective.

Using the 55/45 split in pillowing and manufacturing errors resulted in the following:

1) Required surface accuracy = 0.0012-m rms at 10 GHz and 1/25 of a wavelength;

2) 55% because of pillowing = 0.00066-m rms,
45% because of manufacturing = 0.00054-m rms.

Using Equation 1 for determining rms pillowing errors (Ref 1), and solving for $TS^2$ resulted in a required area bound by the tie points

[1] $$\text{rms pillow} = 0.05 * TS^2/F$$

where $TS^2$ = Mesh Area bound by tie points, $m^2$
$F$ = Focal length, 6.5532 m
rms pillow = 0.00066 m

of 0.0878 $m^2$. Note, in the original equation found in Ref 1, $TS^2$ represented the radial tie spacing squared. However, for the direct tieback tie system, the radial tie spacing along a surface cord does not equal the spacing between radial surface cords, and therefore $TS^2$ was changed to represent the mesh area bound by a set of four tie points. Once $TS^2$ was determined, Equation 2 was used to determine a required radial tie spacing of 0.508 m.

[2] $$TS_{rad} = \sqrt{\frac{TS^2}{0.34}}$$

where $TS^2$ = area bound by tie points, m
$TS_{rad}$ = Radial tie spacing between tie points, m

The constant in Equation 2, 0.34, is based on the relationship between the average area bound by the tie points given a known radial tie spacing.

The manufacturing tolerance is set by three times the required rms manufacturing error or in this case, three times 0.00054-m rms. Therefore, the manufacturing tolerance was set at ± 0.162 cm (0.063 in.).

Table 1 presents a summary of the error budget, tie spacing, and manufacturing tolerance.

*Table 1 Error Budget Summary*

| |
|---|
| **Required rms Surface Accuracy = 0.121 cm at 10 GHz and 1/25 of wavelength** |
| **Pillowing rms Error = 0.066 cm (55%) (0.026 in.)** |
| **Manufacturing rms Error = 0.054 cm (45%) (0.021 in.)** |
| **Required Radial Tie Spacing = 50.8 cm (20 in.)** |
| **Required Manufacturing Tolerance = ± 0.16 cm (± 0.063 in.)** |

After calculating the radial tie spacing of 0.508 m, the mesh tie system generator (Ref 1), was used to generate the tie point coordinates. The result was a tie system consisting of 212 tie points and 20 catenary points. Later, the number of tie points was reduced to 176 because of a change in catenary depth. This is discussed later in the report. Appendix A shows a complete listing of the point coordinates. The program was run for the center-fed configuration. However, Appendix A shows the coordinates of the offset configuration that were hand generated by taking the center-fed coordinates and translating them into the new configuration. Appendix A shows the constants used for this translation process.

The X and Y coordinates for each point were transferred to the CADDS 4X system and a full-scale plot of the points was produced on vellum. This plot made up the template to be used on the mesh stretching table to locate the tie points, the edge catenaries, and the tops of the standoffs.

The X, Y, and Z coordinates were used to determine the tie cord lengths between tie points and the tieback cord length to each point. Figure 5 and Table 2 summarize the results of the length calculations. As with the mesh template, the surface cords were built to the center-fed configuration and required minor changes to be made during installation. The tieback cord lengths were built oversized, and therefore, could easily be revised to match the new geometry.

<u>Tie System Button Design</u>--After having determined the geometry of the tie system, the next step was to determine a design for attaching the tieback cord to the surface cord. Since the tie cords were to be built of graphite tow, breakage could be expected on some of the cords and therefore the design had to facilitate easy repair.

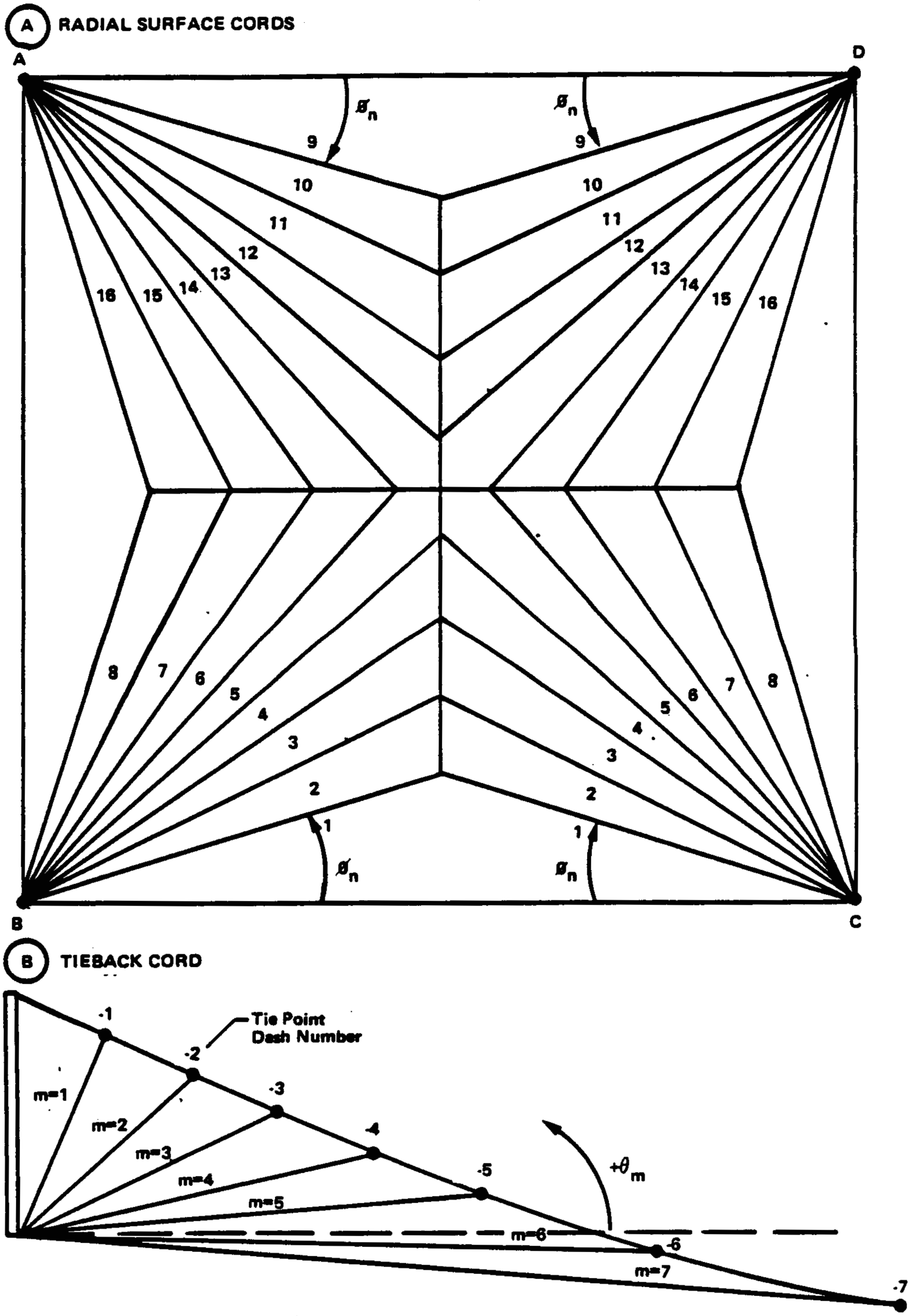


*Figure 5 Tie System Configuration*

ORIGINAL PAGE IS
OF POOR QUALITY

*Table 2 Tie Cord Lengths*

| Radial Surface Cords | $\phi_n$, deg | Distance from Top of Standoff, m -1 | -2 | -3 | -4 | -5 | -6 | -7 |
|---|---|---|---|---|---|---|---|---|
| n= 1 | 14.4 | 0.508 | 1.016 | 1.524 | 1.953 | 2.381 | – | – |
| 2 | 25.4 | 0.508 | 1.016 | 1.524 | 2.031 | 2.299 | 2.566 | – |
| 3 | 34.6 | 0.508 | 1.016 | 1.524 | 2.031 | 2.431 | 2.830 | – |
| 4 | 42.2 | 0.508 | 1.016 | 1.524 | 2.031 | 2.538 | 2.846 | 3.154 |
| 5 | 45.6 | 0.508 | 1.016 | 1.524 | 2.031 | 2.538 | 2.846 | 3.154 |
| 6 | 53.2 | 0.508 | 1.016 | 1.524 | 2.031 | 2.431 | 2.830 | – |
| 7 | 62.7 | 0.508 | 1.016 | 1.524 | 2.031 | 2.299 | 2.566 | – |
| 8 | 74.0 | 0.508 | 1.016 | 1.524 | 1.953 | 2.381 | – | – |
| 9 | 15.7 | 0.508 | 1.016 | 1.524 | 1.953 | 2.381 | – | – |
| 10 | 26.4 | 0.508 | 1.016 | 1.524 | 2.031 | 2.299 | 2.566 | – |
| 11 | 35.6 | 0.508 | 1.016 | 1.524 | 2.031 | 2.431 | 2.830 | – |
| 12 | 43.0 | 0.508 | 1.016 | 1.524 | 2.031 | 2.538 | 2.846 | 3.154 |
| 13 | 46.4 | 0.508 | 1.016 | 1.524 | 2.031 | 2.538 | 2.846 | 3.154 |
| 14 | 54.0 | 0.508 | 1.016 | 1.524 | 2.031 | 2.431 | 2.830 | – |
| 15 | 63.2 | 0.508 | 1.016 | 1.524 | 2.031 | 2.299 | 2.566 | – |
| 16 | 74.4 | 0.508 | 1.016 | 1.524 | 1.953 | 2.381 | – | – |

**Note: The distance calculations are based on the center-fed configuration.**

| Tieback Cord | -1 | | -2 | | -3 | | -4 | | -5 | | -6 | | -7 | |
|---|---|---|---|---|---|---|---|---|---|---|---|---|---|---|
| | L, m | θ, deg | L, m | θ, deg | L, m | θ, deg | L, m | θ, deg | L, m | θ, deg | L, m | θ, deg | L, m | θ, deg |
| n= 1 | 0.625 | 45.2 | 1.044 | 24.3 | 1.514 | 15.6 | 1.928 | 12.0 | 2.350 | 9.9 | – | – | – | – |
| 2 | 0.617 | 46.0 | 1.039 | 25.4 | 1.506 | 16.8 | 1.996 | 12.7 | 2.258 | 11.4 | 2.522 | 10.5 | – | – |
| 3 | 0.610 | 46.8 | 1.031 | 26.5 | 1.499 | 17.9 | 1.986 | 13.8 | 2.380 | 12.1 | 2.774 | 11.0 | – | – |
| 4 | 0.597 | 47.5 | 1.024 | 27.5 | 1.497 | 19.0 | 1.976 | 14.9 | 2.494 | 12.8 | 2.779 | 12.1 | 3.086 | 11.6 |
| 5 | 0.589 | 47.9 | 1.021 | 27.9 | 1.488 | 19.5 | 1.974 | 15.4 | 2.471 | 13.3 | 2.776 | 12.6 | 3.084 | 12.1 |
| 6 | 0.615 | 48.6 | 1.039 | 29.0 | 1.506 | 20.6 | 1.991 | 16.6 | 2.383 | 14.8 | 2.776 | 13.8 | – | – |
| 7 | 0.635 | 49.4 | 1.059 | 30.3 | 1.524 | 22.1 | 2.012 | 18.1 | 2.273 | 16.9 | 2.535 | 16.0 | – | – |
| 8 | 0.655 | 50.4 | 1.082 | 31.8 | 1.547 | 23.8 | 1.961 | 20.4 | 2.380 | 18.4 | – | – | – | – |
| 9 | 0.594 | 41.1 | 1.008 | 18.4 | 1.483 | 9.3 | 1.902 | 5.5 | 2.327 | 3.5 | – | – | – | – |
| 10 | 0.572 | 39.3 | 0.986 | 15.5 | 1.463 | 6.2 | 1.961 | 1.9 | 2.225 | 0.6 | 2.492 | -0.3 | – | – |
| 11 | 0.549 | 38.1 | 0.965 | 13.5 | 1.445 | 4.0 | 1.943 | -0.3 | 2.342 | -2.1 | 2.741 | -3.2 | – | – |
| 12 | 0.531 | 37.2 | 0.947 | 12.2 | 1.427 | 2.7 | 1.928 | -1.7 | 2.433 | -3.9 | 2.743 | -4.6 | 3.053 | -5.1 |
| 13 | 0.526 | 36.9 | 0.945 | 11.8 | 1.425 | 2.2 | 1.925 | -2.2 | 2.433 | -4.4 | 2.741 | -5.1 | 3.051 | -5.6 |
| 14 | 0.536 | 36.4 | 0.950 | 11.0 | 1.433 | 1.3 | 1.933 | -3.0 | 2.334 | -4.9 | 2.733 | -5.9 | – | – |
| 15 | 0.546 | 36.2 | 0.958 | 10.6 | 1.438 | 0.9 | 1.941 | -3.5 | 2.207 | -4.8 | 2.474 | -5.8 | – | – |
| 16 | 0.556 | 36.3 | 0.965 | 10.8 | 1.443 | 1.1 | 1.864 | -2.8 | 2.291 | -4.9 | – | – | – | – |

**Note: Dimension and angles are based on offset configuration—lengths are also based on adjustment fitting geometry.**

The solution was to sandwich the surface cord and the end of the tieback cord between two 1.27-cm diameter 0.508-mm thick aluminum buttons (Fig. 6). The lower button had a 1.27-mm diameter hole drilled in the center so that the tieback cord could be threaded through the center. If a tieback cord should break, which they did too frequently, a new button would be bonded to the bottom. If the surface cord should break, a new surface cord segment, i.e., the piece of cord between two tie points, would be replaced by bonding a new button to the top.

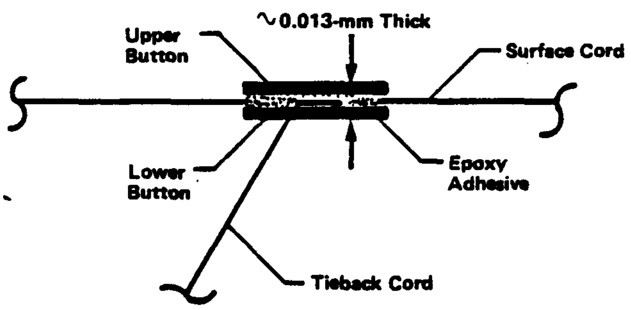


*Figure 6 Tie System Button Design*

## 2.2 FABRICATION OF THE REFLECTOR SURFACE

The fabrication of the reflector surface consisted of three basic steps: (1) stretch and mark the mesh; (2) install the edge catenaries; and (3) build the tie system.

### 2.2.1 Mesh Surface Fabrication

The mesh material is a tricot-knit, 0.003-cm diameter, gold-plated molybdenum monofilament wire mesh that has 5.5 openings/cm. The mesh has the desirable properties of high rf reflectivity, corrosion resistance, low weight, wrinkle resistance, low-spring rate, puncture resistance, and radiation resistance. Figure 7 shows the mesh knit. An 2.286 by 4.572-m wooden table was fabricated and used for stretching the mesh surface, installing the edge catenaries, and marking the tie point locations on the mesh. The vellum template locating the tie points, edge catenaries, and top of standoffs was placed over the table. The table was then covered with Mylar and all edges were smoothed with Mylar tape to minimize the friction between the mesh and the table.

ORIGINAL PAGE IS
OF POOR QUALITY

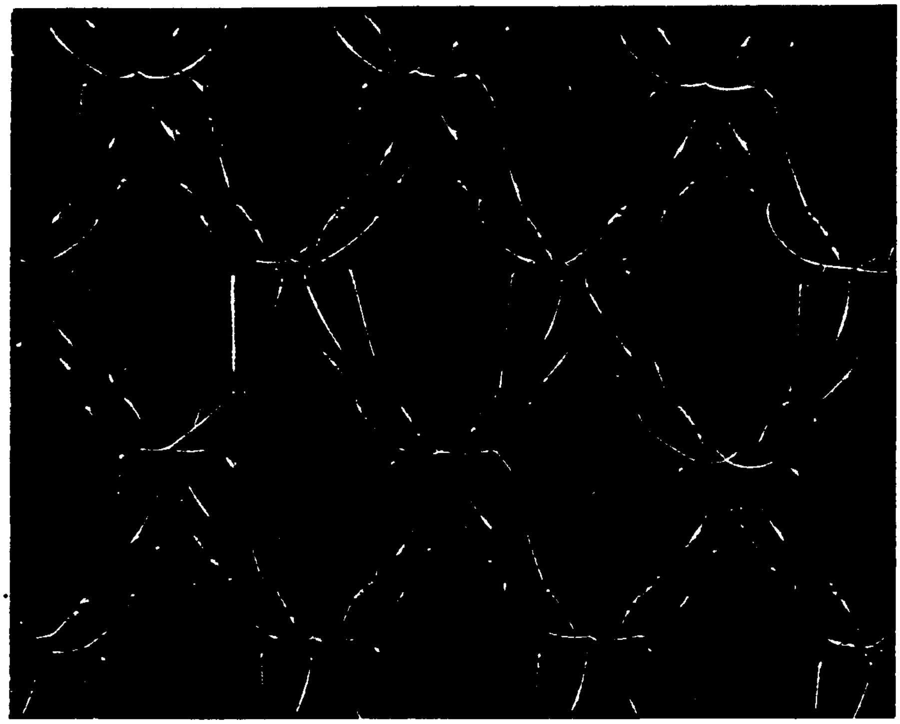

*Figure 7 Tricot Knit Weave*

Since one of the features to be demonstrated in this task was sewing seams in reflective mesh, a 0.61 by 1.219-m patch was sewn into one corner (Fig. 8). It was sewn to the main body of the mesh by first stretching the patch to the appropriate tension level, then applying 5.08-cm wide Mylar tape to the raw edges to be sewn. The same was done to the main body of the mesh surface. The taped edges were then pressed together with the mesh edges sandwiched in between. A hand held sewing machine using nylon sewing thread was then used to produce the final seam (Fig. 9). The tape edge was used as a guide to assure a straight seam. After the sewing was complete, the tape was removed and the excess mesh material was trimmed to approximately 0.6-cm. Because both pieces of mesh had been prestretched before being sewn, the seam did not need to stretch. The final result was an almost invisible seam that produced no apparent discontinuities in the surface.

Once the sewing process was complete, the entire mesh was laid on the stretching table with the material bias at 45 deg to the sides of the table (Fig. 8). The mesh was oversized, approximately 5.5 by 5.5 m, so that the mesh edges would overhang the table to allow for attachments of weights for stretching the mesh. A total of 540 weights, each being 45.5 grams, were hung 5.08 cm apart along the mesh periphery to produce a biaxial tension field in the mesh of approximately 0.088 N/cm. This higher biaxial tension field was used to compensate for gravity. However, the level was too high and caused the mesh to stretch to the point were it was no longer pliable. Therefore, each weight was reduced to 24 grams resulting in a biaxial tension field of approximately 0.046 N/cm. The table was then subjected to a vibration cycle. The vibration was induced by two Vibrolator air-driven motors powered by $6.895 \times 10^5$ N/$m^2$ nitrogen pressure. The vibration, coupled with the weights, caused the mesh to fully expand and remain under tension.

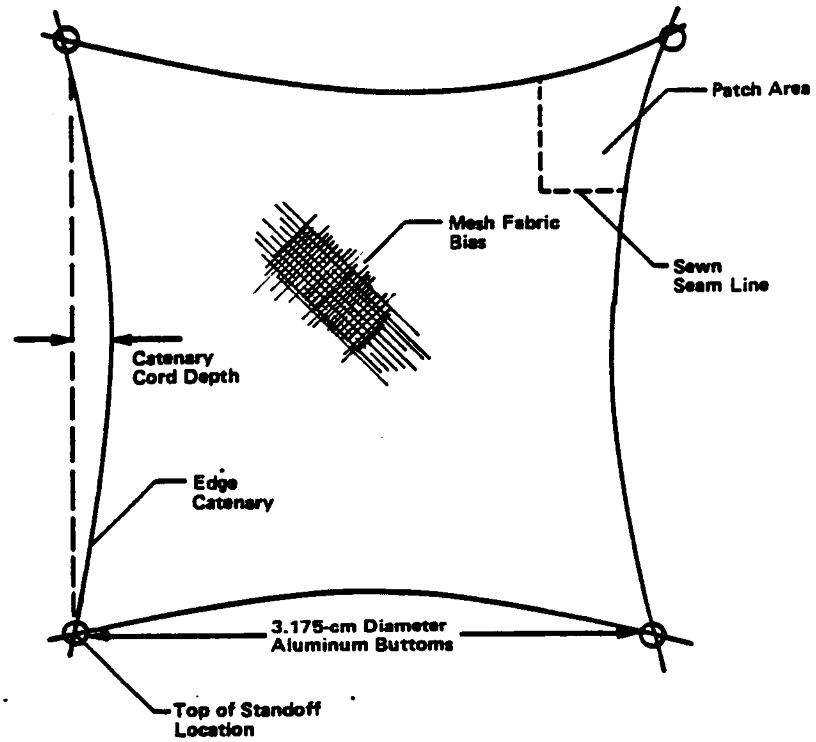


*Figure 8 Mesh Fabric*

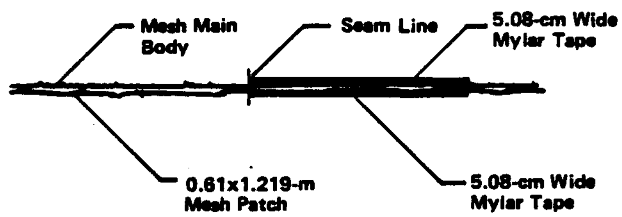


*Figure 9 Reflective Mesh Seam*

Next, catenary cords (12000 tow teflon-coated Celion graphite cord) were laid on the mesh per the template and whipstitched in place with standard black sewing thread using about a 2.5-cm loop. This was accomplished on half of the mesh at a time. The catenaries were then preloaded with approximately 13.6 kg, i.e., the force needed to react the biaxial tensioned mesh.

Once the catenary cords were in place and preloaded, a 3.175-cm diameter, 0.508-mm thick aluminum button was bonded to the mesh and each end of the catenary cord. The Teflon coating on the graphite cords was etched for bonding using Tetra-etch (Gore) and the bonding adhesive was Hysol EA934NA. The location of the buttons corresponded to the tops of the standoffs (Fig. 8). After bonding, a clearance hole was drilled in each button for mechanical attachment of the mesh surface to the top of the standoffs.

The final step was to mark the mesh for each tie point location by tying a black thread to the mesh at each location dictated by the template. The thread markings served as locators for pulling each tieback cord through the mesh during installation of the tie system onto the mesh surface.

2.2.2 Tie System Fabrication

The tie system was built using 3000 tow Celion Teflon-coated graphite cord and 0.508-mm thick by 1.27-mm diameter aluminum buttons. Using the lengths in Table 2, lines were drawn on the template, which connected the tie points along each surface cord and denoted the various angles required by the system (Fig. 10).

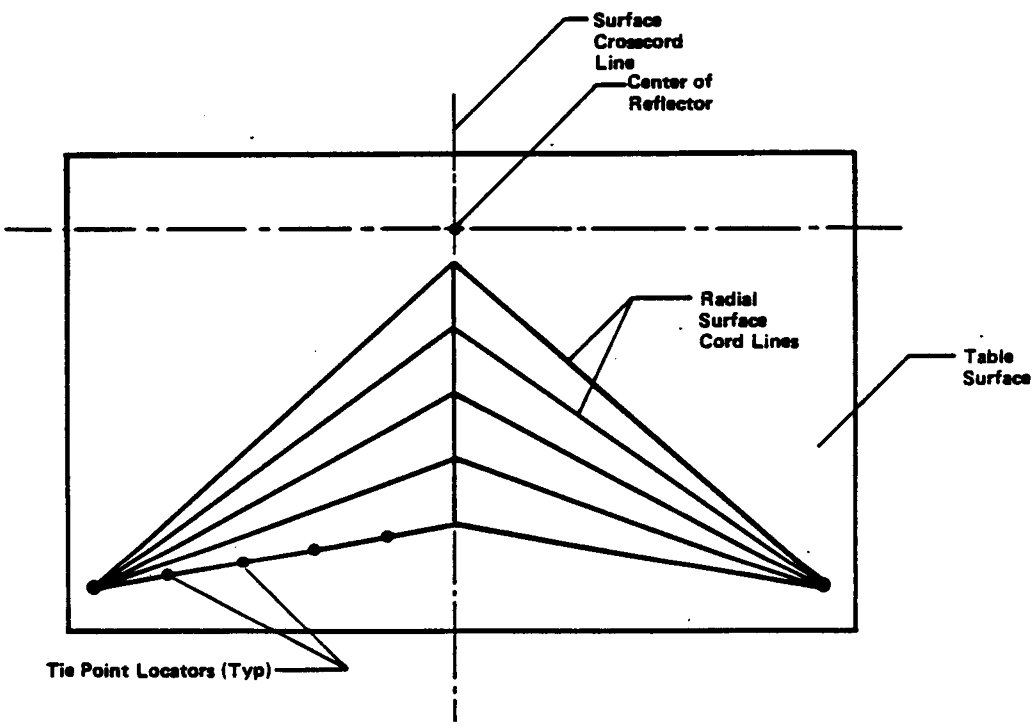


*Figure 10*
*Tie System Fabrication Table (½ of Tie System "Fishbone")*

The first operation involved cutting each tieback cord and surface cord to the proper length. Surface cord lengths were obtained from the template. Tieback lengths are found in Table 2. However, the tieback cords were cut 30-cm oversize.

The next step involved attaching each tieback cord to its corresponding radial surface cord. This was accomplished by first taping the radial surface cord onto the template. Then, at each tie point, a single tieback cord was threaded through an aluminum button with a hole. The tieback and radial surface cord were then sandwiched between a top and bottom button. They were bonded with Hysol EA934NA epoxy adhesive and cured for 16 hours minimum at room temperature using a deadweight system. The tieback cords were bonded at the appropriate angle to the surface cords, shown in Table 2, to assure that when pulled they would not have to bend at the attachment point.

After all the tieback cords had been bonded to the 40 radial surface cords, the surface cross cords were laid on the template and the two radial surface cords and two tieback cords were bonded at the appropriate locations. The radial surface cords were bonded to the surface cross cords at the appropriate angle to minimize any bending of the cord at the attachment point.

Before bonding, the bond area of all the buttons was grit blasted and primed with BR127 epoxy primer. The primer was cured at 250°F ± 10°F for 30 to 60 minutes. The Teflon coating on the graphite cords was etched with Tetra-etch for bonding at each of the tie point locations.

The end result was a pair of "fishbone" surface cord assemblies, the X set and Y set with respect to the reflector coordinate system. When the adhesive was cured, each "fishbone" was individually rolled on separate 7.6-cm diameter spools for simplified handling and transportation.

### 2.2.3 Box Truss Standoffs and Tie Cord Adjustments

Before the reflector could be installed on the box truss, the standoffs and tieback cord adjustment mechanisms needed to be designed and built. The height of each standoff was chosen to be 0.5715 m (22.5 in.). This value was calculated as the optimum standoff height by the Mesh Tie System Generator (Ref 1). Included in the 0.5715-m standoff length was an adjustment fitting to allow adjustment of each tieback cord.

Tieback Cord Adjustment Hardware--The tieback cord adjustment hardware consisted of two components: pairs of 0.3175-cm (1/8-in.) diameter coarse adjustment tubes and 2-56 fine adjustment set screws, one pair per tieback cord (Fig. 11), and an adjustment fitting made up of aluminum angle, one per standoff (Fig. 12).

The coarse adjustment tubes are 5.715-cm long 304 stainless tubing. The OD of the tube was threaded with a 6-32 die to establish a grip area for the O-ring stop (Fig. 11). The coarse adjustment tube adapted to the adjustment fitting (Fig. 13). The clearance holes drilled in the aluminum angle allowed the tubes to move their full length in the adjustment fitting. Since the tieback cords were under low tension when the mesh was in a properly configured paraboloid, O-ring stops were suffi- cient to prevent the coarse adjustment tubes from pulling out of the adjustment fitting. The O-ring size was 2-004 (type Buna 71).

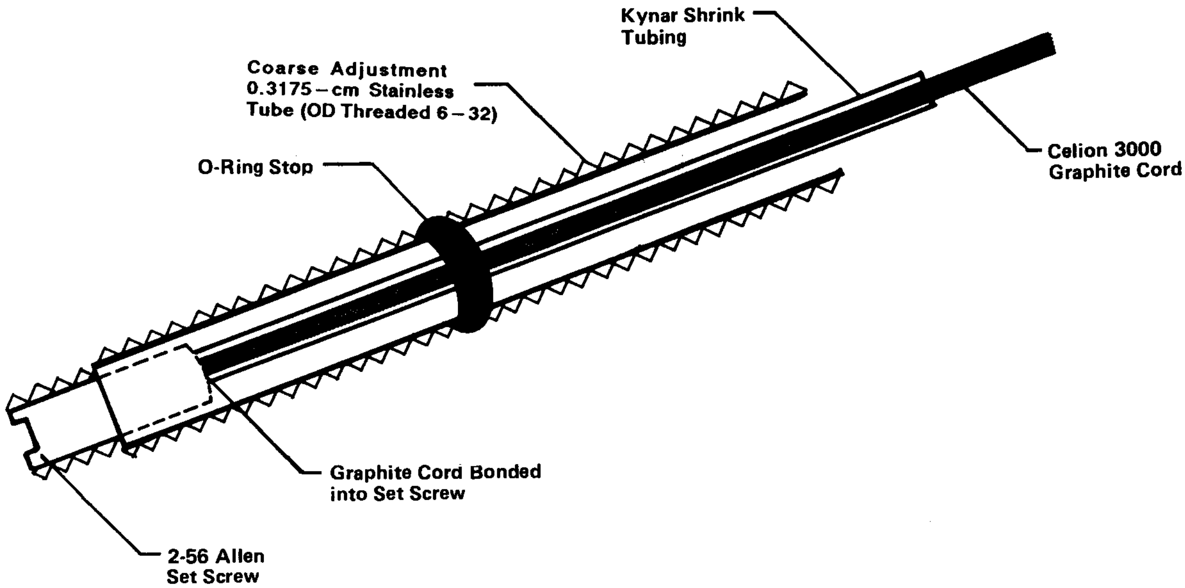


*Figure 11 Tieback Cord Adjustment Hardware*

The fine adjustment, 2-56 allen set screws, are 0.64-cm long and screw inside the outer end of the coarse adjustment tube. The inside end of the allen screw contained a 0.102-cm diameter hole into which the graphite tieback cord was bonded, using Shell EPON 828 resin with 10% of diethylene triamine (DETA) catalyst. The graphite cord was etched with Tetra-etch to remove the Teflon coating before bonding. The fine adjustment yields ± 1.78-mm of movement at the mesh tie points.

The area of the graphite cords, which was located inside of the coarse adjustment tubes, was protected from fraying by heat shrinkable tubing (Kynar 0.119-cm diameter).

The adjustment fitting was fabricated from 0.635-cm (1/4-in.) thick aluminum angle and had 8.15-cm legs. Each side of the angle had 27 holes, each drilled at a compound angle. The holes were drilled at compound angles to accept the coarse adjustment tubes. The drilling was accomplished using a milling machine with a two-axis tilt head. Each hole location was marked on the outside faces of the angle with a height gage. The angle was then placed in the mill. Each hole was started with a 0.635-cm (1/4-in.) starter drill and drilled to 0.3175-cm (0.125-in.) with a 0.3175-cm (1/8-in.) bit and reamer. This allowed a slide fit for the coarse adjustment tube.

<u>Box Truss Standoffs</u>--The overall standoff assembly is presented in Figure 14. The assembly was constructed from aluminum plate, 3.81-cm (1.5-in.) aluminum tubing, and 0.635-cm (1/4-in.) mild steel plate.

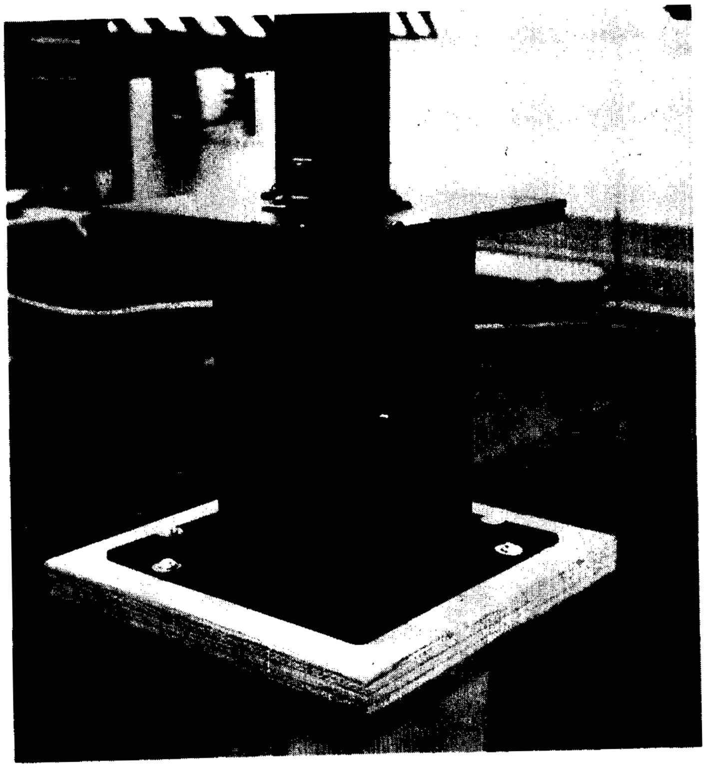

Outside View

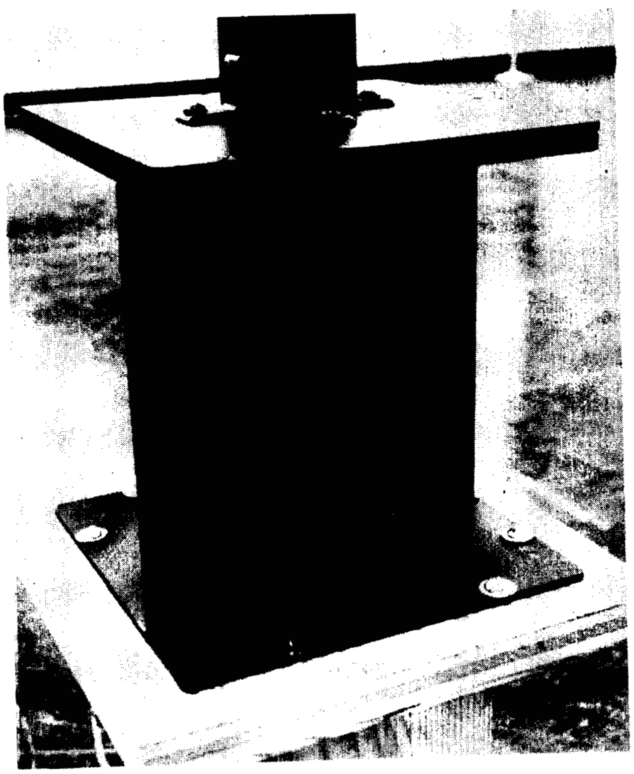

Inside View

*Figure 12 Aluminum Adjustment Fitting*

ORIGINAL PAGE IS
OF POOR QUALITY

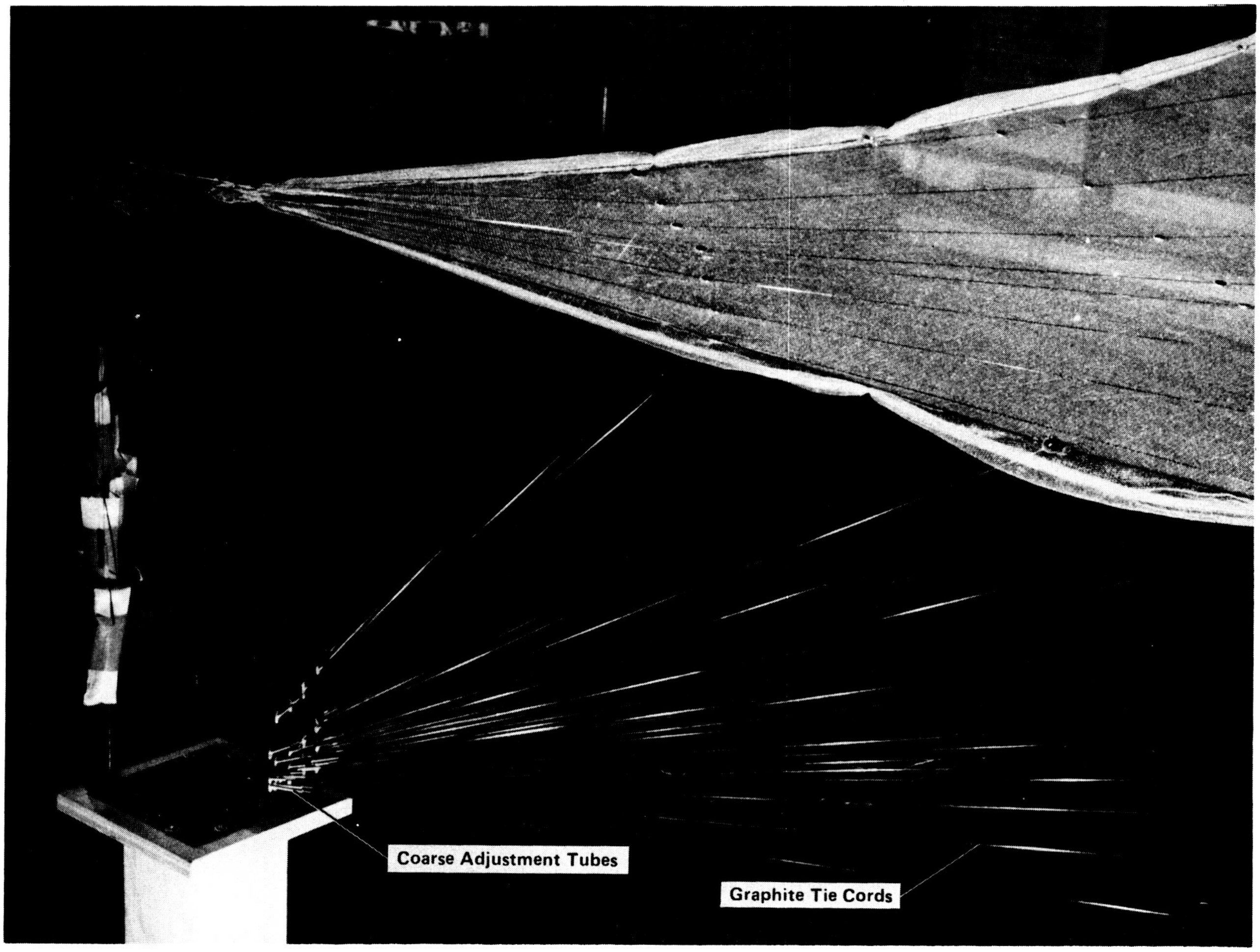


*Figure 13 Attachment Fitting with Adjustment Hardware Installed*

The mesh attachment plates were tilted 22 deg toward the reflector center on the upper standoffs and the lower standoffs were tilted 10 deg towards each other. This closely approximated the curvature of the paraboloid at the top of the standoffs and allowed the mesh surface to assume the paraboloidal shape without having to bend over a shape edge. The 3.175-cm aluminum discs were mechanically attached to the mesh attachment plates with 6-32 screws. The notches at the radius of the mesh attachment plates were guides for the surface cords and their weights. All plates were attached to the 3.81-cm (1.5-in.) square tubes with aluminum angles and screws.

The 0.3175-cm (1/8-in.) flat plates provided both load transfer into the graphite truss and bending stability. The 0.635-cm (1/4-in.) steel plate was needed for more rigidity since the 3.81-cm (1.5-in.) tube did not extend through the adjustment hardware box (Fig. 12). This was done to allow greater access to the adjustment screws. Figure 12 also shows a stability leg opposite of the adjustment fitting.

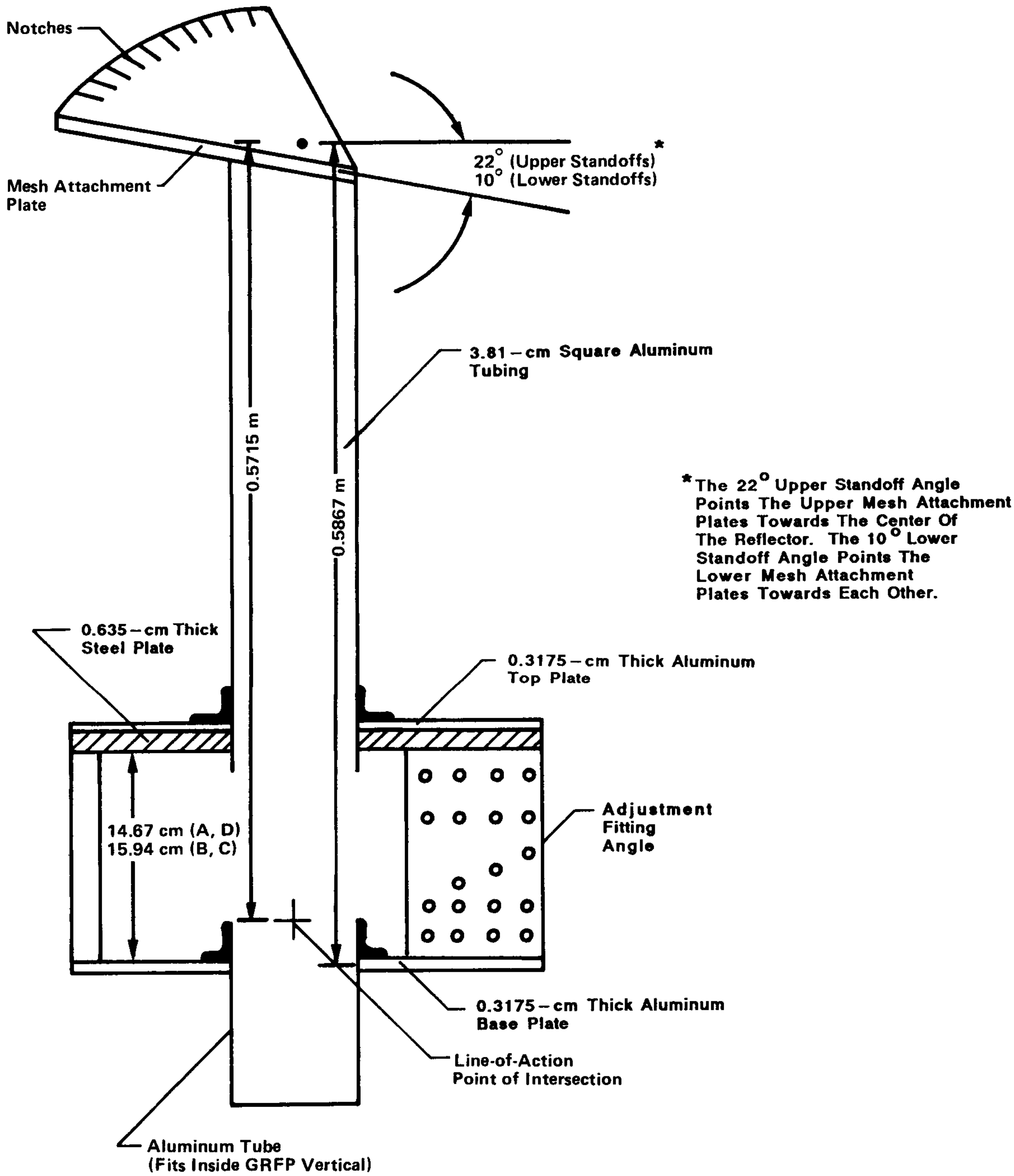


*Figure 14 Standoff Assembly*

The most critical dimension of the standoff assembly was the 0.5715-meter from the attachment point of the mesh to the point of intersection of the tieback cords (Fig. 14). This lines-of-action intersection point was 1.524-cm above the base plate to gain more clearance for the coarse adjustment tubes. The adjustment fitting aluminum angle varied from 14.67-cm high for the upper standoff assemblies to 15.94-cm for the lower standoffs. The aluminum tube below the base plate was machined to 3.49-cm to allow for a slip fit into the top end of the square tube vertical member of the graphite truss.

ORIGINAL PAGE IS
OF POOR QUALITY

## 3.0 INTEGRATION OF REFLECTOR AND SURFACE SETTING

Integration of the reflector onto the box truss and setting the surface was completed in two main steps. First, the mesh and tie system were assembled onto the standoffs and the surface initially set with the standoffs installed in ground level wooden stands. Then the standoffs were installed in the box truss and a final surface setting was completed. This two-step process was used so no major scaffolding was needed to mate the tie system to the mesh or to set the surface.

## 3.1 WOODEN STANDS FOR MESH ASSEMBLY

Wooden positioning stands were fabricated to support the standoffs during the mating process of the tie system to the mesh fabric. They consisted of a 2.54-cm (1-in.) plywood base with four leveling screws, a tower made from 2x4 lumber and supported with pine gussets, and a 1x6 pine top plate with a centered square hole to which the standoffs were bolted for support.

A pair of support boxes were fabricated to elevate the upper standoffs 0.97-m higher than the lower standoffs. They were constructed from 2.54-cm (1-in.) plywood with access holes for weights and manipulation of the four leveling screws (Fig. 15).

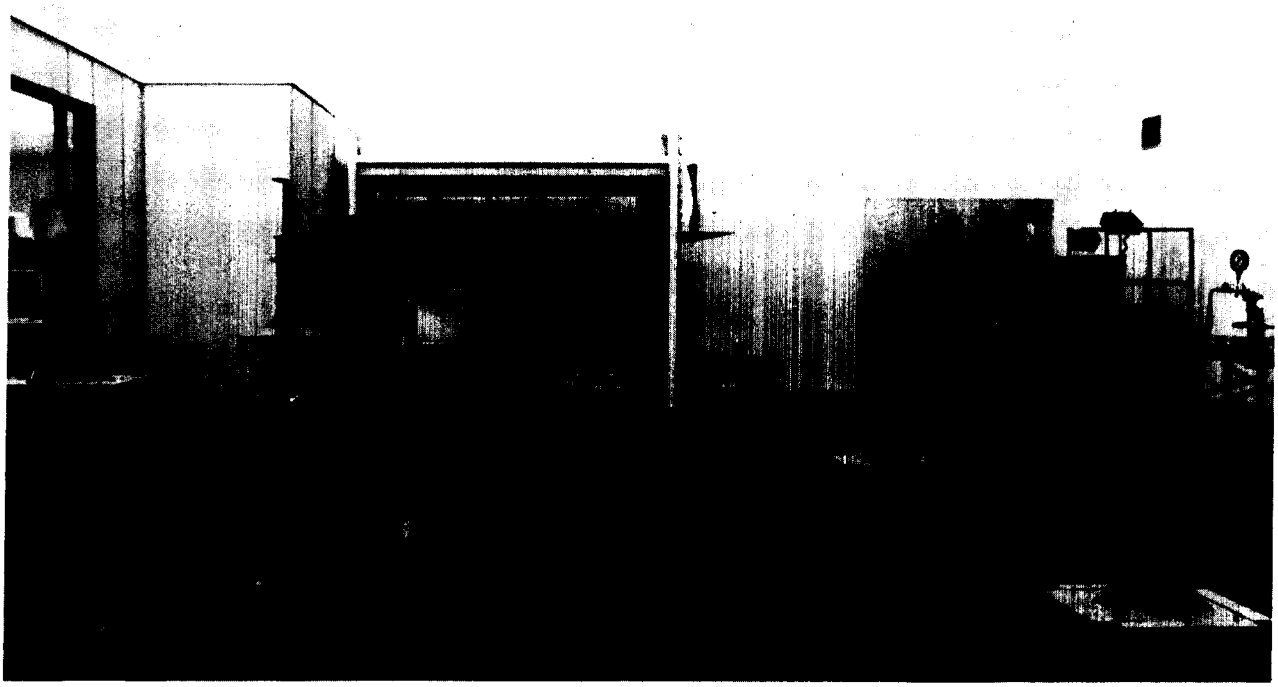

*Figure 15 Wood Stands and Standoffs*

The wood stands were positioned with the aid of a surveyor's transit. The stands were first leveled and then raised or lowered to bring the two lower stand top plates into the same plane. The upper stands were then adjusted to the same plane and 0.97- m higher than the lower top plate plane. This configured the standoffs for a 12.53-deg skew of the box truss (Fig. 4).

The standoffs were then adjusted to meet dimensional requirements. A standard tape measure was used for locating distances. The standoffs were set for 4.572-m between the upper set of two. Adjustments were made for obtaining a distance of 4.569-m between lower and upper standoffs on the 12.54 deg angle and 4.466-m between lower and upper standoffs in the horizontal plane. Diagonally, the setup measured 6.464-m from upper standoff to lower standoff.

## 3.2 INSTALLING THE MESH AND TIE SYSTEM ONTO THE STANDOFFS

The mesh fabric was installed on the corner fittings by mechanically attaching the 3.175-cm aluminum discs to the standoff top plates with a 6-32 screw. Next, the mesh was released from the two lower standoffs and carefully folded back so that one of the tie system's "fishbone" assemblies could be installed starting at the upper side and working down. The tieback cords were threaded through the mesh fabric at the premarked locations denoted by the black thread. As the tie system was installed the mesh was pulled back into place until finally all tieback cords were through the mesh and the mesh was reattached to the standoffs. The same approach was used to install the second "fishbone" assembly only this time the mesh was released from one upper and one lower standoff. Figure 16 shows the reflector surface installed on the standoff before installing the tieback cords into the adjustment fitting.

When the installation was complete, the tieback cords were then cut to the required lengths (Table 2), the ends prepared for bonding with Tetra-etch and the adjustment hardware was bonded to the tie cord ends as previously described in Subsection 2.2.3. The tieback cords were mated with the standoff adjustment fitting by inserting the coarse adjustment tube into the appropriate hole in the angle. A 113.4-gram weight was suspended from each of the surface cords to assure the preload in each cord was equal to the tension of the mesh.

At this point, two problems occurred. First, the 10.16-cm deep catenaries that were originally installed for the center-fed configuration could not be pulled down into shape for the offset reflector without creating extremely high tension levels in the catenaries . Second, the tieback cords going to the upper standoffs were slack and the tieback cords going to the lower standoffs were extremely tight, i.e., it appeared the entire tie cord system was positioned too far toward the upper standoffs.

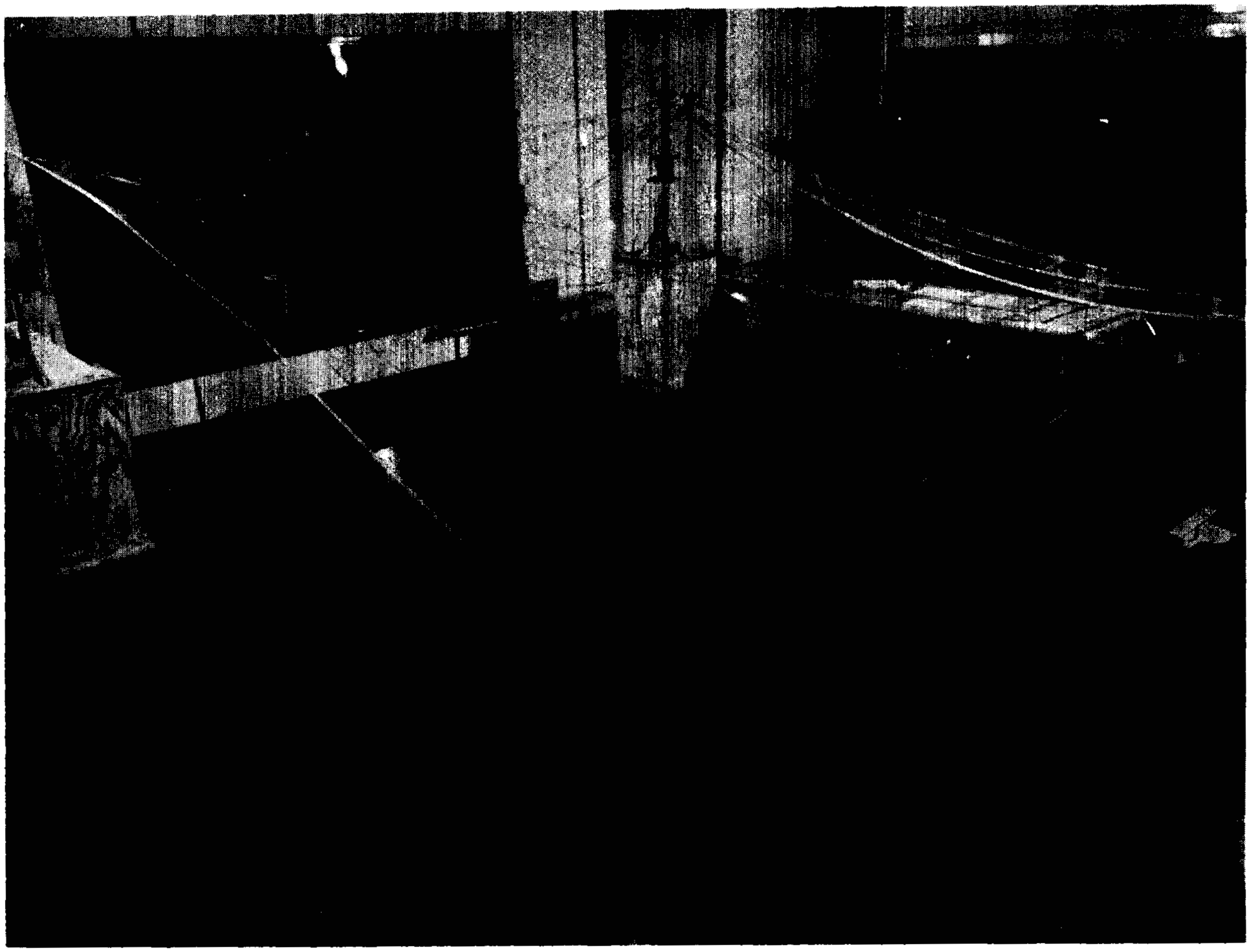

*Figure 16 Reflector Surface before Tie System Tensioning*

To fix the catenaries, new catenary cords were sewn into place at a nominal 30.5-cm depth using a tighter whipstitch loop to provide more uniform mesh tension. Since catenary tension is inversely proportional to the depth, changing the edge catenary depth from 10.16 to 30.5 cm lowered the catenary pretension level to a manageable level. The new catenary depth of 30.5 cm was chosen using engineering judgment. Also, since the actual distance between tops of standoffs, i.e., the distance along the paraboloid, had increased going from the center-fed to offset fed configuration, the mesh tension had increased and therefore needed to be reduced. This was accomplished by drilling new attachment holes in the standoff top plates. The 3.175-cm aluminum discs were each moved 1.0-cm toward mesh center.

This change had several effects:

1) The catenary depth changed from 31.24 to 33.53 cm;

2) The diagonal mesh dimension changed from 6.454 to 6.450 m;

3) The gravitational droop at mesh center changed from 8.9 to 15.24 cm.

To verify that the change had reduced the mesh tension to the proper level, the approximate droop in the center of the reflector was hand calculated. The result showed that at 0.0464 N/cm, the mesh should sag 14.48 cm, close to the 15.24 cm measured.

To fix the tie system, it was necessary to relocate all the tie points on the mesh surface. Again, the problem occurred because of the change in configuration. For the upper half of the reflector, which is further up on the paraboloid in the offset configuration, the distance between any single tie point and the bottom of the standoff had decreased. The opposite was true for the lower half of the reflector. Therefore, new tie point locations were approximated and the mesh was marked to identify each new position. The location changes are presented in Table 3. Overall, the tie system was moved approximately 6.4 cm toward the lower standoffs. When the tie system was inplace, the tieback cords were again inserted into the adjustment fitting. The lengths appeared to be acceptable. However, when the tieback cords were drawn into tension and the mesh surface began to assume a parabolic shape, some of the surface cords remained slack. The solution to this problem required a third and final tie system relocation.

*Table 3 Tie Point Location Change*

| Tie Point | Delta, cm | Tie Point | Delta, cm | Tie Point | Delta, cm | Tie Point | Delta, cm |
|---|---|---|---|---|---|---|---|
| B&C 1-1 | 1.346 | B&C 1-2 | 2.697 | A&D 9-1 | 1.346 | A&D 9-2 | 2.697 |
| B&C 1-3 | 4.054 | B&C 1-4 | 5.202 | A&D 9-3 | 4.054 | A&D 9-4 | 5.202 |
| B&C 1-5 | 6.350 | B&C 2-1 | 1.247 | A&D 10-5 | 6.350 | A&D 10-1 | 1.247 |
| B&C 2-2 | 2.502 | B&C 2-3 | 3.759 | A&D 10-2 | 2.502 | A&D 10-3 | 3.759 |
| B&C 2-4 | 5.019 | B&C 2-5 | 5.685 | A&D 10-4 | 5.019 | A&D 10-5 | 5.685 |
| B&C 2-6 | 6.350 | B&C 3-1 | 1.130 | A&D 10-6 | 6.350 | A&D 11-1 | 1.130 |
| B&C 3-2 | 2.266 | B&C 3-3 | 3.404 | A&D 11-2 | 2.266 | A&D 11-3 | 3.404 |
| B&C 3-4 | 4.547 | B&C 3-5 | 5.448 | A&D 11-4 | 4.547 | A&D 11-5 | 5.448 |
| B&C 3-6 | 6.350 | B&C 4-1 | 1.011 | A&D 11-6 | 6.350 | A&D 12-1 | 1.011 |
| B&C 4-2 | 2.032 | B&C 4-3 | 3.053 | A&D 12-2 | 2.032 | A&D 12-3 | 3.053 |
| B&C 4-4 | 4.077 | B&C 4-5 | 5.103 | A&D 12-4 | 4.077 | A&D 12-5 | 5.103 |
| B&C 4-6 | 5.725 | B&C 4-7 | 6.350 | A&D 12-6 | 5.725 | A&D 12-7 | 6.350 |
| B&C 5-1 | 0.955 | B&C 5-2 | 1.915 | A&D 13-1 | 0.955 | A&D 13-2 | 1.915 |
| B&C 5-3 | 2.875 | B&C 5-4 | 3.840 | A&D 13-3 | 2.875 | A&D 13-4 | 3.840 |
| B&C 5-5 | 4.808 | B&C 5-6 | 5.624 | A&D 13-5 | 4.808 | A&D 13-6 | 5.624 |
| B&C 5-7 | 5.984 | B&C 6-1 | 0.813 | A&D 13-7 | 5.984 | A&D 14-1 | 0.813 |
| B&C 6-2 | 1.631 | B&C 6-3 | 2.457 | A&D 14-2 | 1.631 | A&D 14-3 | 2.451 |
| B&C 6-4 | 3.274 | B&C 6-5 | 3.924 | A&D 14-4 | 3.274 | A&D 14-5 | 3.924 |
| B&C 6-6 | 4.572 | B&C 7-1 | 0.622 | A&D 14-6 | 4.572 | A&D 15-1 | 0.622 |
| B&C 7-2 | 1.247 | B&C 7-3 | 1.872 | A&D 15-2 | 1.247 | A&D 15-3 | 1.872 |
| B&C 7-4 | 2.499 | B&C 7-5 | 2.832 | A&D 15-4 | 2.499 | A&D 15-5 | 2.832 |
| B&C 7-6 | 3.162 | B&C 8-1 | 0.373 | A&D 15-6 | 3.162 | A&D 16-1 | 0.373 |
| B&C 8-2 | 0.747 | B&C 8-3 | 1.120 | A&D 16-2 | 0.747 | A&D 16-3 | 1.120 |
| B&C 8-4 | 1.120 | B&C 8-5 | 1.755 | A&D 16-4 | 1.120 | A&D 16-5 | 1.755 |

ORIGINAL PAGE IS
OF POOR QUALITY

The approach used required that the tie system be isolated from the mesh fabric. First, the tieback cords were released from the adjustment fitting. Then, each surface cord had a 113.4-gram weight suspended from its termination end at the standoff. This placed the entire surface cord system into tension and resulted in the surface cords moving upward, suspended above the mesh surface. This positioned all the surface cords in one flat plane, above and isolated from, the mesh surface. The fabric was also in a static state under tension and free from any surface cord influence.

At this point, the surface cross cords were aligned to the center of the mesh surface in the offset direction and aligned in the other direction to be perpendicular. The system was now prepared to relocate the tieback cord positions. The tieback cords were extracted from the mesh individually and reinserted through the mesh at a point directly below the tie point and in plane with the mesh surface.

After all the tieback cords were through the mesh, they were inserted into the adjustment fitting and held in place with the O-ring stops. This caused the mesh to be drawn into a roughly paraboloidal shape and placed the surface cords into proper tension. Figure 17 shows the final reflector integrated on the standoffs. The next step was to set the surface.

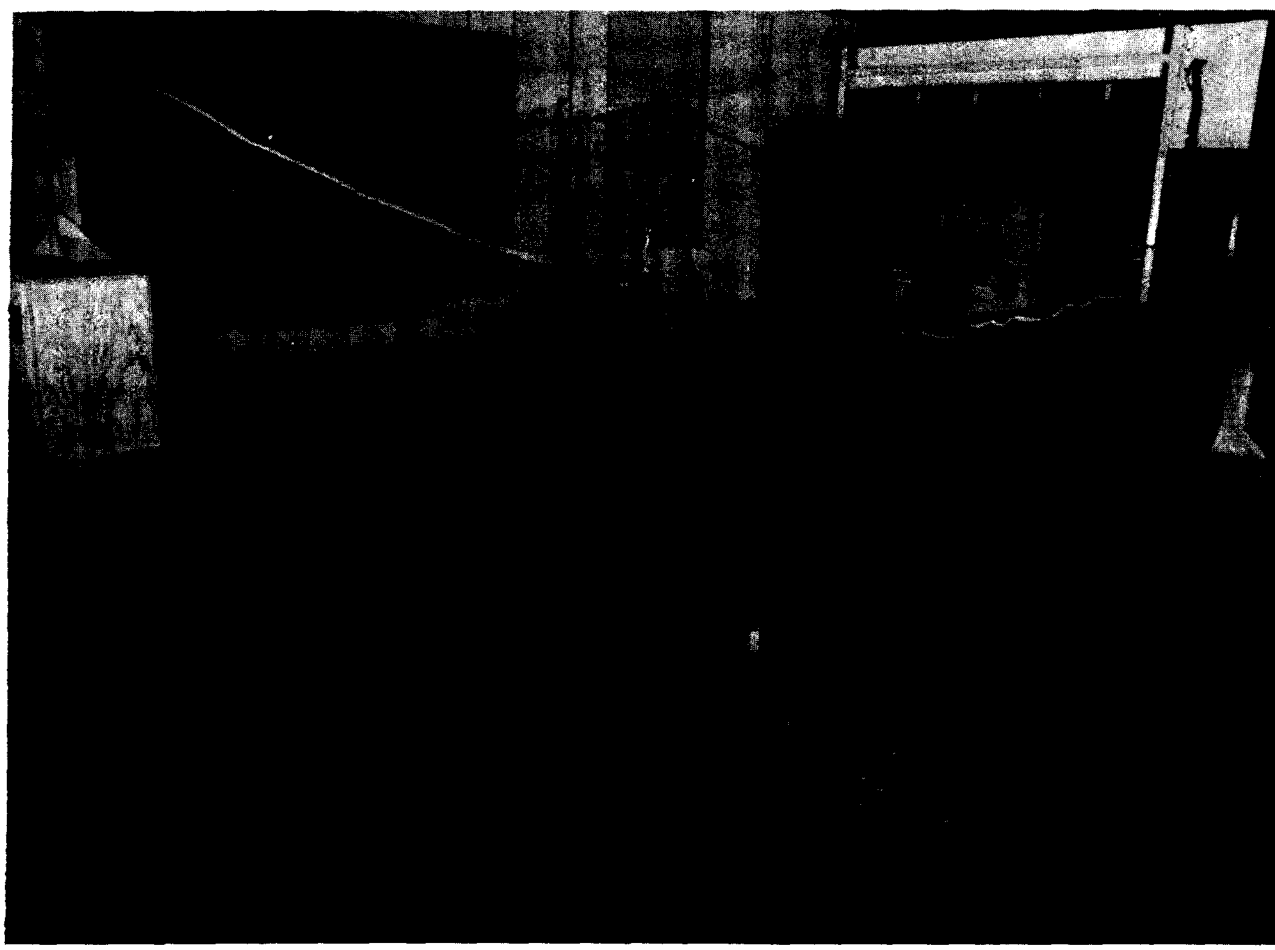

*Figure 17 Reflector Surface with Tie System Installed and Tensioned*

## 3.3 AIMS THEODOLITE MEASURING SYSTEM

Before actual adjustment of the mesh surface, an initialization of the theodolite system was compulsory. The theodolite system was a K&E (Keuffel & Esser) AIMS-R/T (real-time measuring system). It was comprised of two encoder-type optical theodolites with portable base stands. The theodolites were linked to a computer/video monitor that contained the capability of performing parabolic functions.

The theodolite system initialization involved:

1) Theodolite coarse and electronic leveling;

2) Pointing both theodolites at a common azimuth reference;

3) Pointing the theodolites at each other to give the computer the location of each theodolite;

4) Entering into the computer a scale factor of 68.00 in. by pointing the theodolites at the 1-in. and 69-in. marks on a calibrated scale;

5) Pointing the theodolites at reference targets on each lower standoff of the mesh assembly;

6) Entering into the computer the X, Y, and Z coordinates (in in.) of the zero point of the parabola;

7) Entering into the computer the coordinate dimensions of five points of the parabola (in in.), which are minus X, plus X, zero, plus Y, and minus Y;

8) Setting up the computer stack sequence by pointing the theodolites at five imaginary points that simulate the previously entered coordinate dimensions;

9) Using a function key that allows the computer to calculate the theoretical parabola from the input and theodolite data.

The theodolite system required reinitializing approximately every 2 days because of error accumulation from handling and floor movement.

## 3.4 COARSE ADJUSTMENT OF MESH SURFACE

After theodolite initialization, coarse adjustment of the mesh surface was begun. The technique proceeded by pointing the theodolites at each target, i.e., a tie point button twice. First in the direct mode and next in the reverse mode. The two measurements are automatically averaged by the computer to reduce the pointing error by half. To assure that each theodolite operator was pointing at the same target, each tie point was identified with a label generated from Figure 5.

Except for the tie points along the surface cross cords, the labeling was based on the standoff letter, the radial surface cord number, and a dash number. For example, target C5-1 is the first tie point out from the "C" standoff along the number 5 radial surface cord. C5-6 would be the sixth tie point out from the same standoff along the same radial surface cord. For the tie points along the surface cross cord, the label was based on the standoff letters and a dash number, i.e., AD-1 is the first tie point on the surface cross cord between standoffs "A" and "D." The parabolic function was calculated and the results were displayed on the monitor. The display included the pointing error of the theodolites (X.XXXX in.) and the deviation from the required paraboloid, either plus or minus (X.XXXX in.).

The tie point being measured was then adjusted up or down (plus or minus) to within 0.254 cm of the paraboloid. This was achieved by moving the coarse adjustment tube (Fig. 11) either in or out of the standoff adjustment hardware angle. The O-ring stop was repositioned accordingly to prevent the adjustment tube from being pulled free from the angle while under tension.

The tie points were adjusted in a circular pattern beginning at the center of the reflector. The center four points were adjusted first (AB-4, BC-4, CD-4, and AD-4). The -6 points were adjusted next, one quadrant at a time (C4-6, C5-6, D4-6, D5-6, etc). Next, -5s were adjusted for each quadrant, then -4s and so on, until all points, including catenaries, were coarse adjusted to within 0.254 cm from theoretical parabola.

## 3.5 FABRICATION OF STEEL DIAGONALS

Before the reflector was installed on the box truss, two sets of equal length graphite diagonals were replaced with unequal lengths to skew the box truss into the offset fed configuration (Fig. 4). Without enough lead time to order new graphite material and to keep costs down, the graphite diagonals were replaced with steel cable and aluminum end fittings. Each set of steel diagonals were required to be two different lengths, 5.675 m for the shorter diagonal and 7.055 m for the longer diagonal. The aluminum end fittings were of similar design as the graphite end fitting they replaced (Fig. 18).

The assembly of the diagonals involved a tool that consisted of two flat aluminum plates each having a vertical 0.318-cm diameter pin protruding from its center. Two tools of this type were fabricated. The plates were positioned on a work table with the pin-to-pin distance being 5.675 m for the shorter set of diagonals and 7.055 m for the longer set. The steel cables were bonded to end fittings on one end only. After grit blast, the end fittings were positioned on the 0.318-cm tool pins. The steel cables were extended through the second set of end fittings and draped over the end of the work table with a 6.8 kg preload weight attached. The second end fittings were bonded in this configuration.

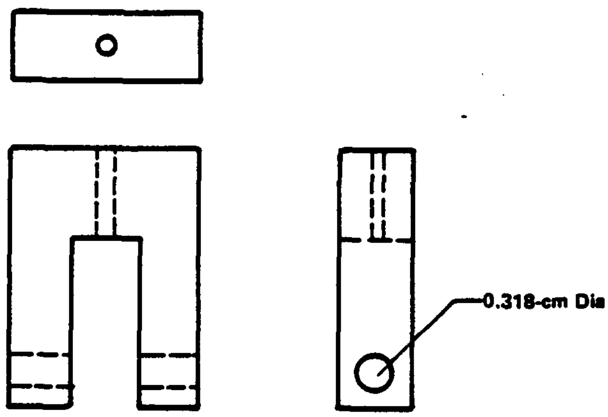


*Figure 18 Diagonal Assembly End Fitting*

## 3.6 INSTALLATION ONTO THE BOX TRUSS

Installation was started by attaching two of the mesh standoffs to the truss vertical members after the truss had been set on its side and fully opened in the nonskewed direction. The truss was then slowly deployed in the skewed direction using a hoist and sling to control the truss level for an even deployment. At three-quarters deployment, the two remaining standoffs were attached to the truss vertical members. The deployment was then completed by locking all the box-truss midlink hinges in the deployed position.

At the final stage of deployment, eight of the center tieback cords broke. The probable cause for the breakage was the fact that the graphite truss was not as flexible as the wooden stands used for the mesh/tie system assembly. The wooden stands had allowed the tops of the standoffs to move diagonally 1.27 cm. The graphite truss moved far less, and therefore, caused the entire tie system to rise which over tensioned the graphite tieback cords.

To compensate for the difference in movement, the 3.175-cm aluminum discs at the corners of the mesh were moved diagonally towards the mesh center approximately 0.635 cm. Also, 0.318-cm thick aluminum shims were installed between the outer edge of the graphite corner fittings and the standoffs. This tilted the standoffs toward mesh center. This was still not enough movement, and therefore, the center of the reflector was still under too much tension. This made it necessary to move the four center tie point locations outward by increasing the length of the surface cross cords between the tie points by approximately 1.9 cm for each point (AB-4, BC-4, CD-4, AD-4, Fig. 5). The broken tieback cords were repaired and the truss assembly was turned upright. The four truss corners were leveled in the skewed position with the lower surface tube at 12.54 deg with reference to the floor. Leveling was achieved with a surveyor's transit; the upper standoffs were 0.97-m above the lower standoffs with reference to level.

The theodolites were initialized per the process, which was discussed previously. Approximately 25% of the O-ring stops needed to be replaced because of excessive wear from the coarse adjustment process. The mesh surface tie points were adjusted per the previously discussed procedure with a goal of ± 0.16 cm from the theoretical paraboloid. The adjusting sequence did not follow a circular pattern. Instead, each quadrant was adjusted individually beginning with the tie points at the mesh center and adjusting one arc row at a time working towards the quadrant corner. The quadrant sequence was A, C, D, and B. Interaction between tie points did not appear to be a major factor. The majority of adjusting required the fine adjustment screw versus the coarse adjustment tube.

After each point was set, procedures called for each point to be retargeted by the theodolite system. However, schedule constraints did not permit this verification process. Instead, random tie points were retargeted to verify that the ± 0.16-cm tolerance had been achieved. After verification, the coarse tubes were locked in place with a drop of silicone adhesive. The surface cords were isolated from the 113.4-gram weights by a locking plate that was attached to the standoff top plate. This sandwiched the surface cords between the standoff top plate and the locking plate, which terminated further surface cord movement.

This Page Left Intentionally Blank

## 4.0 VERIFICATION OF REFLECTIVE SURFACE

The verification of the reflective surface required that the surface be photogrammetrically measured and the results be analyzed to determine the best-fit paraboloid. From these two operations the actual rms manufacturing error and rms pillowing error were determined.

Since there has always been some concern that deployable tension stabilized mesh reflectors would change shape once they have been set, stowed, then deployed, i.e., repeatability, the verification process was performed twice. First, immediately following the theodolite surface setting, and again, after the reflector had been partially stowed and redeployed. Both sets of results are presented.

### 4.1 PHOTOGRAMMETRIC MEASUREMENTS

The photogrammetric measurements of the surface were performed by Dick Adams of NASA Langley Research Center at Martin Marietta's facility. To take the photographs, each tie point button had a special reflective target installed on the top. This target was actually installed at the time the tie system was being built. In addition, two sections of mesh bound by tie points were targeted every two inches. These targets were used later to determine the extent of mesh pillowing.

Each target was referenced by a number in order for the photographs to be analyzed by Geodetic Services, Inc of Melbourne, FL. Figures 19 shows the numbering of the tie points and the mesh targets. In addition, twelve of the targets were marked with special target numbers. The targets, along with the location of these targets according to the theodolite measurements, enable Geodetic Services to transform the photographed coordinates of each tie point into the reflector coordinate system. Figure 19 shows the location of the 12 points. Table 4 gives the theodolite coordinates used for the transformation.

Taking the metric camera measurements required that the camera be positioned at six different clock angles around the reflector and remain at a fixed distance (~4.88-m) above the plane of the reflector. To achieve this requirement, the box truss was laid flat on the floor (Fig. 20). Figure 21 shows the six camera positions relative to the box truss.

The first set of pictures took Dick Adams a day to shoot and develop. After he verified that the photos were good, the truss was set upright and partially stowed. Since the contract schedule did not permit full stowage, the box truss was stowed in both directions about 1 to 1.25 m. This totally relaxed the reflector surface and allowed the surface to realign itself if necessary. Then the truss was redeployed, again laid flat on the floor and the second set of photographs were taken.



PRECEDING PAGE BLANK NOT FILMED

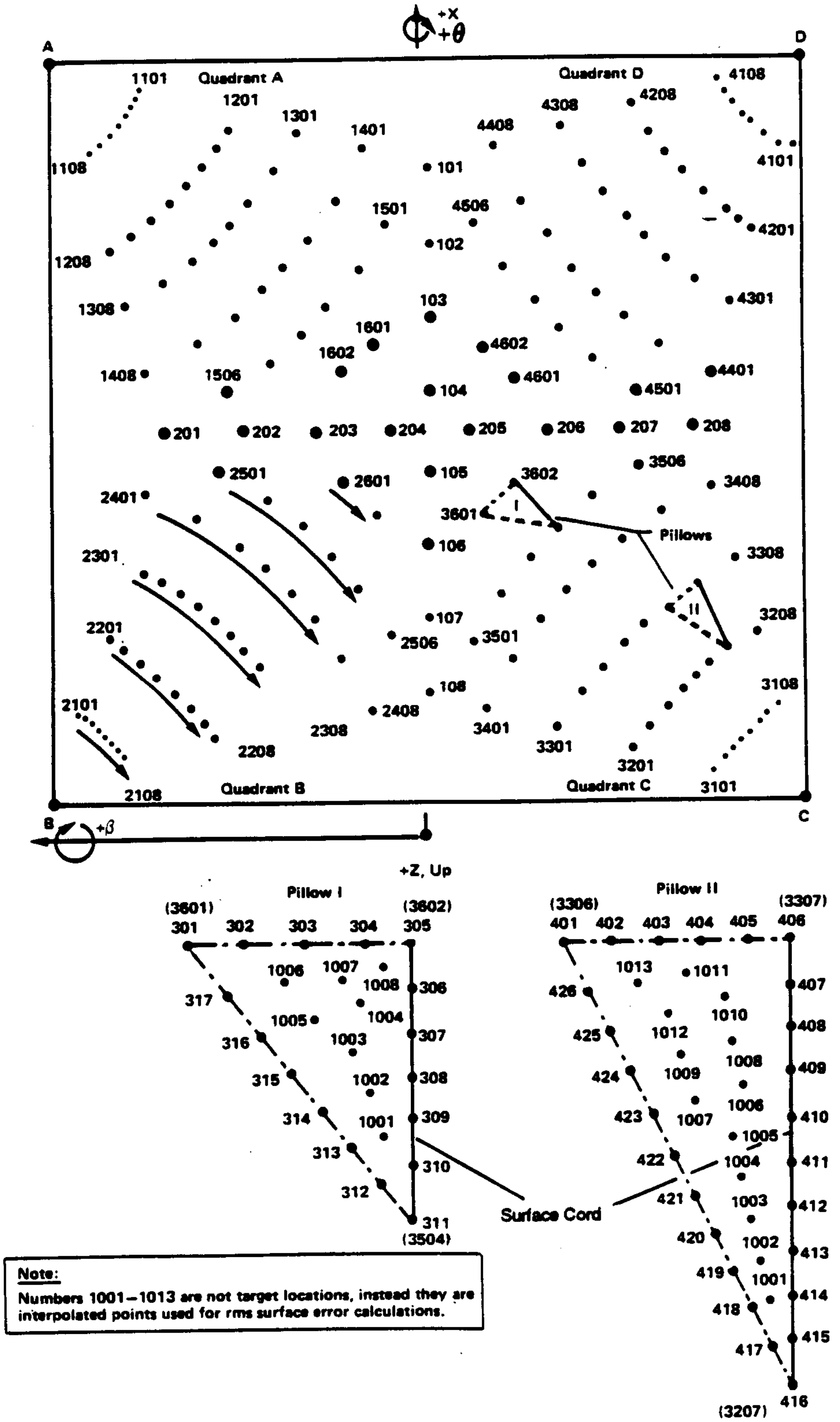


*Figure 19 Tie Point and Pillowing Target Numbers*

ORIGINAL PAGE IS
OF POOR QUALITY

*Table 4 Baseline Coordinates for Photogrammetric Transformation*

| Target | Label | X, m | Y, m | Z, m |
|---|---|---|---|---|
| 1 | 1101 | 4.916 | 1.782 | 1.044 |
| 2 | 1108 | 4.571 | 2.117 | 0.970 |
| 3 | 201 | 2.836 | 1.655 | 0.413 |
| 4 | 2101 | 1.044 | 2.145 | 0.218 |
| 5 | 2108 | 0.759 | 1.815 | 0.149 |
| 6 | 108 | 1.181 | -0.007 | 0.055 |
| 7 | 3101 | 0.764 | -1.833 | 0.152 |
| 8 | 3108 | 1.040 | -2.153 | 0.219 |
| 9 | 208 | 2.841 | -1.669 | 0.415 |
| 10 | 4101 | 4.565 | -2.113 | 0.967 |
| 11 | 4108 | 4.923 | -1.785 | 1.047 |
| 12 | 101 | 4.430 | -0.003 | 0.749 |

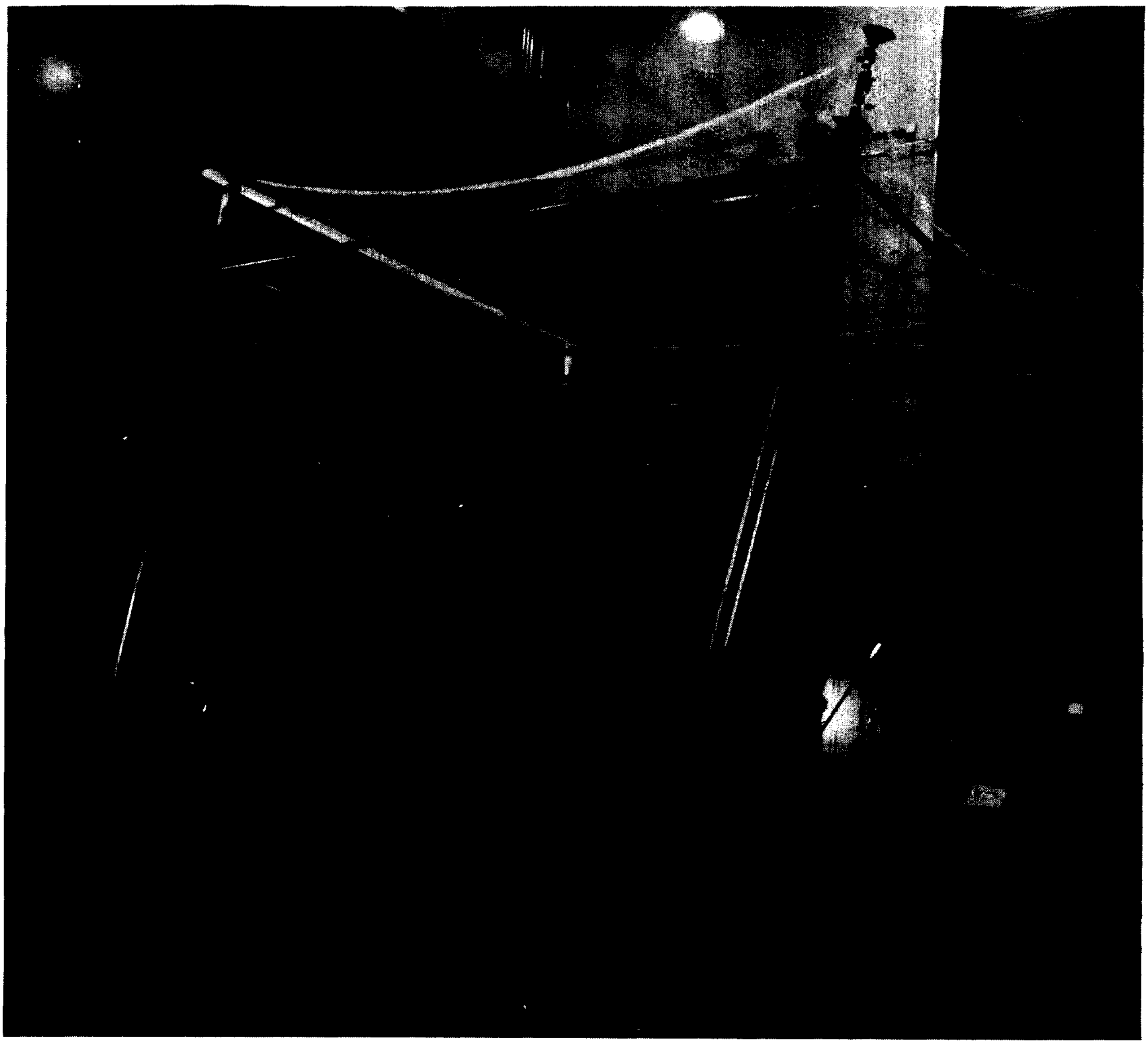

*Figure 20 Truss Configuration for Photogrammetric Pictures*

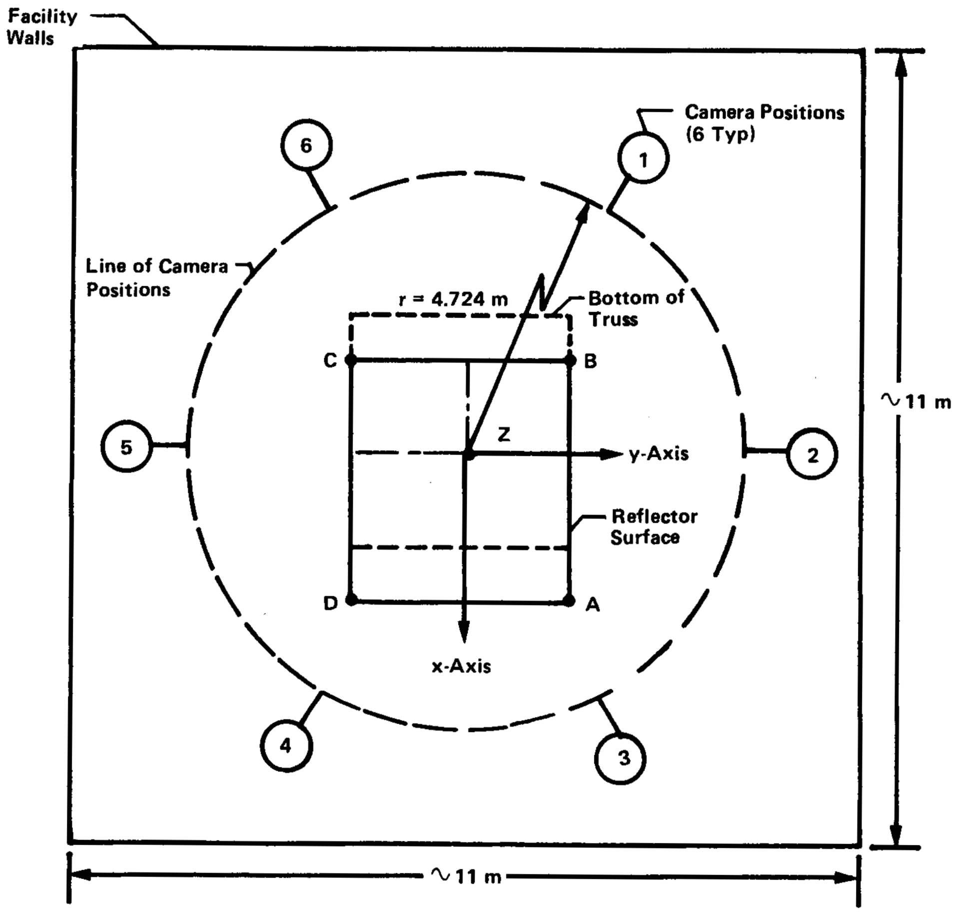


*Figure 21 Photogrammetric Camera Positions*

From the two metric camera measurements the coordinates of each tie point and mesh pillowing target were determined in a coordinate system best represented by the 12 reference points from the theodolite measurements. The rms standard errors for the metric camera measurements was about 0.025 m in X, Y, and Z with triangulation closures of about 1.4 microns, for both measurement sets. Appendix B contains the coordinates of each target for both sets.

## 4.2 BEST-FIT ANALYSIS

Using the metric camera coordinates of each tie point, a "best-fit" analysis was performed to isolate the systematic errors in the reflector from the random errors caused by manufacturing and setting. This was achieved by writing a small IBM PC BASIC program, which manipulated the actual tie point coordinates to best-fit perfect surface. The program listing is shown in Appendix C. This program was modeled after the best-fit surface routine (Ref 1).

The manipulations, roll, pitch, change in focal length and surface translations ( $\Delta X$, $\Delta Y$, and $\Delta Z$), all contribute to systematic errors, e.g., axial defocus, beam scanning, etc (Fig. 22). The difference in the Z- coordinate of the tie point and the corresponding point on the perfect surface is defined as the random error. The best-fit surface is that paraboloidal surface that shows a minimum rms of random surface error (Eq 3).

[3]

$$MANUF_{rms} = \sqrt{\frac{\sum_{i=1}^{N} \left(Z_d - Z_p\right)^2}{N}}$$

where Zd = Z- oordinate of tie point
Zp = Z- coordinate of best-fit surface
N = total number of tie points, 176
Manuf rms = rms of random surface error because of manufacturing and setting

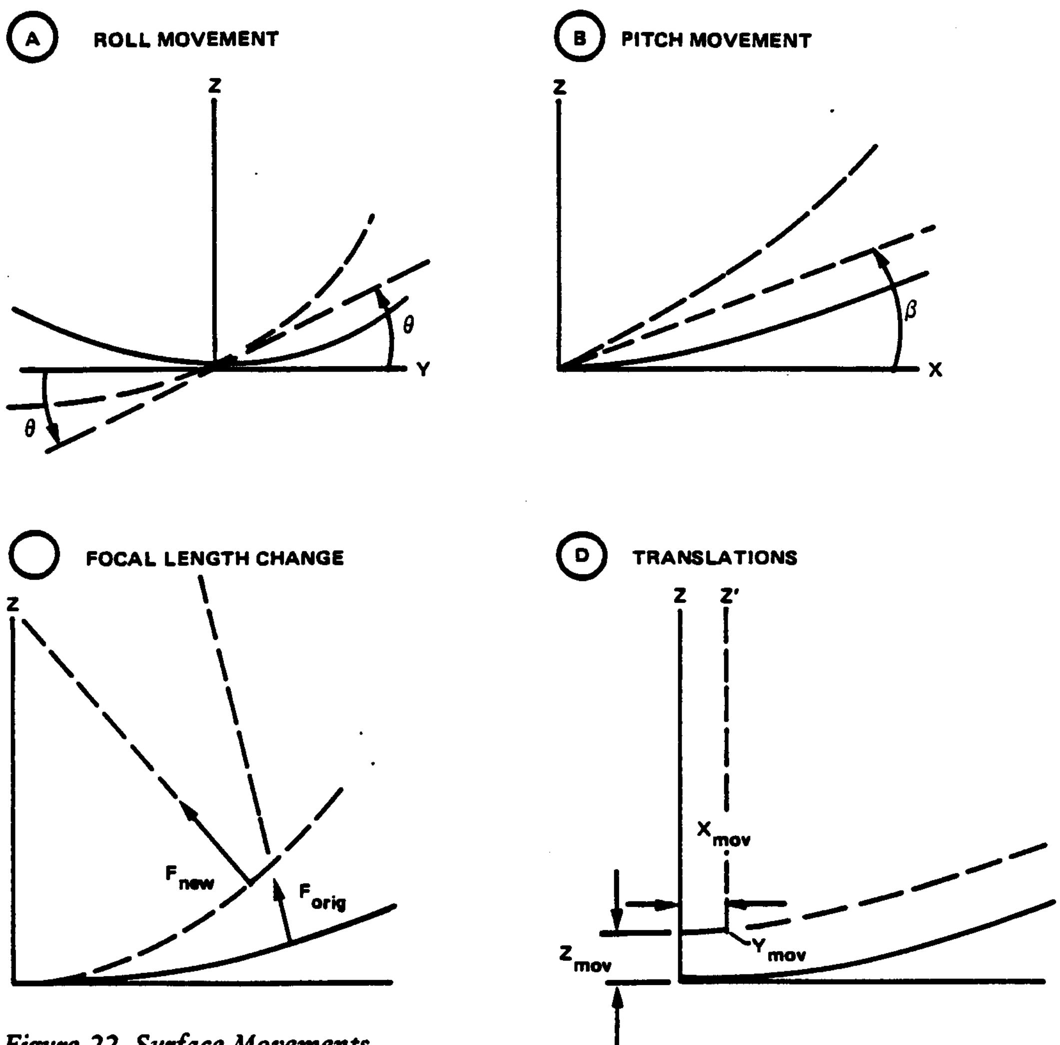


*Figure 22 Surface Movements*

Before the metric camera measurements could be used in the best-fit computer program, the Z- coordinate had to be revised to account for the tie point button thickness since the targets were placed on the top of the buttons and the mesh was under the buttons. Also, quite a few tieback cords had broken during the installation of the tie system to the mesh and many of the buttons were 3 and 4 (buttons) thick. By measuring a representative number of buttons, a standard tie point, i.e., a surface cord and tieback cord sandwiched between one top button and one bottom button was found to 1.27-m thick. For a tie point with 3 buttons it varied from 1.65 to 1.90-mm thick and for 4 buttons 2.16 to 2.54-mm thick. Therefore, Z- coordinate was reduced by 1.27, 1.78, and 2.29 mm for 2, 3, and 4 button tie points, respectively. Appendix C shows the value used at each point.

During the best-fit analysis of the surface, it became apparent that quadrant C, i.e., tie points 3101 through 3602, was uniformly 2.03-mm lower than all other quadrants. This problem was apparently caused by improper initialization of the theodolite system on the day Quadrant C was adjusted. Therefore, two best-fit analysis cases, one of the whole surface and the other removing all points within Quadrant C, were performed.

The best-fit analysis results showed the following. For the first set of metric camera coordinates, Set 1, i.e, the photos taken immediately following the theodolite surface setting, the minimum rms random surface error was 1.27 mm for the whole surface and 1.02 mm for the partial surface. For the set of coordinates after partial stowage, Set 2, the minimum rms random surface error was 1.25 mm for the whole surface and 1.04 mm for the partial surface. To show repeatability, the second set of metric camera measurements used the identical surface manipulations values as the first. In other words, the same $\Delta X$, $\Delta Y$, and $\Delta Z$ translations, the same roll and pitch, and the same focal length.

The results show that the surface is extremely stable and repeatability is excellent. However, a more stringent test might require the surface to be fully stowed for some length of time and then redeployed and measured.

Table 5 shows the resulting surface manipulations from performing the best-fit analysis.

*Table 5 Best-Fit Surface Manipulations*

| | Whole Surface | Partial Surface |
|---|---|---|
| ΔX, cm | 0.0 | 0.0 |
| ΔY, cm | 0.0 | 0.064 |
| ΔZ, cm | 0.157 | 0.036 |
| F, m | 6.538 | 6.553 |
| Θ Roll, deg | 0.0150 | 0.0003 |
| β Pitch, deg | -0.0010 | 0.0047 |

4.3 MESH PILLOWING

Using the metric camera coordinates of the mesh targets, an analysis was performed to determine the rms surface error caused by mesh pillowing.

As with the best-fit analysis, a short BASIC program was written, which took the photographed coordinates and solved for the rms surface error. Appendix D includes a listing of the program.

To isolate pillowing errors from manufacturing errors, the analysis solved for two different flat planes between the three tie points that bound the targeted mesh. For Pillow I, these points were 301, 305, and 311 or 3601, 3602, and 3504, respectively, using the whole surface numbering scheme (Fig. 19). For Pillow II, these points were 401, 406, and 416 or 3306, 3307, and 3207, respectively.

The first flat plane was generated using the X, Y, and Z- coordinates of the three tie points. The second flat plane was generated using only the X and Y coordinates of the tie points and solved for the Z-coordinate using a perfect paraboloid, i.e., a focal length of 6.553 m. Then the distance normal between the first plane and the mesh target point, $d_1$, was added to the distance normal between the second plane and the perfect paraboloid at the mesh target, $d_2$. This way the manufacturing errors of the corner tie points were removed. This process is better understood by looking at a two-dimensional illustration (Fig. 23).

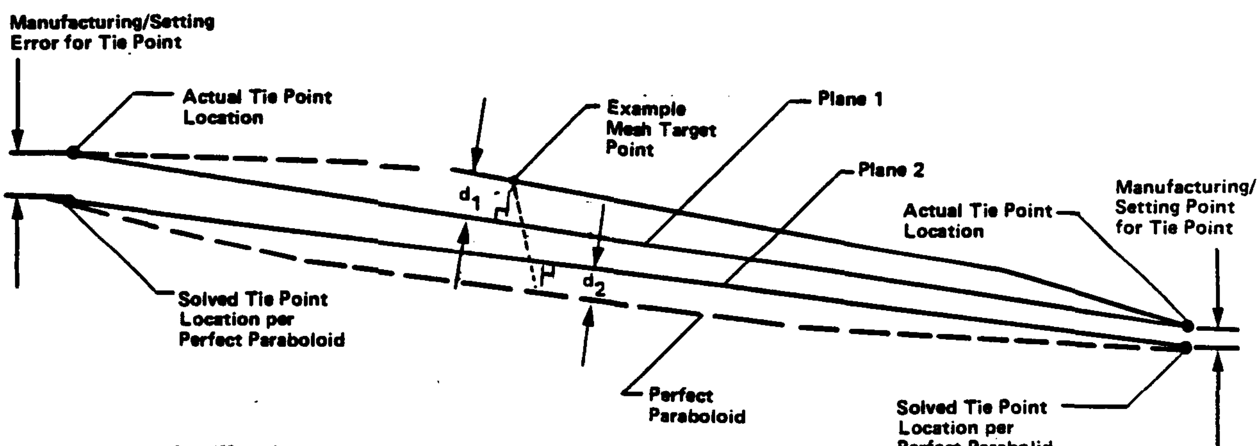


*Figure 23 Mesh Pillowing*

Once the distance from the paraboloid was determined for each mesh target ($d_1 + d_2$), additional surface points were linearly interpolated so that the mesh pillow could be better represented by a group of points. Figure 19 shows the location of the interpolated points.

Finally, to find the minimum rms surface error because of pillowing, an offset value, $d_{ref}$, was used for all points. The program iterated on the $d_{ref}$ value until the minimum rms value was found. Equation 4 shows how the rms pillowing error was determined.

[4]

$$Pillow_{rms} = \sqrt{\frac{\sum_{i=1}^{N} M \times \left(d_{TOT} - d_{ref}\right)^{2}}{N}}$$

where $d_{TOT}$ = distance from paraboloid to mesh, ($d_1 + d_2$)
$d_{ref}$ = offset value used for all points
M = Multipoint factor, 2 for interpolated points, 1 for mesh targets
N = number of total points used to calculate rms
$Pillow_{rms}$ = rms error because of pillowing

Note that within Equation 4 there is a multipoint factor, M, for the interpolated tie points since only half the area bound by tie points was represented by targets.

The analysis results showed that Pillow I has an rms error of 0.043 cm and Pillow II has an rms error of 0.086 cm. Since the two targeted pillow areas represented the upper and lower bounds of mesh pillowing, the two rms values were averaged to determine the rms pillowing error for the whole surface. The average value is 0.066 cm.

## 4.4 SURFACE AREA SUMMARY

Combining manufacturing errors with pillowing errors results in the following total rms surface error (Table 6).

*Table 6 rms Surface Error Summary*

| | Whole Surface/ Set 1 | Partial Surface/ Set 1 | Whole Surface/ Set 2 | Partial Surface/ Set 2 |
|---|---|---|---|---|
| rms Manufacturing Error, cm | 0.127 | 0.102 | 0.124 | 0.104 |
| rms Pillowing Error (ave), cm | 0.066 | 0.066 | 0.066 | 0.066 |
| Worst-Case Sum, cm | 0.193 | 0.168 | 0.191 | 0.170 |
| rss of rms Errors, cm | 0.142 | 0.122 | 0.140 | 0.124 |
| Average of Worst-Case/ rss, cm | 0.168 | 0.145 | 0.165 | 0.147 |

Since the actual rms surface error will be somewhere in between the worst-case sum of the errors and the rss of the errors, an average total surface error was determined. For the whole surface, the average rms surface error of 0.168 cm represents an achieved surface accuracy of 1/18 of a wavelength of 10 GHz. For the partial surface, the total surface error of 0.145 cm represents an achieved surface accuracy of 1/21 of a wavelength.

Although the goal of 1/25 of a wavelength was not achieved, as a first effort for integrating a mesh reflector to a box truss and considering the configuration was changed from centered to offset midway through the effort, the achieved surface accuracy of 1/18 of a wavelength is a remarkable result. It also shows that by going back and readjusting the surface one additional time, the 1/25 of a wavelength goal can be achieved.

This Page Left Intentionally Blank

# 5.0 COMPARISON OF RESULTS WITH ANALYTICAL PREDICTIONS

The schedule did not permit the loads in the tie system to be measured so that they could be compared with the analytical predictions using software (Ref 1). However, two major assumptions within the software could be verified, i.e., mesh pillowing and manufacturing rms surface errors.

## 5.1 MESH PILLOWING EQUATION

In Reference 1 we presented the equation shown below, Equation 5, for predicting the rms surface error because of pillowing for box truss antenna systems which use the direct tieback tie system.

[5] $$\text{rms (pillow)} = \frac{0.05 \times TS^2}{F}$$

where TS = Radial Tie Spacing, m
F = Antenna Focal Length, m and
rms (pillow) = rms surface error caused by pillowing, m

The equation assumed a square tie point pattern. However, the direct tieback tie system does not produce a square tie point pattern, therefore, $TS^2$ should be equal to the area of mesh bound by the tie points. For a square pattern tie system, the tie spacing square and $TS^2$ are equal. Using this correction and comparing it to the measured pillow shapes results in Table 7.

***Table 7 Verification of Pillowing Error Equation***

**Pillow I**

**Mesh Area Bound by Tie Points = 18.8 cm x 30.5 cm = 573.4 cm² (0.057 m²)**

**Analytically Predicted rms Error Caused by Pillowing** $= \frac{0.05\,(0.057)}{6.5532} = 4.349 \times 10^{-4}$ m (0.043 cm)

**Measured rms Error**
**Caused by Pillowing = 0.043 cm**
**% Difference = 0.0**

**Pillow II**

**Mesh Area Bound by Tie Points = 20.3 cm x 50.8 cm = 1031.24 cm² (0.103 m²)**

**Analytically Predicted rms Error Caused by Pillowing** $= \frac{0.05\,(0.103)}{6.5532} = 7.859 \times 10^{-4}$ m (0.079 cm)

**Measured rms Error**
**Caused by Pillowing = 0.086 cm**
**% Difference = 8.1**



PRECEDING PAGE BLANK NOT FILMED

As shown in Table 7, the equation will predict the rms surface error caused by pillowing within 10% or less.

## 5.2 MANUFACTURING EQUATION

Along with the mesh pillowing equation, the equation shown below, Equation 6 was presented in Reference 1 for predicting the rms surface error because of a defined manufacturing tolerance.

[6] rms(manuf) = MT/3

where MT = manufacturing tolerance, and
rms(manuf) = rms surface error caused by manufacturing errors

Although this task attempted to achieve a manufacturing tolerance of ± 0.16 cm, this was not the case. Instead, the best-fit analysis showed the following achieved manufacturing tolerances and rms surface error for each case analyzed (Table 8). Included in the table is the predicted rms error using Equation 6.

*Table 8 Verification of Manufacturing Error Equation*

| | Manuf Tolerance, cm | Actual rms Error, cm | Predicted rms Error, cm | % Difference |
|---|---|---|---|---|
| Whole Surface/Set 1 | 0.432 | 0.127 | 0.144 | 13.3 |
| Partial Surface/Set 1 | 0.343 | 0.102 | 0.114 | 12.6 |
| Whole Surface/Set 2 | 0.419 | 0.124 | 0.140 | 12.2 |
| Partial Surface/Set 2 | 0.356 | 0.104 | 0.118 | 13.8 |

As shown in Table 8, the manufacturing error equation will predict the rms surface error conservatively, and within 15% or less.

## 6.0 SUMMARY AND RECOMMENDATIONS

Task 3 results have shown that the box truss is a viable candidate for supporting lightweight mesh reflectors. The 4.572-m, 1.5 F/D, offset fed reflector built under this task achieved a surface accuracy of 1/18 of a wavelength at 10 GHz. This was accomplished by using 3000 tow Celion graphite cords to produce a direct tieback tie system consisting of 176 tie points. Adjustment fittings at each corner allow each tie point to be adjusted.

Although this reflector uses a single box truss cube, multiple bay box truss structures could use the same technology to produce large reflective surfaces. This means each box section of mesh could be manufactured separately, drastically reducing the cost and complexity over other large reflector concepts. The process for sewing the mesh sections together was also included in this study.

Task 3 has solved many of the problems associated with designing and building box truss mesh reflectors. It has also produced a number of recommendations to follow for continued efforts. The following will reduce the cost and complexity, as well as improve the stability and accuracy of installing mesh reflectors on box truss structures.

1) During the fabrication and installation of this reflector, over 24 tieback cords were broken either at the tie point or at the adjustment fitting. This was because of the sensitivity of the Celion graphite cord to handling and bending. Consider using either Kevlar cord, quartz cord or if the thermal and stiffness requirements dictate, use Celion cord with an outer nylon wrapping. For R&D work, Kevlar seems the most durable and coatings have been developed to reduce the ultraviolet degradation effects.

2) The present design bonded the ends of the catenaries in place on the stretching table. Later, during the installation and coarse setting they were pulled down into shape, thereby increasing the tension in the cords. Instead, the catenaries should be installed on the stretching table, but not bonded. When the mesh is installed on the standoffs and the catenaries are pulled into shape, the catenary can then be tensioned by hanging weights and bonded. This process provides the flexibility of adjusting the catenary depth and the tension level if required without having to replace the catenary cords.

3) An improvement can be made to the tieback cord adjustment hardware. Presently, the graphite cord is bonded directly to the fine adjustment allen screw that is located at the end of the coarse adjustment tube (Fig. 11). The coarse adjustment tube cannot be turned in a threaded fixture for adjustment; this would cause the tieback cords to twist excessively and cause premature breakage. Therefore, the tube is moved in or out of the adjustment fitting, which does not twist the graphite cord.

A metal cable should be bonded to the fine adjustment allen screw and extend outward from the end of the coarse tube. A swivel should be attached to the end of the wire to which the tieback cord will be attached. This allows the coarse adjustment tube to be threaded into the adjustment fitting and would greatly increase the ease of coarse adjustment.

4) A redesign of the adjustment fitting is desirable to simplify the physical arrangement of the adjustment hardware. The tieback lines-of-action converge at the center of the square tube at the base of the standoff. When all the coarse adjustment tubes (48 each) are installed into the adjustment angle fitting along their line-of-action, the ends of the adjustment tubes are close to touching and access to some of the fine adjustment allen screws is very difficult.

   If the adjustment hardware is modified per Item 3 above, it is possible to relocate the adjustment angle fitting to the lower outside (opposing) corner of the cube corner fitting. This provides access to both the coarse adjustment screw and fine adjustment screw from the outside of the adjustment fitting angle. The angle presently used for installing the adjustment hardware would remain to guide the tieback cords and an eyelet or multiple eyelets would be located at the line-of-action point of intersection. The placement of the adjustment hardware in the new adjustment angle could be along horizontal rows of threaded holes and therefore spacing between adjustment screws could be smaller allowing for many more tieback cords to be added to the design. The metal cable attached to a tieback would be routed through the top inside angle through the eyelet and into the coarse adjustment screw on the bottom outside angle. Figure 24 illustrates this concept. Note that the tieback cords pass through what is presently the base plate of the cube corner fitting. Therefore, the base plate of the fitting would have to be modified with an access hole.

   This design would make it possible to adjust the surface for multibay box truss antennas at locations where one standoff is used by up to four different box truss cabes. If the metal cables should prove too bulky through the eyelet, an alternative would be to use Kevlar which will tolerate the wear of the cord through the eyelet.

5) Finally, the single bay reflector was adjusted for a parabolic shape while it was set up on the wooden stands (Fig. 17). Although this greatly eased the assembly process, i.e., not having to work 4.8 meters in the air, it caused some tieback cords to fail since the stands did not precisely duplicate the truss stiffness. That is, when the tensioned tie system was later installed on the box truss and the box truss did not deflect as much as the wooden stands, the tieback cords became overloaded and failed. In the

future, the floor stands should be used solely for installing the tie system onto the mesh surface. At this point the reflector should be installed on the box truss and surface set to the paraboloidal shape. This means either scaffolding must be used or the box truss must be lowered into a pit so that access to the adjustment fittings requires minimal effort.

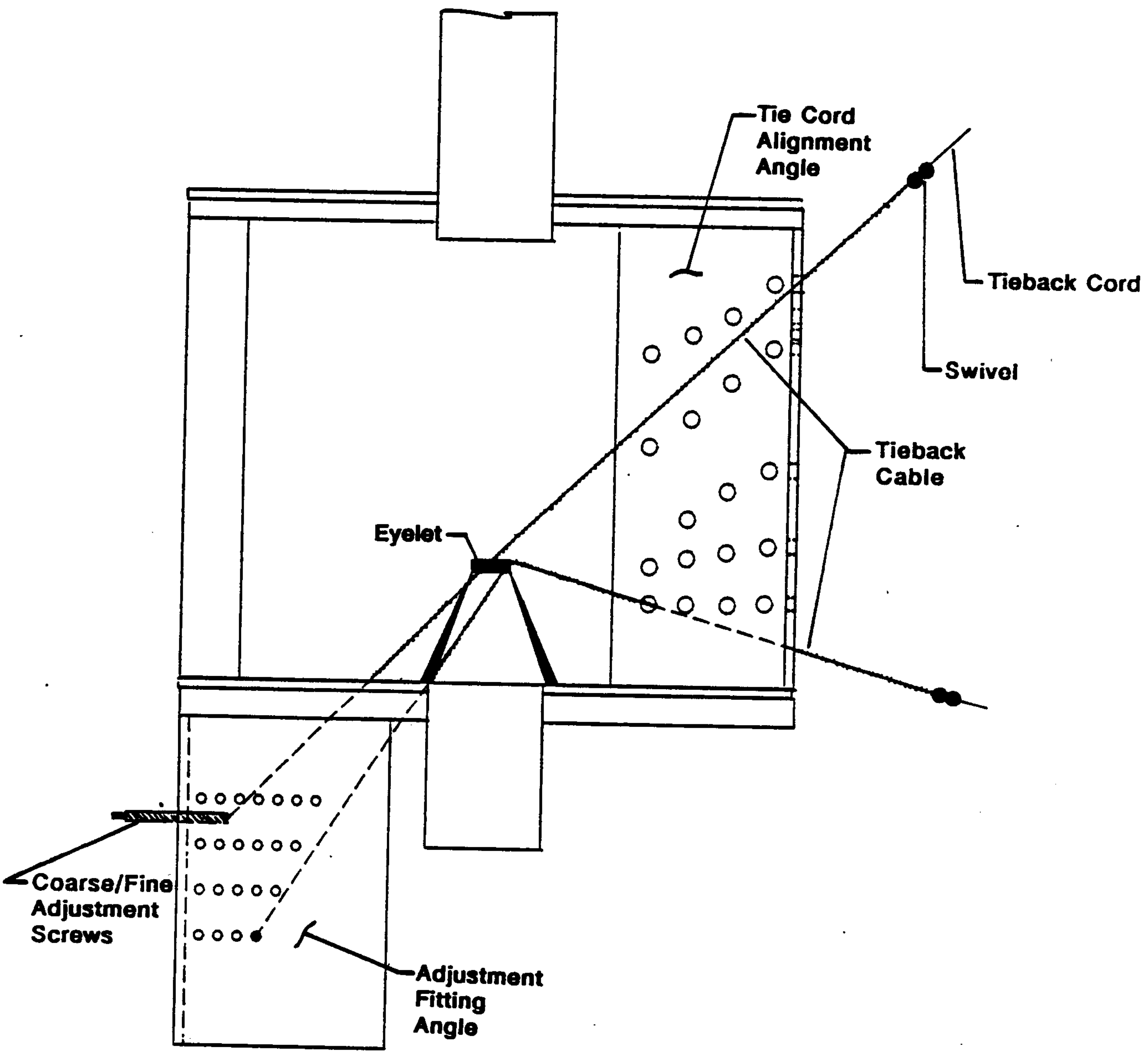


*Figure 24 Redesigned Attachment Fitting*

This Page Left Intentionally Blank.

## 7.0 REFERENCE

1. E. E. Bachtell et al.: "Box Truss Analysis and Technology Development, Task 1--Mesh Analysis and Control." NASA CR-172570, August 1985.



PRECEDING PAGE BLANK NOT FILMED

# APPENDIX A

The following coordinates define the location of each tie point on the mesh reflector. The coordinates where hand generated by translating the center-fed configuration defined in Section 2.1, page 9. The translation consisted of a 2.8956-m translation along the X-axis and a 12.2368-degree rotation about the Y-axis.

TIE POINT COORDINATES IN METERS

| TIE POINT | X,m | Y,m | Z,m | TIE POINT | X,m | Y,m | Z,m |
|---|---|---|---|---|---|---|---|
| A | 5.0752 | 2.2860 | 1.1820 | A15-1 | 4.6247 | 2.0621 | 0.9782 |
| B | 0.6096 | 2.2860 | 0.2135 | A15-2 | 4.1838 | 1.8374 | 0.7966 |
| C | 0.6096 | -2.2860 | 0.2135 | A15-3 | 3.7416 | 1.6120 | 0.6332 |
| D | 5.0752 | -2.2860 | 1.1820 | A15-4 | 3.2983 | 1.3860 | 0.4883 |
| AB-1 | 2.8298 | 1.6537 | 0.4098 | A15-5 | 3.0641 | 1.2666 | 0.4194 |
| AB-2 | 2.8298 | 1.1472 | 0.3557 | A16-1 | 4.5900 | 2.1519 | 0.9804 |
| AB-3 | 2.8298 | 0.6398 | 0.3211 | A16-2 | 4.1145 | 2.0173 | 0.8011 |
| AB-4 | 2.8298 | 0.1319 | 0.3062 | A16-3 | 3.6377 | 1.8824 | 0.6400 |
| BC-1 | 1.2136 | 0.0 | 0.0562 | A16-4 | 3.2338 | 1.7681 | 0.5182 |
| BC-2 | 1.7087 | 0.0 | 0.1114 | B1-1 | 0.7268 | 0.1801 | 0.1439 |
| BC-3 | 2.2045 | 0.0 | 0.1854 | B1-2 | 0.8583 | 1.3146 | 0.0940 |
| BC-4 | 2.7009 | 0.0 | 0.2783 | B1-3 | 0.9902 | 0.8267 | 0.0635 |
| CD-1 | 2.8298 | -1.6537 | 0.4098 | B1-4 | 1.1019 | 0.4134 | 0.0528 |
| CD-2 | 2.8298 | -1.1472 | 0.3557 | B2-1 | 0.8145 | 1.8366 | 0.1540 |
| CD-3 | 2.8298 | -0.6398 | 0.3211 | B2-2 | 1.0342 | 1.3855 | 0.1140 |
| CD-4 | 2.8298 | -0.1319 | 0.3062 | B2-3 | 1.2545 | 0.9330 | 0.0932 |
| AD-1 | 4.4460 | 0.0 | 0.7541 | B2-4 | 1.4753 | 0.4794 | 0.0918 |
| AD-2 | 3.9510 | 0.0 | 0.5955 | B2-5 | 1.5920 | 0.2397 | 0.0989 |
| AD-3 | 3.4551 | 0.0 | 0.4554 | B3-1 | 0.8822 | 1.8790 | 0.1644 |
| AD-4 | 2.9588 | 0.0 | 0.3340 | B3-2 | 1.1698 | 1.4704 | 0.1347 |
| A9-1 | 4.9328 | 1.8011 | 1.0520 | B3-3 | 1.4583 | 1.0604 | 0.1240 |
| A9-2 | 4.8013 | 1.3146 | 0.9454 | B3-4 | 1.7475 | 0.6494 | 0.1326 |
| A9-3 | 4.6694 | 0.8267 | 0.8579 | B3-5 | 1.9760 | 0.3247 | 0.1530 |
| A9-4 | 4.5577 | 0.4134 | 0.7990 | B4-1 | 0.9318 | 1.9211 | 0.1739 |
| A10-1 | 4.8451 | 1.8366 | 1.0242 | B4-2 | 1.2692 | 1.5547 | 0.1537 |
| A10-2 | 4.6255 | 1.3855 | 0.8894 | B4-3 | 1.6077 | 1.1870 | 0.1524 |
| A10-3 | 4.4052 | 0.9330 | 0.7735 | B4-4 | 1.9470 | 0.8186 | 0.1702 |
| A10-4 | 4.1844 | 0.4794 | 0.6767 | B4-5 | 2.2870 | 0.4494 | 0.2072 |
| A10-5 | 4.0677 | 0.2397 | 0.6334 | B4-6 | 2.4940 | 0.2247 | 0.2392 |
| A11-1 | 4.7775 | 1.8790 | 1.0054 | B5-1 | 0.9524 | 1.9422 | 0.1785 |
| A11-2 | 4.4899 | 1.4704 | 0.8515 | B5-2 | 1.3104 | 1.5969 | 1.6280 |
| A11-3 | 4.2014 | 1.0604 | 0.7163 | B5-3 | 1.6696 | 1.2506 | 1.6600 |
| A11-4 | 3.9121 | 0.6494 | 0.5999 | B5-4 | 2.0298 | 0.9033 | 0.1883 |
| A11-5 | 3.6836 | 0.3247 | 0.5217 | B5-5 | 2.3906 | 0.5554 | 0.2298 |
| A12-1 | 4.7278 | 1.9211 | 0.9935 | B5-6 | 2.6102 | 0.3437 | 0.2644 |
| A12-2 | 4.3905 | 1.5547 | 0.8276 | B6-1 | 0.9935 | 1.9930 | 0.1892 |
| A12-3 | 4.0520 | 1.1871 | 0.6801 | B6-2 | 1.3929 | 1.6987 | 0.1841 |
| A12-4 | 3.7126 | 0.8186 | 0.5514 | B6-3 | 1.7935 | 1.4034 | 0.1978 |
| A12-5 | 3.3726 | 0.4494 | 0.4416 | B6-4 | 2.1952 | 1.1075 | 0.2306 |
| A12-6 | 3.1657 | 0.2247 | 0.3842 | B6-5 | 2.5125 | 0.8737 | 0.2699 |
| A13-1 | 4.7073 | 1.9422 | 0.9892 | B7-1 | 1.0350 | 2.0621 | 0.2031 |
| A13-2 | 4.3492 | 1.5969 | 0.8189 | B7-2 | 1.4758 | 2.8374 | 0.2119 |
| A13-3 | 3.9900 | 1.2506 | 0.6670 | B7-3 | 1.9180 | 1.6120 | 0.2395 |
| A13-4 | 3.6298 | 0.9033 | 0.5338 | B7-4 | 2.3613 | 1.3860 | 0.2860 |
| A13-5 | 3.2690 | 0.5554 | 0.4194 | B7-5 | 2.5956 | 1.2666 | 0.3182 |
| A13-6 | 3.0494 | 0.3437 | 0.3593 | B8-1 | 1.0696 | 2.1519 | 0.2203 |
| A14-1 | 4.6661 | 1.9929 | 0.9821 | B8-2 | 1.5451 | 2.0173 | 0.2463 |
| A14-2 | 4.2668 | 1.6987 | 0.8046 | B8-3 | 2.0219 | 1.8824 | 0.2911 |
| A14-3 | 3.8661 | 1.4034 | 0.6453 | B8-4 | 2.4259 | 1.7681 | 0.3438 |
| A14-4 | 3.4645 | 1.1075 | 0.5047 | | | | |
| A14-5 | 3.1472 | 0.8737 | 0.4070 | | | | |

TIE POINT COORDINATES IN METERS

| TIE POINT | X,m | Y,m | Z,m | TIE POINT | X,m | Y,m | Z,m |
|---|---|---|---|---|---|---|---|
| C1-1 | 0.7268 | -0.1801 | 0.1439 | D9-1 | 4.9328 | -1.8011 | 1.0520 |
| C1-2 | 0.8583 | -1.3146 | 0.0940 | D9-2 | 4.8013 | -1.3146 | 0.9454 |
| C1-3 | 0.9902 | -0.8267 | 0.0635 | D9-3 | 4.6694 | -0.8267 | 0.8579 |
| C1-4 | 1.1019 | -0.4134 | 0.0528 | D9-4 | 4.5577 | -0.4134 | 0.7990 |
| C2-1 | 0.8145 | -1.8366 | 0.1540 | D10-1 | 4.8451 | -1.8366 | 1.0242 |
| C2-2 | 1.0342 | -1.3855 | 0.1140 | D10-2 | 4.6255 | -1.3855 | 0.8894 |
| C2-3 | 1.2545 | -0.9330 | 0.0932 | D10-3 | 4.4052 | -0.9330 | 0.7735 |
| C2-4 | 1.4753 | -0.4794 | 0.0918 | D10-4 | 4.1844 | -0.4794 | 0.6767 |
| C2-5 | 1.5920 | -0.2397 | 0.0989 | D10-5 | 4.0677 | -0.2397 | 0.6334 |
| C3-1 | 0.8822 | -1.8790 | 0.1644 | D11-1 | 4.7775 | -1.8790 | 1.0054 |
| C3-2 | 1.1698 | -1.4704 | 0.1347 | D11-2 | 4.4899 | -1.4704 | 0.8515 |
| C3-3 | 1.4583 | -1.0604 | 0.1240 | D11-3 | 4.2014 | -1.0604 | 0.7163 |
| C3-4 | 1.7475 | -0.6494 | 0.1326 | D11-4 | 3.9121 | -0.6494 | 0.5999 |
| C3-5 | 1.9760 | -0.3247 | 0.1530 | D11-5 | 3.6836 | -0.3247 | 0.5217 |
| C4-1 | 0.9318 | -1.9211 | 0.1739 | D12-1 | 4.7278 | -1.9211 | 0.9935 |
| C4-2 | 1.2692 | -1.5547 | 0.1537 | D12-2 | 4.3905 | -1.5547 | 0.8276 |
| C4-3 | 1.6077 | -1.1870 | 0.1524 | D12-3 | 4.0520 | -1.1871 | 0.6801 |
| C4-4 | 1.9470 | -0.8186 | 0.1702 | D12-4 | 3.7126 | -0.8186 | 0.5514 |
| C4-5 | 2.2870 | -0.4494 | 0.2072 | D12-5 | 3.3726 | -0.4494 | 0.4416 |
| C4-6 | 2.4940 | -0.2247 | 0.2392 | D12-6 | 3.1657 | -0.2247 | 0.3842 |
| C5-1 | 0.9524 | -1.9422 | 0.1785 | D13-1 | 4.7073 | -1.9422 | 0.9892 |
| C5-2 | 1.3104 | -1.5969 | 1.6280 | D13-2 | 4.3492 | -1.5969 | 0.8189 |
| C5-3 | 1.6696 | -1.2506 | 1.6600 | D13-3 | 3.9900 | -1.2506 | 0.6670 |
| C5-4 | 2.0298 | -0.9033 | 0.1883 | D13-4 | 3.6298 | -0.9033 | 0.5338 |
| C5-5 | 2.3906 | -0.5554 | 0.2298 | D13-5 | 3.2690 | -0.5554 | 0.4194 |
| C5-6 | 2.6102 | -0.3437 | 0.2644 | D13-6 | 3.0494 | -0.3437 | 0.3593 |
| C6-1 | 0.9935 | -1.9930 | 0.1892 | D14-1 | 4.6661 | -1.9929 | 0.9821 |
| C6-2 | 1.3929 | -1.6987 | 0.1841 | D14-2 | 4.2668 | -1.6987 | 0.8046 |
| C6-3 | 1.7935 | -1.4034 | 0.1978 | D14-3 | 3.8661 | -1.4034 | 0.6453 |
| C6-4 | 2.1952 | -1.1075 | 0.2306 | D14-4 | 3.4645 | -1.1075 | 0.5047 |
| C6-5 | 2.5125 | -0.8737 | 0.2699 | D14-5 | 3.1472 | -0.8737 | 0.4070 |
| C7-1 | 1.0350 | -2.0621 | 0.2031 | D15-1 | 4.6247 | -2.0621 | 0.9782 |
| C7-2 | 1.4758 | -2.8374 | 0.2119 | D15-2 | 4.1838 | -1.8374 | 0.7966 |
| C7-3 | 1.9180 | -1.6120 | 0.2395 | D15-3 | 3.7416 | -1.6120 | 0.6332 |
| C7-4 | 2.3613 | -1.3860 | 0.2860 | D15-4 | 3.2983 | -1.3860 | 0.4883 |
| C7-5 | 2.5956 | -1.2666 | 0.3182 | D15-5 | 3.0641 | -1.2666 | 0.4194 |
| C8-1 | 1.0696 | -2.1519 | 0.2203 | D16-1 | 4.5900 | -2.1519 | 0.9804 |
| C8-2 | 1.5451 | -2.0173 | 0.2463 | D16-2 | 4.1145 | -2.0173 | 0.8011 |
| C8-3 | 2.0219 | -1.8824 | 0.2911 | D16-3 | 3.6377 | -1.8824 | 0.6400 |
| C8-4 | 2.4259 | -1.7681 | 0.3438 | D16-4 | 3.2338 | -1.7681 | 0.5182 |

Note: Tie Point labeling is based on the standoff letter, the radial surface cord number and a dash number, i.e., tie point C5-3 is the third tie point out from the 'C' standoff along the number 5 radial surface cord. For the tie points along the surface cross cords, the label is based on the standoff letters and a dash number, i.e., AD-2 is the second tie point on the surface cross cord between standoffs 'A' and 'D'.

APPENDIX B

Coordinates of Target Points for Set 1 of Metric Camera Measurements
Coordinates shown in inches

| Target # | X | Y | Z | Button Thk. | Z corrected |
|---|---|---|---|---|---|
| 101 | 174.5767 | -0.0849 | 29.5592 | 0.0700 | 29.4892 |
| 102 | 155.6399 | -0.0218 | 23.6123 | 0.0500 | 23.5623 |
| 103 | 136.3680 | -0.2272 | 18.1078 | 0.0700 | 18.0378 |
| 104 | 116.9635 | -0.4078 | 13.4705 | 0.0700 | 13.4005 |
| 105 | 105.3839 | -0.2522 | 10.8110 | 0.0700 | 10.7410 |
| 106 | 85.7402 | 0.1377 | 7.1285 | 0.0700 | 7.0585 |
| 107 | 65.7344 | -0.2518 | 4.2018 | 0.0700 | 4.1318 |
| 108 | 46.1923 | -0.2570 | 2.1364 | 0.0700 | 2.0664 |
| 201 | 111.7774 | 65.1213 | 16.3123 | 0.0500 | 16.2623 |
| 202 | 111.4182 | 45.3427 | 14.0399 | 0.0500 | 13.9899 |
| 203 | 111.5721 | 25.4650 | 12.7729 | 0.0700 | 12.7029 |
| 204 | 111.1280 | 5.6150 | 12.1745 | 0.0700 | 12.1045 |
| 205 | 111.0440 | -6.1907 | 12.1071 | 0.0700 | 12.0371 |
| 206 | 111.3583 | -26.1304 | 12.6630 | 0.0500 | 12.6130 |
| 207 | 111.4585 | -46.1052 | 14.0316 | 0.0500 | 13.9816 |
| 208 | 111.7537 | -65.6485 | 16.2997 | 0.0500 | 16.2497 |
| 301 | 97.4224 | -8.9365 | 9.1682 | 0.0900 | 9.0782 |
| 302 | 98.6564 | -10.0846 | 9.4053 | 0.0000 | 9.4053 |
| 303 | 99.8601 | -11.4735 | 9.7068 | 0.0000 | 9.7068 |
| 304 | 101.1683 | -12.8488 | 9.9978 | 0.0000 | 9.9978 |
| 305 | 102.3508 | -14.3144 | 10.2949 | 0.0900 | 10.2049 |
| 306 | 100.9648 | -15.6418 | 10.0375 | 0.0000 | 10.0375 |
| 307 | 99.5466 | -16.9990 | 9.8086 | 0.0000 | 9.8086 |
| 308 | 98.1149 | -18.3449 | 9.5769 | 0.0000 | 9.5769 |
| 309 | 96.6949 | -19.7945 | 9.3594 | 0.0000 | 9.3594 |
| 310 | 95.2242 | -21.2189 | 9.1177 | 0.0000 | 9.1177 |
| 311 | 93.6654 | -22.6603 | 8.9018 | 0.0500 | 8.8518 |
| 312 | 94.1246 | -20.6130 | 8.8876 | 0.0000 | 8.8876 |
| 313 | 94.7198 | -18.6885 | 8.9476 | 0.0000 | 8.9476 |
| 314 | 95.2228 | -16.8052 | 8.9753 | 0.0000 | 8.9753 |
| 315 | 95.7076 | -14.7426 | 9.0046 | 0.0000 | 9.0046 |
| 316 | 96.2214 | -12.9111 | 9.0446 | 0.0000 | 9.0446 |
| 317 | 96.7810 | -10.8633 | 9.0766 | 0.0000 | 9.0766 |
| 401 | 69.8125 | -55.9920 | 7.7258 | 0.0500 | 7.6758 |
| 402 | 70.8117 | -57.5998 | 8.0343 | 0.0000 | 8.0343 |
| 403 | 71.8563 | -59.2457 | 8.3809 | 0.0000 | 8.3809 |
| 404 | 72.8589 | -60.8685 | 8.7069 | 0.0000 | 8.7069 |
| 405 | 73.9062 | -62.5257 | 9.0352 | 0.0000 | 9.0352 |
| 406 | 74.9145 | -64.2212 | 9.3796 | 0.0500 | 9.3296 |
| 407 | 73.2890 | -65.1566 | 9.2597 | 0.0000 | 9.2597 |
| 408 | 71.4937 | -66.0965 | 9.1572 | 0.0000 | 9.1572 |
| 409 | 69.6656 | -66.9724 | 9.0394 | 0.0000 | 9.0394 |
| 410 | 67.9156 | -67.9061 | 8.9434 | 0.0000 | 8.9434 |
| 411 | 65.9943 | -68.8105 | 8.8206 | 0.0000 | 8.8206 |
| 412 | 64.2557 | -69.7271 | 8.7176 | 0.0000 | 8.7176 |
| 413 | 62.4960 | -70.5873 | 8.6113 | 0.0000 | 8.6113 |
| 414 | 60.6350 | -71.5437 | 8.5059 | 0.0000 | 8.5059 |
| 415 | 58.8515 | -72.4576 | 8.3918 | 0.0000 | 8.3918 |
| 416 | 57.0763 | -73.2636 | 8.3309 | 0.0700 | 8.2609 |
| 417 | 58.1689 | -71.4972 | 8.1875 | 0.0000 | 8.1875 |
| 418 | 59.3320 | -69.9030 | 8.1206 | 0.0000 | 8.1206 |
| 419 | 60.4152 | -68.2033 | 8.0332 | 0.0000 | 8.0332 |
| 420 | 61.6712 | -66.5807 | 7.9743 | 0.0000 | 7.9743 |
| 421 | 62.7548 | -65.1380 | 7.9251 | 0.0000 | 7.9251 |
| 422 | 64.0453 | -63.3957 | 7.8673 | 0.0000 | 7.8673 |

| | | | | | |
|---|---|---|---|---|---|
| 423 | 65.2702 | -61.8297 | 7.8115 | 0.0000 | 7.8115 |
| 424 | 66.4150 | -60.3084 | 7.7769 | 0.0000 | 7.7769 |
| 425 | 67.4998 | -58.7030 | 7.7226 | 0.0000 | 7.7226 |
| 426 | 68.7570 | -57.0959 | 7.6823 | 0.0000 | 7.6823 |
| 1101 | 193.4932 | 70.1454 | 41.0864 | 0.0500 | 41.0364 |
| 1102 | 190.0705 | 71.4708 | 40.0305 | 0.0500 | 39.9805 |
| 1103 | 187.1378 | 72.8225 | 39.1319 | 0.0500 | 39.0819 |
| 1104 | 185.2847 | 74.1967 | 38.6618 | 0.0500 | 38.6118 |
| 1105 | 184.0883 | 74.9196 | 38.3411 | 0.0900 | 38.2511 |
| 1106 | 182.3985 | 77.2971 | 38.1135 | 0.0900 | 38.0235 |
| 1107 | 180.7293 | 79.7782 | 37.8708 | 0.0500 | 37.8208 |
| 1108 | 179.8449 | 83.2785 | 38.1264 | 0.0500 | 38.0764 |
| 1201 | 188.4927 | 51.1894 | 37.0552 | 0.0500 | 37.0052 |
| 1202 | 181.9847 | 53.9113 | 34.9745 | 0.0500 | 34.9245 |
| 1203 | 176.4385 | 56.9213 | 33.3742 | 0.0900 | 33.2842 |
| 1204 | 172.4823 | 60.2516 | 32.3959 | 0.0500 | 32.3459 |
| 1205 | 170.5274 | 61.7095 | 31.9191 | 0.0900 | 31.8291 |
| 1206 | 167.1863 | 66.2441 | 31.4044 | 0.0900 | 31.3144 |
| 1207 | 164.0406 | 71.1783 | 31.0734 | 0.0900 | 30.9834 |
| 1208 | 161.6957 | 78.4058 | 31.3688 | 0.0500 | 31.3188 |
| 1301 | 183.2253 | 32.2751 | 33.6631 | 0.0900 | 33.5731 |
| 1302 | 173.5559 | 36.2483 | 30.5202 | 0.0900 | 30.4302 |
| 1303 | 165.1652 | 41.1127 | 28.1583 | 0.0900 | 28.0683 |
| 1304 | 159.4310 | 46.1458 | 26.8054 | 0.0900 | 26.7154 |
| 1305 | 156.6585 | 48.4936 | 26.1642 | 0.0900 | 26.0742 |
| 1306 | 151.9946 | 54.6319 | 25.3162 | 0.0500 | 25.2662 |
| 1307 | 147.0394 | 62.6210 | 24.8325 | 0.0500 | 24.7825 |
| 1308 | 143.3535 | 73.3788 | 25.2219 | 0.0500 | 25.1719 |
| 1401 | 178.7323 | 16.1132 | 31.2847 | 0.0500 | 31.2347 |
| 1402 | 164.8184 | 18.7651 | 26.7197 | 0.0500 | 26.6697 |
| 1403 | 153.9915 | 25.3033 | 23.6651 | 0.0500 | 23.6151 |
| 1404 | 146.2951 | 31.9295 | 21.7991 | 0.0500 | 21.7491 |
| 1405 | 142.8212 | 35.0229 | 21.0407 | 0.0900 | 20.9507 |
| 1406 | 136.5846 | 43.2229 | 19.9674 | 0.0500 | 19.9174 |
| 1407 | 129.9898 | 53.8496 | 19.3475 | 0.0900 | 19.2575 |
| 1408 | 127.6505 | 69.1274 | 20.4931 | 0.0500 | 20.4431 |
| 1501 | 160.2233 | 9.3601 | 25.0508 | 0.0500 | 25.0008 |
| 1502 | 145.0508 | 12.6303 | 20.6114 | 0.0500 | 20.5614 |
| 1503 | 133.0706 | 17.6290 | 17.5720 | 0.0500 | 17.5220 |
| 1504 | 128.7877 | 21.5795 | 16.6115 | 0.0500 | 16.5615 |
| 1505 | 124.1851 | 34.1906 | 16.1225 | 0.0500 | 16.0725 |
| 1506 | 120.8110 | 49.4802 | 16.5832 | 0.0500 | 16.5332 |
| 1601 | 124.9363 | 8.9021 | 15.3279 | 0.0900 | 15.2379 |
| 1602 | 120.0979 | 13.4703 | 14.2761 | 0.0500 | 14.2261 |
| 2101 | 41.0954 | 84.4063 | 8.5835 | 0.0500 | 8.5335 |
| 2102 | 39.2844 | 81.7885 | 8.0541 | 0.0900 | 7.9641 |
| 2103 | 37.7449 | 79.7257 | 7.5886 | 0.0900 | 7.4986 |
| 2104 | 36.3673 | 77.7158 | 7.1860 | 0.0500 | 7.1360 |
| 2105 | 35.8127 | 76.9654 | 7.0008 | 0.0500 | 6.9508 |
| 2106 | 34.2347 | 75.6460 | 6.7400 | 0.0500 | 6.6900 |
| 2107 | 32.1110 | 73.3690 | 6.2922 | 0.0500 | 6.2422 |
| 2108 | 29.8886 | 71.4858 | 5.8521 | 0.0500 | 5.8021 |
| 2201 | 60.3751 | 79.1729 | 9.7049 | 0.0500 | 9.6549 |
| 2202 | 57.2637 | 73.1150 | 8.4038 | 0.0500 | 8.3538 |
| 2203 | 53.9547 | 68.0504 | 7.4697 | 0.0900 | 7.3797 |
| 2204 | 50.9789 | 64.1042 | 6.5812 | 0.0500 | 6.5312 |
| 2205 | 49.4009 | 62.3338 | 6.1737 | 0.0500 | 6.1237 |
| 2206 | 45.5922 | 59.2640 | 5.4587 | 0.0500 | 5.4087 |
| 2207 | 40.7204 | 55.4286 | 4.6075 | 0.0900 | 4.5175 |
| 2208 | 35.0044 | 52.2432 | 3.9073 | 0.0500 | 3.8573 |

| | | | | | |
|---|---|---|---|---|---|
| 2301 | 79.4588 | 73.6942 | 11.4132 | 0.0500 | 11.3632 |
| 2302 | 75.0242 | 63.8325 | 9.4215 | 0.0900 | 9.3315 |
| 2303 | 70.0386 | 56.1066 | 7.8060 | 0.0500 | 7.7560 |
| 2304 | 65.2817 | 50.0270 | 6.5766 | 0.0500 | 6.5266 |
| 2305 | 62.9373 | 47.6173 | 6.0801 | 0.0500 | 6.0301 |
| 2306 | 57.1129 | 42.8124 | 4.9388 | 0.0500 | 4.8888 |
| 2307 | 49.3765 | 37.3047 | 3.7584 | 0.0500 | 3.7084 |
| 2308 | 39.5886 | 32.8892 | 2.5356 | 0.0500 | 2.4856 |
| 2401 | 95.6987 | 69.1337 | 13.4968 | 0.0500 | 13.4468 |
| 2402 | 92.5918 | 54.6085 | 11.2051 | 0.0900 | 11.1151 |
| 2403 | 85.8451 | 44.0460 | 9.0728 | 0.0500 | 9.0228 |
| 2404 | 79.4191 | 35.9707 | 7.4310 | 0.0900 | 7.3410 |
| 2405 | 76.2924 | 32.7320 | 6.6702 | 0.0500 | 6.6202 |
| 2406 | 68.3794 | 26.4192 | 5.2642 | 0.0500 | 5.2142 |
| 2407 | 57.6833 | 19.2307 | 3.6183 | 0.0500 | 3.5683 |
| 2408 | 43.2259 | 16.3175 | 2.1082 | 0.0500 | 2.0582 |
| 2501 | 101.9652 | 49.8853 | 12.4429 | 0.0500 | 12.3929 |
| 2502 | 98.3813 | 34.5278 | 10.6467 | 0.0900 | 10.5567 |
| 2503 | 93.7261 | 22.1672 | 9.0025 | 0.0500 | 8.9525 |
| 2504 | 89.6228 | 17.9903 | 8.1320 | 0.0500 | 8.0820 |
| 2505 | 77.1976 | 13.3113 | 5.9504 | 0.0500 | 5.9004 |
| 2506 | 61.9989 | 9.5955 | 3.8126 | 0.0500 | 3.7626 |
| 2601 | 102.3279 | 13.7740 | 10.3613 | 0.0500 | 10.3113 |
| 2602 | 97.6269 | 8.9271 | 9.3622 | 0.0900 | 9.2722 |
| 3101 | 30.1247 | -72.0489 | 5.8817 | 0.0500 | 5.8317 |
| 3102 | 32.2623 | -73.7029 | 6.3146 | 0.0500 | 6.2646 |
| 3103 | 34.4242 | -75.6635 | 6.7377 | 0.0500 | 6.6877 |
| 3104 | 36.0300 | -77.3497 | 7.1066 | 0.0900 | 7.0166 |
| 3105 | 36.5052 | -78.3762 | 7.3176 | 0.0900 | 7.2276 |
| 3106 | 37.8009 | -80.0123 | 7.6564 | 0.0900 | 7.5664 |
| 3107 | 39.1940 | -82.2219 | 8.1010 | 0.0700 | 8.0310 |
| 3108 | 41.0236 | -84.7568 | 8.6962 | 0.0500 | 8.6462 |
| 3201 | 34.6846 | -52.7204 | 3.8489 | 0.0500 | 3.7989 |
| 3202 | 40.8645 | -55.7496 | 4.6204 | 0.0500 | 4.5704 |
| 3203 | 45.9010 | -59.3453 | 5.4334 | 0.0500 | 5.3834 |
| 3204 | 49.5664 | -62.6437 | 6.1589 | 0.0900 | 6.0689 |
| 3205 | 50.9383 | -64.5991 | 6.5751 | 0.0900 | 6.4851 |
| 3206 | 53.8615 | -68.0756 | 7.3154 | 0.0900 | 7.2254 |
| 3207 | 57.0759 | -73.2634 | 8.3316 | 0.0700 | 8.2616 |
| 3208 | 60.2704 | -79.4508 | 9.6547 | 0.0500 | 9.6047 |
| 3301 | 39.1772 | -33.3355 | 2.5073 | 0.0500 | 2.4573 |
| 3302 | 49.2493 | -37.6024 | 3.7306 | 0.0500 | 3.6806 |
| 3303 | 57.1410 | -42.7391 | 4.8838 | 0.0500 | 4.8338 |
| 3304 | 62.9973 | -47.8048 | 6.0009 | 0.0500 | 5.9509 |
| 3305 | 65.2145 | -50.4852 | 6.5532 | 0.0500 | 6.5032 |
| 3306 | 69.8127 | -55.9919 | 7.7262 | 0.0500 | 7.6762 |
| 3307 | 74.9142 | -64.2213 | 9.3794 | 0.0500 | 9.3294 |
| 3308 | 79.4083 | -74.1105 | 11.4409 | 0.0500 | 11.3909 |
| 3401 | 43.0282 | -16.8491 | 2.0506 | 0.0500 | 2.0006 |
| 3402 | 57.5570 | -19.4475 | 3.5145 | 0.0500 | 3.4645 |
| 3403 | 68.2880 | -26.2355 | 5.0907 | 0.0500 | 5.0407 |
| 3404 | 76.3242 | -32.9350 | 6.6242 | 0.0500 | 6.5742 |
| 3405 | 79.3130 | -36.4131 | 7.3646 | 0.0900 | 7.2746 |
| 3406 | 85.9804 | -44.3854 | 9.0376 | 0.0500 | 8.9876 |
| 3407 | 92.4287 | -54.9164 | 11.1320 | 0.0700 | 11.0620 |
| 3408 | 95.6621 | -69.6339 | 13.4965 | 0.0500 | 13.4465 |
| 3501 | 61.9067 | -9.8741 | 3.7726 | 0.0500 | 3.7226 |
| 3502 | 77.1688 | -13.1981 | 5.8126 | 0.0500 | 5.7626 |
| 3503 | 89.6283 | -18.1605 | 7.9575 | 0.0500 | 7.9075 |
| 3504 | 93.6654 | -22.6604 | 8.9019 | 0.0500 | 8.8519 |

| | | | | | |
|---|---|---|---|---|---|
| 3505 | 98.6985 | -35.1352 | 10.5799 | 0.0500 | 10.5299 |
| 3506 | 101.9068 | -50.4489 | 12.4686 | 0.0500 | 12.4186 |
| 3601 | 97.4221 | -8.9365 | 9.1684 | 0.0700 | 9.0984 |
| 3602 | 102.3506 | -14.3142 | 10.2946 | 0.0700 | 10.2246 |
| 4101 | 179.9516 | -83.3150 | 38.1654 | 0.0500 | 38.1154 |
| 4102 | 180.9599 | -80.0690 | 38.0323 | 0.0500 | 37.9823 |
| 4103 | 183.1373 | -77.3167 | 38.3744 | 0.0900 | 38.2844 |
| 4104 | 184.2894 | -75.1733 | 38.4897 | 0.0900 | 38.3997 |
| 4105 | 185.4376 | -73.7870 | 38.6913 | 0.0900 | 38.6013 |
| 4106 | 187.3985 | -73.0381 | 39.1944 | 0.0500 | 39.1444 |
| 4107 | 189.8021 | -71.5387 | 39.9656 | 0.0500 | 39.9156 |
| 4108 | 193.7239 | -70.2583 | 41.1898 | 0.0500 | 41.1398 |
| 4201 | 161.8294 | -78.2566 | 31.4118 | 0.0700 | 31.3418 |
| 4202 | 164.2810 | -71.5465 | 31.1476 | 0.0500 | 31.0976 |
| 4203 | 167.9926 | -66.1407 | 31.6571 | 0.0900 | 31.5671 |
| 4204 | 170.7847 | -61.9697 | 32.0405 | 0.0900 | 31.9505 |
| 4205 | 172.4839 | -59.9096 | 32.3777 | 0.0900 | 32.2877 |
| 4206 | 176.3381 | -57.4522 | 33.3586 | 0.0500 | 33.3086 |
| 4207 | 181.4122 | -54.1551 | 34.7705 | 0.0500 | 34.7205 |
| 4208 | 188.5808 | -51.3945 | 37.0578 | 0.0500 | 37.0078 |
| 4301 | 143.4660 | -73.3582 | 25.3108 | 0.0700 | 25.2408 |
| 4302 | 147.2944 | -62.9183 | 24.9066 | 0.0500 | 24.8566 |
| 4303 | 152.6240 | -54.9239 | 25.5570 | 0.0500 | 25.5070 |
| 4304 | 156.9365 | -48.6140 | 26.2177 | 0.0900 | 26.1277 |
| 4305 | 159.4156 | -45.9239 | 26.7460 | 0.0900 | 26.6560 |
| 4306 | 165.1239 | -41.6364 | 28.1636 | 0.0700 | 28.0936 |
| 4307 | 173.1775 | -36.4103 | 30.3935 | 0.0500 | 30.3435 |
| 4308 | 183.3873 | -32.4518 | 33.6058 | 0.0500 | 33.5558 |
| 4401 | 127.6768 | -69.2653 | 20.5239 | 0.0500 | 20.4739 |
| 4402 | 130.1991 | -54.3337 | 19.3374 | 0.0500 | 19.2874 |
| 4403 | 137.0768 | -43.6257 | 20.1153 | 0.0500 | 20.0653 |
| 4404 | 143.0862 | -35.2482 | 21.0627 | 0.0500 | 21.0127 |
| 4405 | 146.2644 | -31.7037 | 21.7442 | 0.0500 | 21.6942 |
| 4406 | 154.1788 | -25.6334 | 23.7589 | 0.0500 | 23.7089 |
| 4407 | 164.6713 | -18.7881 | 26.6236 | 0.0500 | 26.5736 |
| 4408 | 178.8449 | -16.2704 | 31.2232 | 0.0900 | 31.1332 |
| 4501 | 120.9334 | -50.0974 | 16.6187 | 0.0500 | 16.5687 |
| 4502 | 124.4628 | -34.9704 | 16.2182 | 0.0500 | 16.1682 |
| 4503 | 128.7368 | -22.1634 | 16.5376 | 0.0500 | 16.4876 |
| 4504 | 132.9299 | -17.5556 | 17.4815 | 0.0500 | 17.4315 |
| 4505 | 145.1764 | -13.0735 | 20.7308 | 0.0900 | 20.6408 |
| 4506 | 160.0735 | -9.4261 | 24.9848 | 0.0700 | 24.9148 |
| 4601 | 120.0467 | -14.0318 | 14.1867 | 0.0900 | 14.0967 |
| 4602 | 124.5202 | -9.0064 | 15.2426 | 0.0900 | 15.1526 |

Coordinates of Target Points for Set 2 of Metric Camera Measurements

Coordinates shown in inches

| Target # | X | Y | Z | Button Thk. | Z corrected |
|---|---|---|---|---|---|
| 101 | 174.5905 | -0.0769 | 29.5670 | 0.0700 | 29.4970 |
| 102 | 155.6454 | -0.0154 | 23.6356 | 0.0500 | 23.5856 |
| 103 | 136.3710 | -0.2296 | 18.1274 | 0.0700 | 18.0574 |
| 104 | 116.9656 | -0.4123 | 13.4805 | 0.0700 | 13.4105 |
| 105 | 105.3810 | -0.2565 | 10.8334 | 0.0700 | 10.7634 |
| 106 | 85.7340 | 0.1270 | 7.1549 | 0.0700 | 7.0849 |
| 107 | 65.7249 | -0.2673 | 4.2342 | 0.0700 | 4.1642 |
| 108 | 46.1811 | -0.2733 | 2.1509 | 0.0700 | 2.0809 |
| 201 | 111.7699 | 65.1274 | 16.3186 | 0.0500 | 16.2686 |
| 202 | 111.4209 | 45.3467 | 14.0177 | 0.0500 | 13.9677 |
| 203 | 111.5714 | 25.4650 | 12.7677 | 0.0700 | 12.6977 |
| 204 | 111.1281 | 5.6126 | 12.1792 | 0.0700 | 12.1092 |
| 205 | 111.0484 | -6.1943 | 12.1138 | 0.0700 | 12.0438 |
| 206 | 111.3678 | -26.1356 | 12.6563 | 0.0500 | 12.6063 |
| 207 | 111.4710 | -46.1084 | 14.0239 | 0.0500 | 13.9739 |
| 208 | 111.7706 | -65.6460 | 16.2816 | 0.0500 | 16.2316 |
| 301 | 97.4180 | -8.9405 | 9.1930 | 0.0900 | 9.1030 |
| 302 | 98.6600 | -10.0961 | 9.4273 | 0.0000 | 9.4273 |
| 303 | 99.8626 | -11.4873 | 9.7226 | 0.0000 | 9.7226 |
| 304 | 101.1693 | -12.8612 | 10.0078 | 0.0000 | 10.0078 |
| 305 | 102.3526 | -14.3144 | 10.2951 | 0.0900 | 10.2051 |
| 306 | 100.9828 | -15.6708 | 10.0543 | 0.0000 | 10.0543 |
| 307 | 99.5703 | -17.0293 | 9.8298 | 0.0000 | 9.8298 |
| 308 | 98.1289 | -18.3625 | 9.5973 | 0.0000 | 9.5973 |
| 309 | 96.7107 | -19.8127 | 9.3663 | 0.0000 | 9.3663 |
| 310 | 95.2404 | -21.2358 | 9.1196 | 0.0000 | 9.1196 |
| 311 | 93.6840 | -22.6781 | 8.8938 | 0.0500 | 8.8438 |
| 312 | 94.1407 | -20.6299 | 8.8903 | 0.0000 | 8.8903 |
| 313 | 94.7378 | -18.7101 | 8.9564 | 0.0000 | 8.9564 |
| 314 | 95.2382 | -16.8272 | 8.9898 | 0.0000 | 8.9898 |
| 315 | 95.7243 | -14.7674 | 9.0222 | 0.0000 | 9.0222 |
| 316 | 96.2401 | -12.9376 | 9.0633 | 0.0000 | 9.0633 |
| 317 | 96.7964 | -10.8840 | 9.1005 | 0.0000 | 9.1005 |
| 401 | 69.7897 | -55.9583 | 7.7065 | 0.0500 | 7.6565 |
| 402 | 70.7971 | -57.5736 | 8.0267 | 0.0000 | 8.0267 |
| 403 | 71.8464 | -59.2107 | 8.3772 | 0.0000 | 8.3772 |
| 404 | 72.8471 | -60.8239 | 8.7037 | 0.0000 | 8.7037 |
| 405 | 73.8917 | -62.4686 | 9.0278 | 0.0000 | 9.0278 |
| 406 | 74.8949 | -64.1706 | 9.3656 | 0.0500 | 9.3156 |
| 407 | 73.2654 | -65.0892 | 9.2521 | 0.0000 | 9.2521 |
| 408 | 71.4736 | -66.0238 | 9.1568 | 0.0000 | 9.1568 |
| 409 | 69.6523 | -66.9082 | 9.0482 | 0.0000 | 9.0482 |
| 410 | 67.8976 | -67.8299 | 8.9523 | 0.0000 | 8.9523 |
| 411 | 65.9740 | -68.7370 | 8.8214 | 0.0000 | 8.8214 |
| 412 | 64.2344 | -69.6505 | 8.7274 | 0.0000 | 8.7274 |
| 413 | 62.4787 | -70.5147 | 8.6125 | 0.0000 | 8.6125 |
| 414 | 60.6225 | -71.4832 | 8.5059 | 0.0000 | 8.5059 |
| 415 | 58.8392 | -72.4000 | 8.3918 | 0.0000 | 8.3918 |
| 416 | 57.0578 | -73.2251 | 8.3183 | 0.0700 | 8.2483 |
| 417 | 58.1542 | -71.4413 | 8.1828 | 0.0000 | 8.1828 |
| 418 | 59.3113 | -69.8436 | 8.1209 | 0.0000 | 8.1209 |
| 419 | 60.3907 | -68.1468 | 8.0383 | 0.0000 | 8.0383 |
| 420 | 61.6366 | -66.5198 | 7.9823 | 0.0000 | 7.9823 |
| 421 | 62.7227 | -65.0813 | 7.9366 | 0.0000 | 7.9366 |
| 422 | 64.0268 | -63.3592 | 7.8815 | 0.0000 | 7.8815 |

| | | | | | |
|---|---|---|---|---|---|
| 423 | 65.2526 | -61.8014 | 7.8264 | 0.0000 | 7.8264 |
| 424 | 66.3943 | -60.2853 | 7.7848 | 0.0000 | 7.7848 |
| 425 | 67.4810 | -58.6850 | 7.7230 | 0.0000 | 7.7230 |
| 426 | 68.7435 | -57.0824 | 7.6746 | 0.0000 | 7.6746 |
| 1101 | 193.4653 | 70.1757 | 41.0976 | 0.0500 | 41.0476 |
| 1102 | 190.0260 | 71.5126 | 40.0350 | 0.0500 | 39.9850 |
| 1103 | 187.1052 | 72.8683 | 39.1378 | 0.0500 | 39.0878 |
| 1104 | 185.2696 | 74.2336 | 38.6668 | 0.0500 | 38.6168 |
| 1105 | 184.0860 | 74.9417 | 38.3437 | 0.0900 | 38.2537 |
| 1106 | 182.4023 | 77.3120 | 38.1166 | 0.0900 | 38.0266 |
| 1107 | 180.7386 | 79.7811 | 37.8740 | 0.0500 | 37.8240 |
| 1108 | 179.8454 | 83.3006 | 38.1333 | 0.0500 | 38.0833 |
| 1201 | 188.4898 | 51.2056 | 37.0693 | 0.0500 | 37.0193 |
| 1202 | 181.9133 | 53.9608 | 34.9697 | 0.0500 | 34.9197 |
| 1203 | 176.4561 | 56.9261 | 33.3808 | 0.0900 | 33.2908 |
| 1204 | 172.4925 | 60.2564 | 32.3973 | 0.0500 | 32.3473 |
| 1205 | 170.5287 | 61.7247 | 31.9152 | 0.0900 | 31.8252 |
| 1206 | 167.2013 | 66.2382 | 31.3985 | 0.0900 | 31.3085 |
| 1207 | 164.0644 | 71.1457 | 31.0670 | 0.0900 | 30.9770 |
| 1208 | 161.7064 | 78.3821 | 31.3667 | 0.0500 | 31.3167 |
| 1301 | 183.2578 | 32.2784 | 33.6760 | 0.0900 | 33.5860 |
| 1302 | 173.4777 | 36.3037 | 30.5460 | 0.0900 | 30.4560 |
| 1303 | 165.1793 | 41.1158 | 28.1622 | 0.0900 | 28.0722 |
| 1304 | 159.4552 | 46.1354 | 26.8011 | 0.0900 | 26.7111 |
| 1305 | 156.6821 | 48.4835 | 26.1549 | 0.0900 | 26.0649 |
| 1306 | 152.0287 | 54.5992 | 25.3048 | 0.0500 | 25.2548 |
| 1307 | 147.0581 | 62.5952 | 24.8185 | 0.0500 | 24.7685 |
| 1308 | 143.3695 | 73.3315 | 25.2115 | 0.0500 | 25.1615 |
| 1401 | 178.7374 | 16.1214 | 31.2926 | 0.0500 | 31.2426 |
| 1402 | 164.9034 | 18.7317 | 26.7524 | 0.0500 | 26.7024 |
| 1403 | 154.0119 | 25.2981 | 23.6667 | 0.0500 | 23.6167 |
| 1404 | 146.3207 | 31.9156 | 21.7877 | 0.0500 | 21.7377 |
| 1405 | 142.8402 | 35.0131 | 21.0247 | 0.0900 | 20.9347 |
| 1406 | 136.6147 | 43.1897 | 19.9506 | 0.0500 | 19.9006 |
| 1407 | 130.0189 | 53.7970 | 19.3315 | 0.0900 | 19.2415 |
| 1408 | 127.6663 | 69.0721 | 20.4787 | 0.0500 | 20.4287 |
| 1501 | 160.2863 | 9.3360 | 25.0944 | 0.0500 | 25.0444 |
| 1502 | 145.0654 | 12.6251 | 20.6137 | 0.0500 | 20.5637 |
| 1503 | 133.0927 | 17.6137 | 17.5568 | 0.0500 | 17.5068 |
| 1504 | 128.8196 | 21.5536 | 16.5904 | 0.0500 | 16.5404 |
| 1505 | 124.2107 | 34.1629 | 16.1037 | 0.0500 | 16.0537 |
| 1506 | 120.8389 | 49.4294 | 16.5669 | 0.0500 | 16.5169 |
| 1601 | 124.9248 | 8.9154 | 15.3178 | 0.0900 | 15.2278 |
| 1602 | 120.1213 | 13.4476 | 14.2634 | 0.0500 | 14.2134 |
| 2101 | 41.0725 | 84.3952 | 8.5777 | 0.0500 | 8.5277 |
| 2102 | 39.2546 | 81.7558 | 8.0447 | 0.0900 | 7.9547 |
| 2103 | 37.7159 | 79.7052 | 7.5798 | 0.0900 | 7.4898 |
| 2104 | 36.3503 | 77.7097 | 7.1764 | 0.0500 | 7.1264 |
| 2105 | 35.7947 | 76.9629 | 6.9941 | 0.0500 | 6.9441 |
| 2106 | 34.2228 | 75.6442 | 6.7311 | 0.0500 | 6.6811 |
| 2107 | 32.0916 | 73.3648 | 6.2841 | 0.0500 | 6.2341 |
| 2108 | 29.8281 | 71.4735 | 5.8497 | 0.0500 | 5.7997 |
| 2201 | 60.3728 | 79.2114 | 9.6982 | 0.0500 | 9.6482 |
| 2202 | 57.2443 | 73.0945 | 8.3911 | 0.0500 | 8.3411 |
| 2203 | 53.9368 | 68.0377 | 7.4615 | 0.0900 | 7.3715 |
| 2204 | 50.9952 | 64.1278 | 6.5675 | 0.0500 | 6.5175 |
| 2205 | 49.3981 | 62.3388 | 6.1637 | 0.0500 | 6.1137 |
| 2206 | 45.6152 | 59.2814 | 5.4426 | 0.0500 | 5.3926 |
| 2207 | 40.7186 | 55.4282 | 4.5972 | 0.0900 | 4.5072 |
| 2208 | 34.8773 | 52.2122 | 3.9047 | 0.0500 | 3.8547 |

| | | | | | |
|---|---|---|---|---|---|
| 2301 | 79.4348 | 73.6494 | 11.4090 | 0.0500 | 11.3590 |
| 2302 | 75.0006 | 63.7987 | 9.4104 | 0.0900 | 9.3204 |
| 2303 | 70.0192 | 56.0909 | 7.8001 | 0.0500 | 7.7501 |
| 2304 | 65.3291 | 50.0802 | 6.5674 | 0.0500 | 6.5174 |
| 2305 | 62.9541 | 47.6350 | 6.0698 | 0.0500 | 6.0198 |
| 2306 | 57.1604 | 42.8419 | 4.9206 | 0.0500 | 4.8706 |
| 2307 | 49.3927 | 37.3093 | 3.7497 | 0.0500 | 3.6997 |
| 2308 | 39.5509 | 32.8765 | 2.5346 | 0.0500 | 2.4846 |
| 2401 | 95.6787 | 69.0981 | 13.4975 | 0.0500 | 13.4475 |
| 2402 | 92.5796 | 54.5920 | 11.1965 | 0.0900 | 11.1065 |
| 2403 | 85.8231 | 44.0220 | 9.0701 | 0.0500 | 9.0201 |
| 2404 | 79.3932 | 35.9454 | 7.4257 | 0.0900 | 7.3357 |
| 2405 | 76.2607 | 32.7085 | 6.6780 | 0.0500 | 6.6280 |
| 2406 | 68.3977 | 26.4295 | 5.2618 | 0.0500 | 5.2118 |
| 2407 | 57.6962 | 19.2298 | 3.6141 | 0.0500 | 3.5641 |
| 2408 | 43.1829 | 16.3003 | 2.1092 | 0.0500 | 2.0592 |
| 2501 | 101.9550 | 49.8683 | 12.4352 | 0.0500 | 12.3852 |
| 2502 | 98.3568 | 34.4961 | 10.6452 | 0.0900 | 10.5552 |
| 2503 | 93.7079 | 22.1465 | 9.0050 | 0.0500 | 8.9550 |
| 2504 | 89.6197 | 17.9887 | 8.1458 | 0.0500 | 8.0958 |
| 2505 | 77.1924 | 13.3024 | 5.9520 | 0.0500 | 5.9020 |
| 2506 | 62.0014 | 9.5889 | 3.8173 | 0.0500 | 3.7673 |
| 2601 | 102.3090 | 13.7524 | 10.3679 | 0.0500 | 10.3179 |
| 2602 | 97.6368 | 8.9350 | 9.3835 | 0.0900 | 9.2935 |
| 3101 | 30.1254 | -72.0812 | 5.8798 | 0.0500 | 5.8298 |
| 3102 | 32.2619 | -73.7325 | 6.3120 | 0.0500 | 6.2620 |
| 3103 | 34.4270 | -75.6890 | 6.7310 | 0.0500 | 6.6810 |
| 3104 | 36.0395 | -77.3816 | 7.1005 | 0.0900 | 7.0105 |
| 3105 | 36.5212 | -78.4165 | 7.3104 | 0.0900 | 7.2204 |
| 3106 | 37.8119 | -80.0416 | 7.6477 | 0.0900 | 7.5577 |
| 3107 | 39.2022 | -82.2463 | 8.0917 | 0.0700 | 8.0217 |
| 3108 | 41.0392 | -84.7999 | 8.6867 | 0.0500 | 8.6367 |
| 3201 | 34.6113 | -52.7300 | 3.8580 | 0.0500 | 3.8080 |
| 3202 | 40.8788 | -55.7801 | 4.6165 | 0.0500 | 4.5665 |
| 3203 | 45.9069 | -59.3677 | 5.4270 | 0.0500 | 5.3770 |
| 3204 | 49.5567 | -62.6512 | 6.1494 | 0.0900 | 6.0594 |
| 3205 | 50.9298 | -64.6058 | 6.5634 | 0.0900 | 6.4734 |
| 3206 | 53.8425 | -68.0572 | 7.3011 | 0.0900 | 7.2111 |
| 3207 | 57.0582 | -73.2252 | 8.3181 | 0.0700 | 8.2481 |
| 3208 | 60.2682 | -79.4140 | 9.6417 | 0.0500 | 9.5917 |
| 3301 | 39.1803 | -33.3608 | 2.5202 | 0.0500 | 2.4702 |
| 3302 | 49.2277 | -37.6097 | 3.7429 | 0.0500 | 3.6929 |
| 3303 | 57.1426 | -42.7528 | 4.8760 | 0.0500 | 4.8260 |
| 3304 | 63.0228 | -47.8360 | 5.9911 | 0.0500 | 5.9411 |
| 3305 | 65.2197 | -50.4978 | 6.5392 | 0.0500 | 6.4892 |
| 3306 | 69.7898 | -55.9586 | 7.7059 | 0.0500 | 7.6559 |
| 3307 | 74.8950 | -64.1709 | 9.3652 | 0.0500 | 9.3152 |
| 3308 | 79.4122 | -74.0757 | 11.4254 | 0.0500 | 11.3754 |
| 3401 | 43.0451 | -16.8738 | 2.0715 | 0.0500 | 2.0215 |
| 3402 | 57.5391 | -19.4638 | 3.5647 | 0.0500 | 3.5147 |
| 3403 | 68.2398 | -26.2196 | 5.1136 | 0.0500 | 5.0636 |
| 3404 | 76.3289 | -32.9431 | 6.6143 | 0.0500 | 6.5643 |
| 3405 | 79.3239 | -36.4265 | 7.3553 | 0.0900 | 7.2653 |
| 3406 | 85.9866 | -44.3876 | 9.0259 | 0.0500 | 8.9759 |
| 3407 | 92.4230 | -54.8847 | 11.1173 | 0.0700 | 11.0473 |
| 3408 | 95.6652 | -69.5822 | 13.4764 | 0.0500 | 13.4264 |
| 3501 | 61.9137 | -9.8994 | 3.8290 | 0.0500 | 3.7790 |
| 3502 | 77.1822 | -13.2235 | 5.8499 | 0.0500 | 5.7999 |
| 3503 | 89.6547 | -18.1897 | 7.9655 | 0.0500 | 7.9155 |
| 3504 | 93.6840 | -22.6783 | 8.8931 | 0.0500 | 8.8431 |

| | | | | | |
|---|---|---|---|---|---|
| 3505 | 98.6790 | -35.1000 | 10.5672 | 0.0500 | 10.5172 |
| 3506 | 101.9170 | -50.4477 | 12.4609 | 0.0500 | 12.4109 |
| 3601 | 97.4179 | -8.9403 | 9.1926 | 0.0700 | 9.1226 |
| 3602 | 102.3524 | -14.3142 | 10.2949 | 0.0700 | 10.2249 |
| 4101 | 179.9744 | -83.3223 | 38.1623 | 0.0500 | 38.1123 |
| 4102 | 180.9966 | -80.0542 | 38.0306 | 0.0500 | 37.9806 |
| 4103 | 183.1690 | -77.3134 | 38.3750 | 0.0900 | 38.2850 |
| 4104 | 184.3149 | -75.1802 | 38.4904 | 0.0900 | 38.4004 |
| 4105 | 185.4727 | -73.7831 | 38.6923 | 0.0900 | 38.6023 |
| 4106 | 187.4140 | -73.0492 | 39.1967 | 0.0500 | 39.1467 |
| 4107 | 189.8274 | -71.5449 | 39.9692 | 0.0500 | 39.9192 |
| 4108 | 193.7420 | -70.2662 | 41.1936 | 0.0500 | 41.1436 |
| 4201 | 161.8564 | -78.2548 | 31.4048 | 0.0700 | 31.3348 |
| 4202 | 164.3060 | -71.5498 | 31.1413 | 0.0500 | 31.0913 |
| 4203 | 168.0167 | -66.1453 | 31.6537 | 0.0900 | 31.5637 |
| 4204 | 170.8057 | -61.9768 | 32.0393 | 0.0900 | 31.9493 |
| 4205 | 172.4936 | -59.9265 | 32.3754 | 0.0900 | 32.2854 |
| 4206 | 176.3292 | -57.4784 | 33.3561 | 0.0500 | 33.3061 |
| 4207 | 181.3843 | -54.1826 | 34.7691 | 0.0500 | 34.7191 |
| 4208 | 188.5732 | -51.4042 | 37.0626 | 0.0500 | 37.0126 |
| 4301 | 143.4915 | -73.3405 | 25.3030 | 0.0700 | 25.2330 |
| 4302 | 147.3189 | -62.9170 | 24.8911 | 0.0500 | 24.8411 |
| 4303 | 152.6421 | -54.9293 | 25.5504 | 0.0500 | 25.5004 |
| 4304 | 156.9345 | -48.6380 | 26.2163 | 0.0900 | 26.1263 |
| 4305 | 159.3923 | -45.9646 | 26.7427 | 0.0900 | 26.6527 |
| 4306 | 165.1268 | -41.6500 | 28.1721 | 0.0700 | 28.1021 |
| 4307 | 173.1720 | -36.4212 | 30.3946 | 0.0500 | 30.3446 |
| 4308 | 183.3958 | -32.4526 | 33.6108 | 0.0500 | 33.5608 |
| 4401 | 127.6992 | -69.2565 | 20.5039 | 0.0500 | 20.4539 |
| 4402 | 130.2255 | -54.3187 | 19.3241 | 0.0500 | 19.2741 |
| 4403 | 137.1010 | -43.6190 | 20.1044 | 0.0500 | 20.0544 |
| 4404 | 143.1086 | -35.2424 | 21.0589 | 0.0500 | 21.0089 |
| 4405 | 146.2682 | -31.7149 | 21.7419 | 0.0500 | 21.6919 |
| 4406 | 154.1876 | -25.6359 | 23.7736 | 0.0500 | 23.7236 |
| 4407 | 164.6711 | -18.7922 | 26.6234 | 0.0500 | 26.5734 |
| 4408 | 178.8018 | -16.2816 | 31.2263 | 0.0900 | 31.1363 |
| 4501 | 120.9585 | -50.0807 | 16.6059 | 0.0500 | 16.5559 |
| 4502 | 124.4700 | -34.9822 | 16.2117 | 0.0500 | 16.1617 |
| 4503 | 128.7316 | -22.1823 | 16.5365 | 0.0500 | 16.4865 |
| 4504 | 132.9274 | -17.5688 | 17.4774 | 0.0500 | 17.4274 |
| 4505 | 145.1646 | -13.0890 | 20.7525 | 0.0900 | 20.6625 |
| 4506 | 160.0727 | -9.4278 | 24.9878 | 0.0700 | 24.9178 |
| 4601 | 120.0613 | -14.0268 | 14.1897 | 0.0900 | 14.0997 |
| 4602 | 124.4985 | -9.0363 | 15.2415 | 0.0900 | 15.1515 |

APPENDIX C

Program listing for Solving Set 1 'Best-Fit' Surface

```
10 DIM XIII(200),YIII(200),ZII(200),NOD(200),ZP(200),X(200),Y(200),Z(200)
20 DIM XI(200),XII(200),YII(200),YI(200),ZI(200),ZIII(200)
30 OPEN "B:XYZTRN1" FOR INPUT AS #1
40 FOCAL=258!:DELTAZ=0!:DELTAX=0:DELTAY=0!:RMSMINT=1:RMSMINP=1
50 N=0
60 INPUT #1,NODE,D1,D2,D3,D4
70 IF NODE>300 AND NODE<599 THEN GOTO 60
80 N=N+1:NOD(N)=NODE:XIII(N)=D1:YIII(N)=D2:ZIII(N)=D3-(D4*.02+.01)
90 IF NODE=4602 THEN NNODE=N:GOTO 100 ELSE GOTO 60
100 BETA=0!:ALPHA=0
110 DELTAZ=0:DELTAY=0:DELTAX=0
120 FOR I=1 TO NNODE:XII(I)=XIII(I)+DELTAX:YII(I)=YIII(I)+DELTAY:ZII(I)=ZIII(I)+
DELTAZ:NEXT I
130 ALPHARAD=ALPHA*3.1415927#/180!
140 FOR I=1 TO NNODE:YI(I)=YII(I)*COS(ALPHARAD)+ZII(I)*SIN(ALPHARAD)
150 ZI(I)=-YII(I)*SIN(ALPHARAD)+ZII(I)*COS(ALPHARAD)
160 XI(I)=XII(I)
170 NEXT I
180 BETARAD=BETA*3.1415927#/180!
190 FOR I=1 TO NNODE:X(I)=XI(I)*COS(BETARAD)+ZI(I)*SIN(BETARAD)
200 Z(I)=-XI(I)*SIN(BETARAD)+ZI(I)*COS(BETARAD)
210 Y(I)=YI(I):NEXT I
220 FOR I=1 TO NNODE:ZP(I)=(X(I)*X(I)+Y(I)*Y(I))/(4!*FOCAL):NEXT I
230 REM PRINT " NODE        X          Y          Z          ZP         DELTAZ"
240 REM FOR I=1 TO NNODE:IF ABS(Z(I)-ZP(I))<.1 THEN GOTO 270
250 REM PRINT USING "####  ";NOD(I);
260 REM PRINT USING "####.####  ";X(I);Y(I);Z(I);ZP(I);Z(I)-ZP(I)
270 REM NEXT I
280 NNODA=0:NNODB=0:NNODC=0:NNODD=0
290 RMSA=0:RMSB=0:RMSC=0:RMSD=0:AVEA=0:AVEB=0:AVEC=0:AVED=0
300 FOR I=1 TO NNODE:IF NOD(I)>1000 AND NOD(I)<2000 THEN NNODA=NNODA+1:RMSA=RMSA
+(Z(I)-ZP(I))*(Z(I)-ZP(I)):AVEA=AVEA+(Z(I)-ZP(I))
310 IF NOD(I)>2000 AND NOD(I)<3000 THEN NNODB=NNODB+1:RMSB=RMSB+(Z(I)-ZP(I))*(Z(
I)-ZP(I)):AVEB=AVEB+(Z(I)-ZP(I))
320 IF NOD(I)>3000 AND NOD(I)<4000 THEN NNODC=NNODC+1:RMSC=RMSC+(Z(I)-ZP(I))*(Z(
I)-ZP(I)):AVEC=AVEC+(Z(I)-ZP(I))
330 IF NOD(I)>4000 AND NOD(I)<5000 THEN NNODD=NNODD+1:RMSD=RMSD+(Z(I)-ZP(I))*(Z(
I)-ZP(I)):AVED=AVED+(Z(I)-ZP(I))
340 NEXT I
350 PRINT "DELTAX =";DELTAX;" DELTAY =";DELTAY;" DELTAZ =";DELTAZ
360 PRINT "ALPHA =";ALPHA;"  BETA =";BETA
370 PRINT "FOCAL LENGTH =";FOCAL
380 PRINT "AVE ERROR IN QUAD A =";AVEA/NNODA;" RMS ERROR IN QUAD A =";SQR(RMSA/N
NODA)
390 PRINT "AVE ERROR IN QUAD B =";AVEB/NNODB;" RMS ERROR IN QUAD B =";SQR(RMSB/N
NODB)
400 PRINT "AVE ERROR IN QUAD C =";AVEC/NNODC;" RMS ERROR IN QUAD C =";SQR(RMSC/N
NODC)
410 PRINT "AVE ERROR IN QUAD D =";AVED/NNODD;" RMS ERROR IN QUAD D =";SQR(RMSD/N
NODD)
420 RMS1=0:N=0:FOR I=1 TO NNODE
430 N=N+1:RMS1=RMS1+((Z(I)-ZP(I))*(Z(I)-ZP(I)))
440 NEXT I
450 RMSTOT=SQR(RMS1/N)
460 RMS2=0:N=0:FOR I=1 TO NNODE
470 IF NOD(I)>3000 AND NOD(I)<4000 THEN GOTO 490
480 N=N+1:RMS2=RMS2+((Z(I)-ZP(I))*(Z(I)-ZP(I)))
```

ORIGINAL PAGE IS
OF POOR QUALITY

```
490 NEXT I
500 RMSPAR=SQR(RMS2/N)
501 GOSUB 10000
510 PRINT "RMS SURFACE ERROR =";RMSTOT
520 PRINT "RMS WITHOUT QUAD C =";RMSPAR
521 PRINT "***********  MIN RMS INFO  ***********"
522 PRINT "WHOLE SURFACE:":PRINT "FOCAL =";FOCALT
523 PRINT "DELTAX =";DXT;"DELTAY =";DYT;"DELTAZ =";DZT
524 PRINT "ALPHA =";ALPHAT;"BETA =";BETAT
525 PRINT "RMS =";RMSMINT
526 PRINT "PARTIAL SURFACE:":PRINT "FOCAL =";FOCALP
527 PRINT "DELTAX =";DXP;"DELTAY =";DYP;"DELTAZ =";DZP
528 PRINT "ALPHA =";ALPHAP;"BETA =";BETAP
529 PRINT "RMS =";RMSMINP
530 PRINT "DO YOU WANT HARDCOPY OF THE INFORMATION (Y/N)":INPUT A$
540 IF A$<>"Y" THEN GOTO 740
550 LPRINT "FOCAL LENGTH =";FOCAL
560 LPRINT "DELTAX =";DELTAX
570 LPRINT "DELTAY =";DELTAY
580 LPRINT "DELTAZ =";DELTAZ
590 LPRINT "ALPHA =";ALPHA
600 LPRINT "BETA =";BETA
610 LPRINT "AVE ERROR IN QUAD A =";AVEA/NNODA;" RMS ERROR IN QUAD A =";SQR(RMSA/
NNODA)
620 LPRINT "AVE ERROR IN QUAD B =";AVEB/NNODB;" RMS ERROR IN QUAD B =";SQR(RMSB/
NNODB)
630 LPRINT "AVE ERROR IN QUAD C =";AVEC/NNODC;" RMS ERROR IN QUAD C =";SQR(RMSC/
NNODC)
640 LPRINT "AVE ERROR IN QUAD D =";AVED/NNODD;" RMS ERROR IN QUAD D =";SQR(RMSD/
NNODD)
650 LPRINT "RMS TOTAL SURFACE ERROR =";RMSTOT
660 LPRINT "RMS SURFACE ERROR WITHOUT QUAD C =";RMSPAR
670 LPRINT "*********************************************************************
"
680 LPRINT " NODE      X          Y          Z          ZP        DELTAZ     DELTAZ^2
"
690 FOR I=1 TO NNODE:LPRINT USING "####  ";NOD(I);
700 LPRINT USING "####.#### ";X(I);Y(I);Z(I);ZP(I);Z(I)-ZP(I);(Z(I)-ZP(I))^2;
710 IF ABS(Z(I)-ZP(I))>.1 THEN LPRINT "****" ELSE LPRINT " "
720 NEXT I
730 LPRINT CHR$(12)
740 PRINT "DO YOU WANT TO CHANGE SOME PARAMETERS (Y/N)":INPUT A$
750 IF A$<>"Y" THEN END
760 INPUT "ENTER NEW VALUE FOR DELTAX ",DELTAXNEW
770 INPUT "ENTER NEW VALUE FOR DELTAY ",DELTAYNEW
780 INPUT "ENTER NEW VALUE FOR DELTAZ ",DELTAZNEW
790 INPUT "ENTER NEW VALUE FOR ALPHA IN DEG. ",ALPHANEW
800 INPUT "ENTER NEW VALUE FOR BETA IN DEG.",BETANEW
810 INPUT "ENTER NEW FOCAL LENGTH ",FOCALNEW
820 IF DELTAXNEW<>DELTAX OR DELTAYNEW<>DELTAY OR DELTAZNEW<>DELTAZ THEN DELTAX=D
ELTAXNEW:DELTAY=DELTAYNEW:DELTAZ=DELTAZNEW:ALPHA=ALPHANEW:BETA=BETANEW:FOCAL=FOC
ALNEW:GOTO 120
830 IF ALPHANEW<>ALPHA THEN FOCAL=FOCALNEW:BETA=BETANEW:ALPHA=ALPHANEW:GOTO 130
840 IF BETANEW<>BETA THEN FOCAL=FOCALNEW:BETA=BETANEW:GOTO 180
850 FOCAL=FOCALNEW:GOTO 220
10000 IF RMSTOT<RMSMINT THEN RMSMINT=RMSTOT:DXT=DELTAX:DYT=DELTAY:DZT=DELTAZ:ALP
HAT=ALPHA:BETAT=BETA:FOCALT=FOCAL
10010 IF RMSPAR<RMSMINP THEN RMSMINP=RMSPAR:DXP=DELTAX:DYP=DELTAY:DZP=DELTAZ:ALP
HAP=ALPHA:BETAP=BETA:FOCALP=FOCAL
10020 RETURN
```

Program listing for Solving Set 2 'Best-Fit' Surface

```
10 DIM XIII(200),YIII(200),ZII(200),NOD(200),ZP(200),X(200),Y(200),Z(200)
20 DIM XI(200),XII(200),YII(200),YI(200),ZI(200),ZIII(200)
30 OPEN "B:XYZTRN2" FOR INPUT AS #1
35 OPEN "B:BUTTON.DAT" FOR INPUT AS #2
40 FOCAL=258!:DELTAZ=0!:DELTAX=0:DELTAY=0!:RMSMINT=1:RMSMINP=1
50 N=0
60 INPUT #1,NODE,D1,D2,D3:INPUT #2,DUM,D4
70 IF NODE>300 AND NODE<599 THEN GOTO 60
80 N=N+1:NOD(N)=NODE:XIII(N)=D1:YIII(N)=D2:ZIII(N)=D3-(D4*.02+.01)
90 IF NODE=4602 THEN NNODE=N:GOTO 100 ELSE GOTO 60
100 BETA=0!:ALPHA=0
110 DELTAZ=0:DELTAY=0:DELTAX=0
120 FOR I=1 TO NNODE:XII(I)=XIII(I)+DELTAX:YII(I)=YIII(I)+DELTAY:ZII(I)=ZIII(I)+
DELTAZ:NEXT I
130 ALPHARAD=ALPHA*3.1415927#/180!
140 FOR I=1 TO NNODE:YI(I)=YII(I)*COS(ALPHARAD)+ZII(I)*SIN(ALPHARAD)
150 ZI(I)=-YII(I)*SIN(ALPHARAD)+ZII(I)*COS(ALPHARAD)
160 XI(I)=XII(I)
170 NEXT I
180 BETARAD=BETA*3.1415927#/180!
190 FOR I=1 TO NNODE:X(I)=XI(I)*COS(BETARAD)+ZI(I)*SIN(BETARAD)
200 Z(I)=-XI(I)*SIN(BETARAD)+ZI(I)*COS(BETARAD)
210 Y(I)=YI(I):NEXT I
220 FOR I=1 TO NNODE:ZP(I)=(X(I)*X(I)+Y(I)*Y(I))/(4!*FOCAL):NEXT I
230 REM PRINT " NODE         X          Y          Z          ZP          DELTAZ"
240 REM FOR I=1 TO NNODE:IF ABS(Z(I)-ZP(I))<.1 THEN GOTO 270
250 REM PRINT USING "####  ";NOD(I);
260 REM PRINT USING "####.####  ";X(I);Y(I);Z(I);ZP(I);Z(I)-ZP(I)
270 REM NEXT I
280 NNODA=0:NNODB=0:NNODC=0:NNODD=0
290 RMSA=0:RMSB=0:RMSC=0:RMSD=0:AVEA=0:AVEB=0:AVEC=0:AVED=0
300 FOR I=1 TO NNODE:IF NOD(I)>1000 AND NOD(I)<2000 THEN NNODA=NNODA+1:RMSA=RMSA
+(Z(I)-ZP(I))*(Z(I)-ZP(I)):AVEA=AVEA+(Z(I)-ZP(I))
310 IF NOD(I)>2000 AND NOD(I)<3000 THEN NNODB=NNODB+1:RMSB=RMSB+(Z(I)-ZP(I))*(Z(
I)-ZP(I)):AVEB=AVEB+(Z(I)-ZP(I))
320 IF NOD(I)>3000 AND NOD(I)<4000 THEN NNODC=NNODC+1:RMSC=RMSC+(Z(I)-ZP(I))*(Z(
I)-ZP(I)):AVEC=AVEC+(Z(I)-ZP(I))
330 IF NOD(I)>4000 AND NOD(I)<5000 THEN NNODD=NNODD+1:RMSD=RMSD+(Z(I)-ZP(I))*(Z(
I)-ZP(I)):AVED=AVED+(Z(I)-ZP(I))
340 NEXT I
350 PRINT "DELTAX =";DELTAX;" DELTAY =";DELTAY;" DELTAZ =";DELTAZ
360 PRINT "ALPHA =";ALPHA;"  BETA =";BETA
370 PRINT "FOCAL LENGTH =";FOCAL
380 PRINT "AVE ERROR IN QUAD A =";AVEA/NNODA;" RMS ERROR IN QUAD A =";SQR(RMSA/N
NODA)
390 PRINT "AVE ERROR IN QUAD B =";AVEB/NNODB;" RMS ERROR IN QUAD B =";SQR(RMSB/N
NODB)
400 PRINT "AVE ERROR IN QUAD C =";AVEC/NNODC;" RMS ERROR IN QUAD C =";SQR(RMSC/N
NODC)
410 PRINT "AVE ERROR IN QUAD D =";AVED/NNODD;" RMS ERROR IN QUAD D =";SQR(RMSD/N
NODD)
420 RMS1=0:N=0:FOR I=1 TO NNODE
430 N=N+1:RMS1=RMS1+((Z(I)-ZP(I))*(Z(I)-ZP(I)))
440 NEXT I
450 RMSTOT=SQR(RMS1/N)
460 RMS2=0:N=0:FOR I=1 TO NNODE
470 IF NOD(I)>3000 AND NOD(I)<4000 THEN GOTO 490
480 N=N+1:RMS2=RMS2+((Z(I)-ZP(I))*(Z(I)-ZP(I)))
```

```
490 NEXT I
500 RMSPAR=SQR(RMS2/N)
501 GOSUB 10000
510 PRINT "RMS SURFACE ERROR =";RMSTOT
520 PRINT "RMS WITHOUT QUAD C =";RMSPAR
521 PRINT "***********  MIN RMS INFO  ***********"
522 PRINT "WHOLE SURFACE:":PRINT "FOCAL =";FOCALT
523 PRINT "DELTAX =";DXT;"DELTAY =";DYT;"DELTAZ =";DZT
524 PRINT "ALPHA =";ALPHAT;"BETA =";BETAT
525 PRINT "RMS =";RMSMINT
526 PRINT "PARTIAL SURFACE:":PRINT "FOCAL =";FOCALP
527 PRINT "DELTAX =";DXP;"DELTAY =";DYP;"DELTAZ =";DZP
528 PRINT "ALPHA =";ALPHAP;"BETA =";BETAP
529 PRINT "RMS =";RMSMINP
530 PRINT "DO YOU WANT HARDCOPY OF THE INFORMATION (Y/N)":INPUT A$
540 IF A$<>"Y" THEN GOTO 740
550 LPRINT "FOCAL LENGTH =";FOCAL
560 LPRINT "DELTAX =";DELTAX
570 LPRINT "DELTAY =";DELTAY
580 LPRINT "DELTAZ =";DELTAZ
590 LPRINT "ALPHA =";ALPHA
600 LPRINT "BETA =";BETA
610 LPRINT "AVE ERROR IN QUAD A =";AVEA/NNODA;" RMS ERROR IN QUAD A =";SQR(RMSA/
NNODA)
620 LPRINT "AVE ERROR IN QUAD B =";AVEB/NNODB;" RMS ERROR IN QUAD B =";SQR(RMSB/
NNODB)
630 LPRINT "AVE ERROR IN QUAD C =";AVEC/NNODC;" RMS ERROR IN QUAD C =";SQR(RMSC/
NNODC)
640 LPRINT "AVE ERROR IN QUAD D =";AVED/NNODD;" RMS ERROR IN QUAD D =";SQR(RMSD/
NNODD)
650 LPRINT "RMS TOTAL SURFACE ERROR =";RMSTOT
660 LPRINT "RMS SURFACE ERROR WITHOUT QUAD C =";RMSPAR
670 LPRINT "*****************************************************************
"
680 LPRINT " NODE      X          Y          Z          ZP       DELTAZ      DELTAZ^2
"
690 FOR I=1 TO NNODE:LPRINT USING "####  ";NOD(I);
700 LPRINT USING "####.#### ";X(I);Y(I);Z(I);ZP(I);Z(I)-ZP(I);(Z(I)-ZP(I))^2;
710 IF ABS(Z(I)-ZP(I))>.1 THEN LPRINT "****" ELSE LPRINT " "
720 NEXT I
730 LPRINT CHR$(12)
740 PRINT "DO YOU WANT TO CHANGE SOME PARAMETERS (Y/N)":INPUT A$
750 IF A$<>"Y" THEN END
760 INPUT "ENTER NEW VALUE FOR DELTAX ",DELTAXNEW
770 INPUT "ENTER NEW VALUE FOR DELTAY ",DELTAYNEW
780 INPUT "ENTER NEW VALUE FOR DELTAZ ",DELTAZNEW
790 INPUT "ENTER NEW VALUE FOR ALPHA IN DEG. ",ALPHANEW
800 INPUT "ENTER NEW VALUE FOR BETA IN DEG.",BETANEW
810 INPUT "ENTER NEW FOCAL LENGTH ",FOCALNEW
820 IF DELTAXNEW<>DELTAX OR DELTAYNEW<>DELTAY OR DELTAZNEW<>DELTAZ THEN DELTAX=D
ELTAXNEW:DELTAY=DELTAYNEW:DELTAZ=DELTAZNEW:ALPHA=ALPHANEW:BETA=BETANEW:FOCAL=FOC
ALNEW:GOTO 120
830 IF ALPHANEW<>ALPHA THEN FOCAL=FOCALNEW:BETA=BETANEW:ALPHA=ALPHANEW:GOTO 130
840 IF BETANEW<>BETA THEN FOCAL=FOCALNEW:BETA=BETANEW:GOTO 180
850 FOCAL=FOCALNEW:GOTO 220
10000 IF RMSTOT<RMSMINT THEN RMSMINT=RMSTOT:DXT=DELTAX:DYT=DELTAY:DZT=DELTAZ:ALP
HAT=ALPHA:BETAT=BETA:FOCALT=FOCAL
10010 IF RMSPAR<RMSMINP THEN RMSMINP=RMSPAR:DXP=DELTAX:DYP=DELTAY:DZP=DELTAZ:ALP
HAP=ALPHA:BETAP=BETA:FOCALP=FOCAL
10020 RETURN
```

# APPENDIX D

Program listing for Solving Pillow I RMS Error

```
1 REM THIS PROGRAM IS FOR MESH PILLOW I IT ADD ADDITIONAL
2 REM POINTS BY INTERPOLATING BETWEEN EXISTING POINTS
3 REM THIS PROGRAM WORKS IDENTICALLY TO "RMSPIL2.TXT"
4 REM "RMSPIL2.TXT" IS FOR PILLOW II
5 DEFDBL A-H,J-Z
10 DIM ZP(40),ZP2(40),NOD(40),DIST(40),X(40),Y(40),Z(40),Z2(40),DIST2(40)
30 OPEN "B:XYZTRN1" FOR INPUT AS #1
40 FOCAL=258!:DELTAZ=0!:DELTAX=0:DELTAY=0!
45 RMSMIN=100
50 N=0
60 INPUT #1,NODE,D1,D2,D3,D4
70 IF NODE<301 OR NODE>320 THEN GOTO 60
80 N=N+1:NOD(N)=NODE:X(N)=D1:Y(N)=D2:Z(N)=D3-(D4*.02+.01)
90 IF NODE=317 THEN GOTO 100 ELSE GOTO 60
100 N=N+1:NOD(N)=1001:X(N)=(X(9)+X(13))/2!
110 Y(N)=(Y(9)+Y(13))/2!
120 Z(N)=(Z(9)+Z(13))/2!
130 N=N+1:NOD(N)=1002:X(N)=(X(8)+X(14))/2!
140 Y(N)=(Y(8)+Y(14))/2!
150 Z(N)=(Z(8)+Z(14))/2!
160 N=N+1:NOD(N)=1003:X(N)=(X(7)+X(15))/2!
170 Y(N)=(Y(7)+Y(15))/2!
180 Z(N)=(Z(7)+Z(15))/2!
190 N=N+1:NOD(N)=1004:X(N)=(X(16)-X(6))/3+X(6)
200 Y(N)=(Y(16)-Y(6))/3+Y(6)
210 Z(N)=(Z(16)-Z(6))/3+Z(6)
220 N=N+1:NOD(N)=1005:X(N)=(X(16)-X(6))*2/3+X(6)
230 Y(N)=(Y(16)-Y(6))*2/3+Y(6)
240 Z(N)=(Z(16)-Z(6))*2/3+Z(6)
250 N=N+1:NOD(N)=1006:X(N)=(X(16)+X(3))/2!
260 Y(N)=(Y(3)+Y(16))/2!
270 Z(N)=(Z(3)+Z(16))/2!
280 N=N+1:NOD(N)=1007:X(N)=(X(22)+X(4))/2!
290 Y(N)=(Y(4)+Y(22))/2!
300 Z(N)=(Z(4)+Z(22))/2!
310 N=N+1:NOD(N)=1008:X(N)=(X(6)+X(4))/2!
320 Y(N)=(Y(4)+Y(6))/2!
330 Z(N)=(Z(4)+Z(6))/2!
350 NNODE=N
360 FOR I=1 TO NNODE:Z2(I)=(X(I)*X(I)+Y(I)*Y(I))/(4!*258)
370 NEXT I
1000 A=-5.35097:B=1!:C=28.1793:D=274.42352#
1010 A2=-6.0544:B2=1!:C2=32.75341:D2=295.00868#
1020 FOR I=1 TO NNODE:T=(-D-A*X(I)-B*Y(I)-C*Z(I))/(A*A+B*B+C*C)
1030 XP=A*T+X(I):YP=B*T+Y(I):ZP(I)=C*T+Z(I)
1040 DIST(I)=SQR((XP-X(I))*(XP-X(I))+(YP-Y(I))*(YP-Y(I))+(ZP(I)-Z(I))*(ZP(I)-Z(I
)))
1050 NEXT I
1060 FOR I=1 TO NNODE:T2=(-D2-A2*X(I)-B2*Y(I)-C2*Z2(I))/(A2*A2+B2*B2+C2*C2)
1070 XP2=A2*T2+X(I):YP2=B2*T2+Y(I):ZP2(I)=C2*T2+Z2(I)
1080 DIST2(I)=SQR((XP2-X(I))*(XP2-X(I))+(YP2-Y(I))*(YP2-Y(I))+(ZP2(I)-Z2(I))*(ZP
2(I)-Z2(I)))
1090 NEXT I
1100 RMS1=0:FOR I=1 TO NNODE:IF NOD(I)>=301 AND NOD(I)<=317 THEN MULT=1 ELSE MUL
T=2
1104 IF NOD(I)=301 OR NOD(I)=305 THEN MULT=0
1105 RMS1=RMS1+MULT*((DIST(I)+DIST2(I)-DELTAZ)*(DIST(I)+DIST2(I)-DELTAZ))
```

```
1107 PRINT NOD(I);MULT
1110 NEXT I
1120 RMS=SQR(RMS1/(NNODE+6)):IF RMS<RMSMIN THEN RMSMIN=RMS:DELTAZMIN=DELTAZ
1130 REM PRINT " NODE        X         Y         Z         DIST        DIST2       DELTA"
1140 REM FOR I=1 TO NNODE
1150 REM PRINT USING "#### ";NOD(I);
1160 REM PRINT USING "####.#### ";X(I);Y(I);Z(I);DIST(I);DIST2(I);DIST(I)+DIST2(
I)-DELTAZ
1170 REM NEXT I
1180 PRINT "DELTAZ =";DELTAZ;"  RMS ERROR =";RMS
1190 PRINT "MIN DELTAZ =";DELTAZMIN;"MIN RMS ERROR =";RMSMIN
1200 PRINT "DO YOU WANT HARDCOPY OF THE INFORMATION (Y/N)":INPUT A$
1210 IF A$<>"Y" THEN GOTO 1310
1220 WIDTH "LPT1:",130
1230 LPRINT "DELTAZ =";DELTAZ
1240 LPRINT "RMS ERROR =";RMS
1250 LPRINT CHR$(27);"&k2S"
1260 LPRINT " NODE       X          Y          Z          ZP        Z2        ZP2
  DIST       DIST2       DELTA"
1270 FOR I=1 TO NNODE:LPRINT USING "####  ";NOD(I);
1280 LPRINT USING "####.#### ";X(I);Y(I);Z(I);ZP(I);Z2(I);ZP2(I);DIST(I);DIST2(I
);DIST(I)+DIST2(I)-DELTAZ
1290 NEXT I
1300 LPRINT CHR$(12)
1310 INPUT "ENTER NEW VALUE FOR DELTAZ ",DELTAZ
1320 GOTO 1100
```

Program listing for Solving Pillow II RMS Error

```
5 REM THIS PROGRAM IS FOR MESH PILLOW NUMBER II
7 REM IT USES LINEAR INTERPOLATION OF KNOWN POINTS TO ADD TO THE
8 REM POINTS ALREADY KNOWN AND MULTIPLIES THOSES POINTS TWICE
10 DEFDBL A-H,J-Z
20 DIM ZP(40),ZP2(40),NOD(40),DIST(40),X(40),Y(40),Z(40),Z2(40),DIST2(40)
30 OPEN "B:XYZTRN1" FOR INPUT AS #1
40 FOCAL=258!:DELTAZ=0!:DELTAX=0:DELTAY=0!
50 RMSMIN=100
60 N=0
70 INPUT #1,NODE,D1,D2,D3,D4
80 IF NODE<401 OR NODE>430 THEN GOTO 70
90 N=N+1:NOD(N)=NODE:X(N)=D1:Y(N)=D2:Z(N)=D3-(D4*.02+.01)
100 IF NODE=426 THEN GOTO 110 ELSE GOTO 70
110 N=N+1:NOD(N)=1001:X(N)=(X(14)+X(18))/2!
120 Y(N)=(Y(14)+Y(18))/2!
130 Z(N)=(Z(14)+Z(18))/2!
140 N=N+1:NOD(N)=1002:X(N)=(X(13)+X(19))/2!
150 Y(N)=(Y(13)+Y(19))/2!
160 Z(N)=(Z(13)+Z(19))/2!
170 N=N+1:NOD(N)=1003:X(N)=(X(12)+X(20))/2!
180 Y(N)=(Y(12)+Y(20))/2!
190 Z(N)=(Z(12)+Z(20))/2!
200 N=N+1:NOD(N)=1004:X(N)=(X(11)+X(21))/2!
210 Y(N)=(Y(11)+Y(21))/2!
220 Z(N)=(Z(11)+Z(21))/2!
230 N=N+1:NOD(N)=1005:X(N)=(X(10)+X(22))/2!
240 Y(N)=(Y(10)+Y(22))/2!
250 Z(N)=(Z(10)+Z(22))/2!
260 N=N+1:NOD(N)=1006:X(N)=(X(23)-X(9))/3+X(9)
270 Y(N)=(Y(23)-Y(9))/3+Y(9)
280 Z(N)=(Z(23)-Z(9))/3+Z(9)
290 N=N+1:NOD(N)=1007:X(N)=(X(23)-X(9))*2/3+X(9)
300 Y(N)=(Y(23)-Y(9))*2/3+Y(9)
310 Z(N)=(Z(23)-Z(9))*2/3+Z(9)
320 N=N+1:NOD(N)=1008:X(N)=(X(24)-X(8))/3+X(8)
330 Y(N)=(Y(24)-Y(8))/3+Y(8)
340 Z(N)=(Z(24)-Z(8))/3+Z(8)
350 N=N+1:NOD(N)=1009:X(N)=(X(24)-X(8))*2/3+X(8)
360 Y(N)=(Y(24)-Y(8))*2/3+Y(8)
370 Z(N)=(Z(24)-Z(8))*2/3+Z(8)
380 N=N+1:NOD(N)=1010:X(N)=(X(35)+X(5))/2!
390 Y(N)=(Y(5)+Y(35))/2!
400 Z(N)=(Z(5)+Z(35))/2!
410 N=N+1:NOD(N)=1011:X(N)=(X(24)-X(4))/3+X(4)
420 Y(N)=(Y(24)-Y(4))/3+Y(4)
430 Z(N)=(Z(24)-Z(4))/3+Z(4)
440 N=N+1:NOD(N)=1012:X(N)=(X(24)-X(4))*2/3+X(4)
450 Y(N)=(Y(24)-Y(4))*2/3+Y(4)
460 Z(N)=(Z(24)-Z(4))*2/3+Z(4)
470 N=N+1:NOD(N)=1013:X(N)=(X(25)+X(3))/2!
480 Y(N)=(Y(3)+Y(25))/2!
490 Z(N)=(Z(3)+Z(25))/2!
500 NNODE=N
510 FOR I=1 TO NNODE:Z2(I)=(X(I)*X(I)+Y(I)*Y(I))/(4!*258)
520 NEXT I
530 A=-.98755:B=1!:C=8.02254:D=63.35594#
```

```
540 A2=-.98484:B2=1!:C2=7.91704:D2=63.30557#
550 FOR I=1 TO NNODE:T=(-D-A*X(I)-B*Y(I)-C*Z(I))/(A*A+B*B+C*C)
560 XP=A*T+X(I):YP=B*T+Y(I):ZP(I)=C*T+Z(I)
570 DIST(I)=SQR((XP-X(I))*(XP-X(I))+(YP-Y(I))*(YP-Y(I))+(ZP(I)-Z(I))*(ZP(I)-Z(I)
))
580 NEXT I
590 FOR I=1 TO NNODE:T2=(-D2-A2*X(I)-B2*Y(I)-C2*Z2(I))/(A2*A2+B2*B2+C2*C2)
600 XP2=A2*T2+X(I):YP2=B2*T2+Y(I):ZP2(I)=C2*T2+Z2(I)
610 DIST2(I)=SQR((XP2-X(I))*(XP2-X(I))+(YP2-Y(I))*(YP2-Y(I))+(ZP2(I)-Z2(I))*(ZP2
(I)-Z2(I)))
620 NEXT I
630 RMS1=0:FOR I=1 TO NNODE:IF NOD(I)>=401 AND NOD(I)<=426 THEN MULT=1 ELSE MULT
=2
640 IF NOD(I)=401 OR NOD(I)=406 THEN MULT=0
650 RMS1=RMS1+MULT*((DIST(I)+DIST2(I)-DELTAZ)*(DIST(I)+DIST2(I)-DELTAZ))
660 REM PRINT NOD(I);MULT
670 NEXT I
680 RMS=SQR(RMS1/(NNODE+6)):IF RMS<RMSMIN THEN RMSMIN=RMS:DELTAZMIN=DELTAZ
690 REM PRINT " NODE       X          Y          Z          DIST       DIST2      DELTA"
700 REM FOR I=1 TO NNODE
710 REM PRINT USING "#### ";NOD(I);
720 REM PRINT USING "####.#### ";X(I);Y(I);Z(I);DIST(I);DIST2(I);DIST(I)+DIST2(I
)-DELTAZ
730 REM NEXT I
740 PRINT "DELTAZ =";DELTAZ;"  RMS ERROR =";RMS
750 PRINT "MIN DELTAZ =";DELTAZMIN;"MIN RMS ERROR =";RMSMIN
760 PRINT "DO YOU WANT HARDCOPY OF THE INFORMATION (Y/N)":INPUT A$
770 IF A$<>"Y" THEN GOTO 870
780 WIDTH "LPT1:",130
790 LPRINT "DELTAZ =";DELTAZ
800 LPRINT "RMS ERROR =";RMS
810 LPRINT CHR$(27);"Q";
820 LPRINT " NODE       X          Y          Z          ZP         Z2         ZP2
 DIST       DIST2      DELTA"
830 FOR I=1 TO NNODE:LPRINT USING "####  ";NOD(I);
840 LPRINT USING "####.#### ";X(I);Y(I);Z(I);ZP(I);Z2(I);ZP2(I);DIST(I);DIST2(I)
;DIST(I)+DIST2(I)-DELTAZ
850 NEXT I
860 LPRINT CHR$(12)
870 INPUT "ENTER NEW VALUE FOR DELTAZ ",DELTAZ
880 GOTO 630
```

ORIGINAL PAGE IS
OF POOR QUALITY

## Standard Bibliographic Page

| | | |
|---|---|---|
| 1. Report No. NASA CR-178228 | 2. Government Accession No. | 3. Recipient's Catalog No. |
| 4. Title and Subtitle The Integration of a Mesh Reflector to a 15-ft Box Truss Structure, Task 3 -- Box Truss Analysis and Technology Development | | 5. Report Date March 1987 |
| | | 6. Performing Organization Code |
| 7. Author(s) E.E. Bachtell, W.F. Thiemet, and G. Morosow | | 8. Performing Organization Report No. MCR-86-669 |
| 9. Performing Organization Name and Address Martin Marietta Corporation Denver Aerospace P.O. Box 179 Denver, Colorado 80201 | | 10. Work Unit No. 506-49-21-01 |
| | | 11. Contract or Grant No. NAS1-17551 |
| 12. Sponsoring Agency Name and Address National Aeronautics and Space Administration Wahshington, DC 20546 | | 13. Type of Report and Period Covered Contractor Report |
| | | 14. Sponsoring Agency Code |

15. Supplementary Notes

Langley technical monitors: U.M. Lovelace and J.W. Goslee
Final Report -- Task 3

16. Abstract

In order to demonstrate the design and integration of a reflective mesh surface to a deployable box truss structure, reflective mesh was installed on a 15-ft prototype box truss cube. The resulting configuration is a off-set fed 15-ft diameter reflector with an F/D of 1.5. The resulting surface accuracy was 1/18 of a wavelength at 10 GHz. The specific features demonstrated included:

1) Sewing seams in reflective mesh;
2) Stretching mesh to a desired preload;
3) Installation of a tensioned tie cord support system;
4) Setting and verificlation of a reflective surface; and
5) Repeatability of the reflector surface

| | |
|---|---|
| 17. Key Words (Suggested by Authors(s)) Large Space Structures, Antennas, Radiometers, Spacecraft | 18. Distribution Statement Unclassified - Unlimited; Subject Category 18 |

| | | | |
|---|---|---|---|
| 19. Security Classif.(of this report) Unclassified | 20. Security Classif.(of this page) Unclassified | 21. No. of Pages 73 | 22. Price A04 |